Characterization of synaptic alterations and the effect of genetic background in a mouse model of Spinal Muscular Atrophy

Mehdi Eshraghi

Thesis submitted to the

Faculty of Graduate and Postdoctoral Studies

in partial fulfillment of the requirements

for the Doctorate in Philosophy degree in Neuroscience

Department of Cellular and Molecular Medicine

Faculty of Medicine

University of Ottawa

Abstract

Spinal muscular atrophy (SMA) is a genetic disorder characterized by muscle weakness and atrophy and death of motor neurons in humans. Although almost all cases of SMA occur due to mutations in a gene called *survival motor neuron 1* (*SMN1*), SMA patients present with a wide range of severities of the symptoms. The most severe cases never achieve any developmental motor milestone and die within a few years after birth. On the other hand, mild cases of SMA have a normal life span and show trivial motor deficits. This suggests the role of other factors (rather than the function of *SMN1*) in the outcome of the disease. Indeed, the copy number of an almost identical gene, called *SMN2*, is the main determining factor for the severity of SMA. In addition, a few other genes (e.g. *Plastin 3*) are proposed as disease modifiers in SMA.

SMN1 is a housekeeping gene, but due to unknown reasons the most prominent pathologies in SMA are atrophy of myofibers and death of motor neurons. However, recent studies showed that some other cell types are also affected in the course of SMA disease.

We investigated the alterations of central synapses in $Smn^{2B/-}$ mice, a model of SMA. We did not observe any degeneration of central synapses in these mice until a post symptomatic stage. However, mass spectrometry (MS) analysis on isolated synaptosomes from spinal cords of these animals revealed widespread alterations in the proteome of their central synapses at a presymptomatic stage. Functional cluster analysis on MS results suggested that several molecular pathways are affected within synapses of spinal cords of $Smn^{2B/-}$ mice prior to onset of any obvious pathology in their motor units. The affected molecular pathways are involved in basic cell biological functions including energy production, protein synthesis, cytoskeleton regulation and intracellular trafficking. We showed that the levels of several proteins involved in actin cytoskeleton regulation are altered in synaptosomes isolated from spinal cords of $Smn^{2B/-}$ mice.

More investigations are required to determine the exact functional abnormalities of affected pathways in central synapses of these mice.

We also generated congenic *Smn*$^{2B/-}$ mice in two different mouse genetic backgrounds; FVB and BL6. Using a systematic approach, we showed that congenic *Smn*$^{2B/-}$ mice in the FVB background show a more severe SMA phenotype than *Smn*$^{2B/-}$ mice in a BL6 background. *Smn*$^{2B/-}$ mice in the FVB background had a shorter survival, higher rate of weight loss, earlier and more severe pathologic changes compared to *Smn*$^{2B/-}$ mice in the BL6 background. We investigated the levels of several actin binding proteins in spinal cords of these animals and found higher induction of plastin 3 in *Smn*$^{2B/-}$ mice in BL6 background. More investigations are underway to determine the role of plastin 3 in severity of the phenotype of *Smn*$^{2B/-}$ mice, and to find other possible SMA modifier genes in these animals.

TABLE OF CONTENTS

List of Tables

LIST OF FIGURES

List of Abbreviations

ChAT	**Choline acetyltransferase**
DAPI	**4', 6-diamidino-2-phenylindole**
DSHB	**Developmental Studies Hybridoma Bank**
EM	**electron microscopy**
ESE	**exonic splicing enhancer**
ESS	**exonic splicing silencer**
GAPDH	**Glyceraldehyde 3-phosphate dehydrogenase**
hnRNP-A1	**heterogeneous nuclear ribonucleoprotein A1**
hSOD1	**human superoxide dismutase 1**
MEP	**motor endplate**
MHC	**myosin heavy chain**
MRI	**magnetic resonance imaging**
NF-M	**neurofilament-medium**
NMD	**neuromuscular disorder**
NMDs	**neuromuscular disorders**
OMIM	**online Mendelian inheritance in man**
PND	**postnatal day**
RHA	**RNA helicase A**
ROCK	**Rho/Rho kinase**
sDMA	**symmetrically dimethylated arginines**
SMA	**Spinal Muscular Atrophy**
snoRNPs	**small nucleolar ribonucleoproteins**
SMN	**Survival Motor Neuron**

snRNA	**small nuclear RNAs**
SnRNP	**small nuclear ribonucleoproteins**
SV2	**synaptic vesicle protein 2**
TA	**tibialis anterior**
TK2	**thymidine kinase 2**
TVA	**transverse abdominis**

Authorization

Chapter 3.2 and Chapter 4.2 were adapted from Eshraghi M, McFall E, Gibeault S, Kothary R. Effect of genetic background on the phenotype of the *Smn*$^{2B/-}$ mouse model of spinal muscular atrophy. Hum Mol Genet. 2016 Oct 15; 25(20):4494-4506.

Acknowledgments

I was extremely fortunate to have great people around who supported me through all of the steps of my PhD. I would like to extend my sincerest thanks and appreciation to them.

Specially, I would like to extend my gratitude towards my supervisor, Dr. Rashmi Kothary. He has a great personality and a unique style of mentorship which guarantees the professional and scientific growth of his trainees. As a PhD student, I had challenging but really enjoyable experiences in his lab. Due to his precious guidance, I feel that now I have a better understanding of science as a molecular biologist.

I would like to acknowledge all of my previous and current lab co-workers especially Yves De Repentigny who is an invaluable asset in Dr Kothary's lab.

I also would like to express my appreciations to the members of my 'Thesis Advisory Committee': Dr. Jocelyn Côté, Dr. Diane Lagace and Dr. Robin Parks for their comments and directions on my PhD projects.

I would like to thank the University of Ottawa for awarding me the 'Ontario Trillium Scholarship (OTS)'.

Finally, special recognition goes out to my wonderful wife, Elham, for all of her supports, encouragements and patience during my pursuit of PhD. Also, to our lovely son, Kian, who missed out on a lot of daddy's time while I was busy at the bench.

Author Contributions

Figure 3.1.2. Sample preparation was performed by M. Eshraghi and microscopic imaging was done by S. Cummings, Dr R. Kothary lab, Ottawa Hospital Research Institute, Ottawa, Canada.

Figure 3.1.5. Synaptosome fractions were prepared by M. Eshraghi and electron microscopy was performed by Y. De Repentigny, Dr R. Kothary lab, Ottawa Hospital Research Institute, Ottawa, Canada.

Figure 3.1.6. Synaptosome fractions were prepared by M. Eshraghi and mass spectrometry (MS) analysis of synaptosome samples was performed by Dr. P. Vacratsis lab, department of Chemistry and Biochemistry, University of Windsor, Windsor, Ontario.

Chapter 1 : General Introduction

Spinal Muscular Atrophy

Spinal muscular atrophies (SMAs) are a heterogeneous group of genetic disorders characterized by lower motor impairment (i.e. hypotonia, muscle weakness, and lack of deep tendon reflexes) and no or little sensory and cognitive deficits (La Spada, Wilson et al. 1991, Monani 2005, Wirth, Brichta et al. 2006). The most common form of SMA is 'proximal autosomal recessive spinal muscular atrophy' (referred to as 'SMA' in this monograph). SMA is the leading cause of infantile mortality with an incidence of 1 in 10,000 live births (Pearn 1978). SMA is caused by mutations or deletions of the *Survival Motor Neuron 1* (*SMN1*) gene (Lefebvre, Burglen et al. 1995, Zerres and Rudnik-Schoneborn 1995). Several types of SMA have been described based on the ages at onset, survival of the affected person and severity of the clinical manifestations. Acute severe cases constitute more than 50% of SMA patients; the disease starts at early infancy and affected individuals have severe motor deficits and usually die before the age of two due to respiratory complications. On the other hand, mild chronic cases of SMA start in early adulthood and present with mild to moderate muscle weakness and usually have a normal lifespan (Pearn 1980, Zerres and Rudnik-Schoneborn 1995).

Severe infantile SMA was first described by Guido Werdnig and Johann Hoffmann during the late 1800s (this type of SMA is also called Werdnig-Hoffmann disease). These scientists provided precise descriptions of the main pathologic features of SMA (including myofiber atrophy and loss of neurons within the anterior horn of the spinal cord) (Hoffmann 1893, Hoffmann 1897, Werdnig 1971). During the first half of the 20th century, several cases of chronic muscular atrophy/dystrophy were described as mild types of SMA. However it is difficult to consider all of these patients as SMA cases because the mentioned reports lack comprehensive clinical and laboratory evaluations (Kugelberg and Welander 1956). In 1956,

Kugelberg and Welander published a report of 12 patients with juvenile muscular atrophy. Comprehensive family history, clinical examinations and laboratory tests suggested that chronic SMA is a hereditary neuromuscular disorder which originates probably from lesions within the spinal cord. The authors also observed that juvenile muscular atrophy occurs usually during late childhood and presents with weakness of the lower limbs at the beginning, and progresses slowly to the upper limbs. They also reported that the muscles with cranial innervations remain unaffected during the course of the disease (Kugelberg and Welander 1956). The authors concluded that this disorder should be distinguished from other forms of muscular dystrophy and from early onset cases of amyotrophic lateral sclerosis (ALS). Interestingly, the authors also concluded that juvenile muscular atrophy is a distinct identity from severe infantile muscular atrophy (Werdnig- Hoffmann disease).

Indeed, it took almost a century to discover the genetic basis of SMA. During the early 1990s, SMA was mapped to a genetic locus on the long arm of human chromosome 5 and in late 1990s it was shown that all types of SMAs happen due to mutations in the *SMN1* gene and different types of SMAs are mainly due to the different copy numbers of an almost identical gene (called *SMN2*). The discovery of the genetic basis of SMA opened a new chapter in the history of the disease. Soon afterwards, huge progress was made regarding understanding the biologic aspects of SMA and as a result new therapeutic strategies have been introduced. Now it is possible that SMA will be no longer an incurable disease in the near future.

Clinical presentations of SMA

SMA is one of the most common autosomal recessive disorders with a carrier frequency of 1 in 40 normal individuals and a disease prevalence of 1 in 6,000-10,000 live births (Pearn 1973, Pearn 1978). The affected individuals show no symptoms at birth but do so after a while; usually by symmetric proximal muscle weakness of the lower limbs (Pearn 1980).

The main clinical findings of SMA patients include extensive hypotonia, symmetrical muscle weakness and atrophy (occurring predominantly in shoulder and pelvic girdles), lack of deep tendon reflexes and tremor in hands and fingers (reflecting the lower motor neuron deficit). The weakness and atrophy of muscles happen first in proximal skeletal muscles and then progress to distal muscles of limbs and eventually involve trunk and axial muscles. The extraoccular muscles and diaphragm are frequently spared until the end stages of the disease and no or little somato-sensory deficit is detected. Severe muscle atrophy will result in paralysis and immobilisation of the patients with type I and II SMA (Simic 2008). Diagnosis is made based on the findings from muscle biopsy (e.g. severe atrophy of muscle fibers), electromyography (e.g. abnormal spontaneous electrical activities with fibrillations), magnetic resonance imaging (MRI) and DNA genotyping (Simic 2008).

So far, SMA cases are categorized into four major types based on (a) age of onset, (b) pattern and severity of motor deficits, and (c) survival of the affected individuals (Table 1.1) (Pearn 1980, Munsat and Davies 1992). More than 50% of SMA patients are Type I. Type II SMA is also more prevalent than Type III and Type IV SMA (Ogino, Leonard et al. 2002).

SMA type	Age of Onset	Maximum Motor Milestone	Life span
Type 0	Before birth	None	Few weeks
Type I (Werdnig-Hoffmann disease)	0 - 6 months	None	<2 years
Type II (intermediate)	6 - 18 months	Sitting	Survive into adulthood
Type III (Kugelberg-Welander disease)	>18 months	Walking but may lose ability to walk	Normal
Type IV (adult)	>20-30 years	Normal with mild motor impairments	Normal

Table 1.1. Clinical classification of spinal muscular atrophy.

SMA is classified based on age of onset, life span and the severity of the symptoms. Type I SMA is the most prevalent type of SMA (accounting for more than 50% of cases). Also, type II SMA is more prevalent than types III and type IV SMA. Patients with intermediate and mild forms of SMA have a relatively longer pre-symptomatic period and usually have a normal life span. Adapted from (Farrar, Park et al. 2016)).

Type I SMA (OMIM number 253300)

Type I SMA is also referred to as severe infantile acute SMA or Werdnig-Hoffman disease and is characterized by the abrupt onset of severe muscle weakness and hypotonia within the first few months after birth (Pearn 1980). Most of the patients with type I SMA are completely asymptomatic at birth (Simic 2008). The affected individuals never manage to sit or walk and death occurs due to fatal respiratory complications before the age of 2 years. Some studies have also reported significant peripheral sensory deficits in type I SMA patients but not in the other types of SMA (Rudnik-Schoneborn, Goebel et al. 2003).

Type II SMA (OMIM number 253550)

Also referred to as chronic childhood SMA, type II SMA is characterized by the onset of the disease between the ages of 6 months and 18 months. The patients reach the ability to sit but never walk independently. They also have a life span more than 2 years (Pearn 1978).

Type III SMA (OMIM number 253400)

Type III SMA is also known as juvenile SMA or Wohlfart-Kugelberg-Welander disease. In type III SMA, the symptoms start after the age of 2 years and the patients gain the ability to walk independently but lose walking ability at the last stages of the disease. More importantly, type III SMA patients have a normal life span. Some researchers subdivide type III SMA to 'type IIIa SMA' (age of the onset before 3 years) and 'type IIIb SMA' (age of the onset after 3 years). On average, patients with 'type IIIb SMA' show less severe phenotypes and remain ambulatory until older ages (Zerres and Rudnik-Schoneborn 1995). Pearn (1978) studied the incidence and prevalence of Kugelberg-Welander disease (type III SMA) in north-east England and reported a disease incidence of 1 in 24,100 live births and a prevalence of 1.2 per 100,000 of the general population (Pearn 1978).

Type IV SMA (OMIM number 271150)

Type IV SMA is generally known as adult-type SMA. Type IV SMA consists of a heterogeneous group of disorders in terms of causative genetic mutations, age of the onset and the severity of the phenotypes (Brahe, Servidei et al. 1995, Zerres, Rudnik-Schoneborn et al. 1995). The age of the onset in Type IV SMA is after 20-30 years (Zerres and Rudnik-Schoneborn 1995). Interestingly, not all the patients with Type IV SMA show homozygous mutations/deletions of the *SMN1* gene; it seems that some of these cases are *SMN1* independent disorders (Brahe, Servidei et al. 1995).

Atypical SMA

There are also atypical cases of SMA (due to homozygous deletion/mutations of *SMN1* gene) with involvement of other parts of the central nervous system (e.g. cerebral or cerebellar atrophy) and other organs (e.g. cardiovascular, urogenital or skeletal defects). However, it remains to be determined if these congenital anomalies are indeed linked to the 5q13 locus (Rudnik-Schoneborn, Forkert et al. 1996).

Genetics of SMA

SMN gene

In the early 1990s, all types of SMA were mapped onto a region on the long arm of human chromosome 5: 5q12-q13 (Brzustowicz, Lehner et al. 1990, Gilliam, Brzustowicz et al. 1990, Melki, Abdelhak et al. 1990, Melki, Sheth et al. 1990). At the time, it was known that this chromosomal region includes a large inverted duplication event, and, at least four genes are present in both telomeric (t) and centromeric (c) segments: *Survival Motor Neuron* (*SMN*), *Neuronal Apoptosis Inhibitory Protein* (*NAIP*), *Basal Transcription Factor subunit p44*

(*BTFp44*) and *Small Edrk-Rich Factor 1A* (*SERF1A*). In 1995, Lefebvre et al. showed that the mutations of the telomeric copy of the *SMN* gene (*SMN1*, OMIM number 600354) are responsible for all types of SMA (Lefebvre, Burglen et al. 1995). Later on, it was shown that the copy number of the centromeric *SMN* (*SMN2*, OMIM number 601627) gene modulates the severity of phenotype and thereby is a major determinant for the type of SMA in affected patients (Lefebvre, Burglen et al. 1998).

SMN1 and *SMN2* are almost identical genes with 99% sequence similarity (Monani, Lorson et al. 1999). Each gene is about 27 Kb in size and includes 9 exons (Chen, Baird et al. 1998). The *SMN* transcript is 1.7 kb in size and the SMN protein includes 294 amino acids (Lefebvre, Burglen et al. 1995). There are only 5 nucleotide differences between *SMN1* and *SMN2* genes: one in intron 6, one in exon 7, two in intron 7, and one in exon 8. The one in exon 7 (a C>T transition) is a silent mutation that does not change the amino acid sequence of the SMN protein, and the one in exon 8 is in the 3' untranslated region (Burglen, Lefebvre et al. 1996, Monani, Lorson et al. 1999).

Further studies revealed that the C>T transition at the sixth base-pair position in exon 7 of *SMN2* disrupts a heptamer motif of an exonic splicing enhancer (ESE). This motif in *SMN1* was shown to be recognized by SF2/ASF (a known splicing activator) and therefore mediates the inclusion of exon 7 in *SMN1* mRNA (Lorson, Hahnen et al. 1999, Monani, Lorson et al. 1999, Cartegni and Krainer 2002). Thus, the C>T transition in *SMN2* results in decreased inclusion of exon 7 in *SMN2* mRNA (i.e. most of the transcripts from the *SMN2* gene are devoid of exon7). Recent studies proposed that this transition also creates an exonic splicing silencer (ESS) which binds to hnRNP A1, a known splicing repressor, and results in exclusion of exon 7 during *SMN2* pre-RNA processing (Kashima and Manley 2003).

SMN genes are ubiquitously expressed genes, but the highest expression of *SMN* is reported in brain, spinal cord, liver and kidney (Coovert, Le et al. 1997, Lefebvre, Burlet et al. 1997). Gennarelli et al. reported the expression of four *SMN* RNA isoforms in skeletal muscles. Sequencing of these transcripts showed that alternative splicing events (i.e. exclusion of exon 5, 7 or both) are responsible for different SMN isoforms. They also showed that the expression level of the biggest transcript (877-nucleotides or the full length *SMN1* mRNA) is highly decreased in samples from SMA patients and the 823-nucleotide isoform (delta7-SMN) was the most abundant isoform (Gennarelli, Lucarelli et al. 1995).

Etiology of SMA

In humans, the *SMN* locus is an unstable genomic region consisting of different copy numbers (0-4) of a 500 Kb duplication/inversion event. This region is prone to deletion events during paternal meiosis (Wirth, Schmidt et al. 1997). Deletion mutations of the *SMN1* gene are responsible for most of the cases of SMA (more than 90%). The frequency of deletions of *SMN1* gene is higher in SMA type I and type II (about 95%) than SMA type III (about 85%) (Clermont, Burlet et al. 1995, Zerres and Rudnik-Schoneborn 1995, Wirth 2000). The loss of *SMN1* gene function in combination with incomplete compensation by *SMN2* gene results in vast depletion of SMN protein within cells (Coovert, Le et al. 1997).

A unique fact about SMA is that almost all patients have at least one or two copies of the *SMN2* gene (Lefebvre, Burglen et al. 1995, Lefebvre, Burlet et al. 1997). Since an alternative RNA splicing event is responsible for production of truncated SMN protein from *SMN2* it provides an opportunity to treat SMA patients by increasing the production of full length SMN protein from *SMN2* (Lim and Hertel 2001, Miyajima, Miyaso et al. 2002, Cartegni and Krainer 2003, Skordis, Dunckley et al. 2003). Indeed, homozygous deletions of the *SMN2* gene are seen

in only 3-5% of human population; a condition that does not have any known clinical consequence in normal individuals (Lefebvre, Burglen et al. 1995).

A small fraction of SMA cases happens due to subtle mutations (e.g. point mutations) in the *SMN1* gene (Wirth, Herz et al. 1999). Most of these patients have compound heterozygous deletion/mutation of *SMN1* (i.e. on one chromosome 5, they carry a *SMN1* deletion and on the other one they have a subtle *SMN1* mutation) (McAndrew, Parsons et al. 1997, Wirth, Herz et al. 1999). The most reported *SMN1* missense mutations are Y272C and 813ins/dup11 mutations (17% and 13%, respectively) (Wirth, Herz et al. 1999). Most of the *SMN1* missense mutations are localized to exon 6 and 7 and result in impairment of self-oligomerization of the SMN protein (Hahnen, Schonling et al. 1997, Talbot, Ponting et al. 1997).

In contrast to childhood and juvenile SMAs which predominantly happen as autosomal recessive disorders, adult onset SMAs are inherited in various genetic forms including autosomal dominant and X-linked as well as autosomal recessive (Pearn, Hudgson et al. 1978). However, only autosomal recessive forms of type IV SMA are due to mutations of *SMN1* gene (Brahe, Servidei et al. 1995), and autosomal dominant forms do not show any linkage to the 5q13 region (Kausch, Muller et al. 1991).

Several *SMN*-independent SMA cases have been reported due to mutations in thymidine kinase 2 gene (TK2, MIM# 188250) (Mancuso, Salviati et al. 2002). *TK2* controls the mtDNA replication and mutations of this gene results in depletion of mtDNA in neurons. A less frequent case of *SMN*-independent SMA is due to mutations in the cytochrome-c oxidase assembly gene (SCO2, MIM# 604377), which is crucial for normal mitochondria function (Tarnopolsky, Bourgeois et al. 2004).

Structure of SMN protein

Both *SMN1* and *SMN2* genes encode for an identical protein called SMN (Coovert, Le et al. 1997). SMN is a 38 kDa protein and consists of 294 amino acids (Lefebvre, Burglen et al. 1995). Within the cells, SMN is mostly localized to the cytoplasm, where it takes part in a protein complex formed by SMN and seven Sm core proteins (including SmB, D1-3, E, F and G). This complex contributes to the assembly of the spliceosomal machinery (Fischer, Liu et al. 1997, Pellizzoni, Kataoka et al. 1998, Pellizzoni, Charroux et al. 1999).

SMN protein has several known domains and motifs (Figure 1.1). It has been shown that most of these motifs are related to binding activities of SMN. The N-terminus of SMN is important for its binding to SIP1 and RNA molecules (Liu, Fischer et al. 1997, Lorson, Strasswimmer et al. 1998). Also, it seems that the function of the N-terminus of SMN is important for its export and localization to the cytoplasm; mutations within the N-terminus region of SMN result in nuclear accumulation of the protein (Le, Coovert et al. 2000). The C-terminus of SMN is critical for SMN self-oligomerization (Lorson, Strasswimmer et al. 1998). SMN also contains a 'Tudor domain' within its central regions (residues 92-144) (Talbot, Miguel-Aliaga et al. 1998). The 'Tudor domain' of SMN mediates its binding to Sm proteins (Buhler, Raker et al. 1999, Cote and Richard 2005).

The 'Tudor domain' is a conserved 50 amino acids motif which is seen in several RNA binding proteins. This domain is comprised of five β-strands with a barrel like fold. The function of the 'Tudor domain' is not fully understood but it exists usually in proteins that are involved in different aspects of RNA metabolism (Pek, Anand et al. 2012). In addition, some of the proteins which contain a 'Tudor domain' are involved in other functions in cells like response to DNA damage and regulation of epigenetic modifications. It seems that the 'Tudor domain', in general,

facilitates protein-protein interactions and the assembly of macromolecular complexes. In this regard, it is known that the ‘Tudor domain’ interacts with methylated lysines or methylated arginines of it target proteins (Pek, Anand et al. 2012).

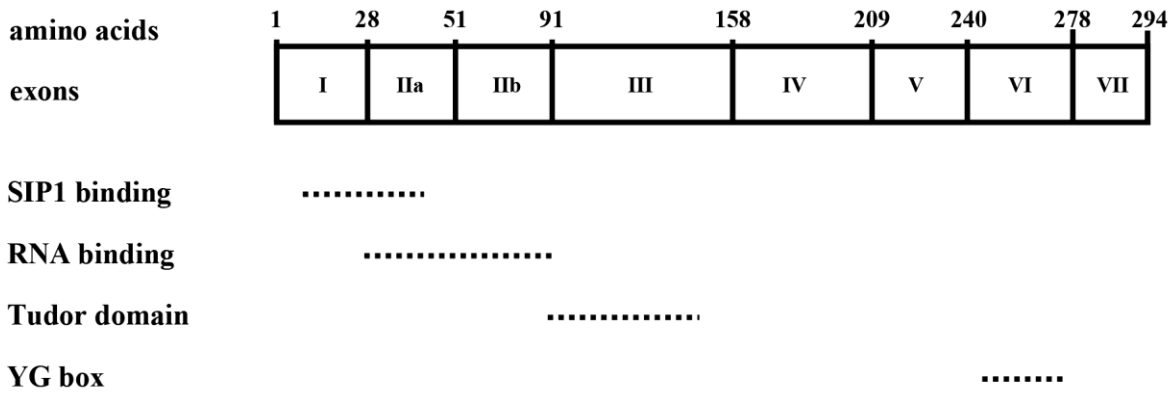

Figure 1.1. Domains of the SMN protein. SMN protein includes several domains and motifs which generally regulate its binding activities. The positions of domains on the protein sequence are shown by dashed lines. The "Tudor domain" of SMN mediates its interaction with Sm proteins. SMN also oligomerizes through it "YG box" domain. The figure is adapted from (Buhler, Raker et al. 1999).

Using heteronuclear multidimensional NMR spectroscopy, Selenko et al. solved the 3D structure of the 'Tudor domain' of SMN (Selenko, Sprangers et al. 2001). They showed that the 'Tudor domain' of SMN has a negatively charged surface which facilitates SMN binding to the positively charged C-terminus of Sm proteins. Interestingly the SMN E134K mutant isoform did not alter the conformation of the 'Tudor domain' of SMN but changed its surface charge, thus, interfering with its binding ability to Sm proteins (Selenko, Sprangers et al. 2001). In addition, posttranslational modifications of the C-terminus tails of Sm D1 and D3 (i.e. symmetrical dimethylation of arginine residues) may play a role in the regulation of interaction of SMN with these proteins (Selenko, Sprangers et al. 2001). Cote et al. showed that 'Tudor domains' of several proteins (including SMN, SPF30 and TDRD3) interact with symmetrical dimethylated arginines of arginine-glycine-rich motifs. They also showed that inhibition of this modification of core Sm proteins results in their cytoplasmic accumulation and inhibition of Sm core assembly (Cote and Richard 2005).

The C-terminus of SMN contains a highly conserved domain called the 'YG box' (correlating to amino acids 254 to 280 of human SMN). SMN oligomerizes through its 'YG box' and the mutations within this domain decrease the ability of SMN to oligomerize (Martin, Gupta et al. 2012, Praveen, Wen et al. 2014, Gupta, Martin et al. 2015).

Recently, Seng et al. solved the three dimensional structure of full length SMN protein (FL-SMN). Beside the known 'Tudor domain' (residues 97-148; exons 2-3), they identified a second 'Tudor domain' (residues 152-195, exons 3-4) in SMN. They found that despite the difference in the sequence, both of these 'Tudor domains' show very similar 3D structures. They also found that the 3D structure of Δ7-SMN is similar to FL-SMN. The authors concluded that Δ7-SMN may retain some activities of FL-SMN at very low levels (Seng, Magee et al. 2015).

Indeed, this is in accordance with previous observations that over-expression of Δ7-SMN extends the survival of a severe mouse model of SMA (Le, Pham et al. 2005). However, the lack of incomplete rescue of the phenotype by Δ7-SMN emphasises the essential role of the C-terminus region of SMN for its function (Burghes and Beattie 2009).

Mouse models of SMA

The discovery of the *Smn* gene made it possible to generate several mouse models of SMA. These models recapitulated a wide range of SMA phenotype severities in the mouse. So far, mouse models of SMA have made significant contributions to the understanding of the biology of *SMN* and pathogenesis of SMA, and for assessing new therapeutic approaches. Unlike human, mouse has one *Smn* gene and homozygous deletions of mouse *Smn* result in early embryonic lethality (Schrank, Gotz et al. 1997, Pellizzoni, Kataoka et al. 1998). However, heterozygous deletion of the *Smn* gene (i.e. $Smn^{+/-}$) does not produce any SMA phenotype in the mouse. And like human, mouse shows the SMA phenotype only when the SMN protein is reduced to the very low levels. (Jablonka, Schrank et al. 2000, Monani, Sendtner et al. 2000).

So far, two main approaches have been utilized to generate mouse models of SMA. In the first approach the mouse *Smn* gene is totally deactivated (i.e. it does not produce any FL-Smn protein) and then low copy numbers of the human *SMN2* gene and/or its variants are introduced into the mouse genome. In the absence of any mouse *Smn* function, exogenous human *SMN2* genes are responsible for the production of FL-SMN protein. Like SMA patients, in these models the amount of SMN protein produced by *SMN2* genes is enough for the animal to survive the embryonic period but the mouse undergoes pathologic changes soon after birth. This approach was used to generate ‘severe SMA’ and ‘delta 7 SMA’ mouse models (Monani, Sendtner et al.

2000, Le, Pham et al. 2005). The 'Taiwanese SMA' mouse model is another example of using this approach; these mice carry two alleles of the '*Δ7-Smn*' gene and two copies of *SMN2* genes (Hsieh-Li, Chang et al. 2000). Interestingly, the severity of the SMA phenotype is variable between the 'Taiwanese SMA' mouse model and the other two mentioned SMA mouse models, suggesting some functions for 'delta 7-SMN' protein. In the second approach, the mouse *Smn* gene is mutated in a way that produces very low levels of Smn protein. $Smn^{2B/-}$ mice and Smn^{C-T} mice are two examples of using this approach (Bowerman, Beauvais et al. 2010, Gladman, Bebee et al. 2010) . A thorough review of all of the existing mouse models of SMA is beyond the scope of this monograph (for more details please see (Bebee, Dominguez et al. 2012).

$Smn^{2B/-}$ mice

The Smn^{2B} allele was generated by introducing mutations in a splicing enhancer element within exon 7 of mouse *Smn*. It was shown that most of the products of this allele are devoid of exon 7, however it still produces low amounts of FL-Smn protein (DiDonato, Lorson et al. 2001). Mice that carry one Smn^{2B} allele and one *Smn* null allele (i.e. $Smn^{2B/-}$ mice) recapitulate SMA phenotypes including loss of motor neurons and atrophy of skeletal muscles. However, the disease in this model is less severe than 'severe SMA', 'delta7 SMA' and 'Taiwanese SMA' mouse models (Bowerman, Beauvais et al. 2010). Interestingly, $Smn^{2B/2B}$ mice show no SMA phenotype and have a normal life span. This model has contributed to solidify the theory of 'SMN threshold for the pathogenesis of SMA' (Bowerman, Murray et al. 2012).

Functions of SMN

Present in both vertebrates and invertebrates, *Smn* is a conserved gene across the animal kingdom. *Smn* orthologues have been found in some unicellular eukaryotes like *Saccharomyces*

pombe (Mier and Perez-Pulido 2012). In multi cellular organisms, *Smn* is ubiquitously expressed in all cell types and is critical for cell viability. This is believed to be due to the housekeeping functions that this gene executes within cells (Fischer, Liu et al. 1997, Liu, Fischer et al. 1997). During embryonic life, *SMN* is highly expressed in all cell types. However, after birth its expression decreases in most of the cell types (including skeletal and cardiac myofibers, fibroblasts and lymphocytes). In adults, the expression of *SMN* remains high in the central nervous system, liver and kidney (Coovert, Le et al. 1997). *SMN* is expressed in various regions of the central nervous system including layer V of the cortex, dentate gyrus of the hippocampus, thalamus, cerebellum and brainstem nuclei, but the highest expression of *SMN* is within the anterior horns of the spinal cord, where lower motor neurons reside (Battaglia, Princivalle et al. 1997, Bechade, Rostaing et al. 1999).

SMN protein is localized to both cytoplasm and nucleus of neurons. Most of the SMN protein is localized in the cytoplasm where it contributes to several essential functions like assembly of small nuclear ribonucleoproteins (snRNPs). SMN shows a speckled pattern distribution within the cytoplasm (Bechade, Rostaing et al. 1999). SMN is imported to the nucleus along with newly assembled snRNPs. In the nucleus, while snRNPs accumulate in Cajal bodies (CB) for further processing (Sleeman and Lamond 1999), SMN is accumulated in structures called gems (Gemini of coiled bodies). These structures are in close association with coil bodies (CBs) and resemble them in number (2-6) and size (0.1-1.0 microns). Coilin, one of the main markers of the CBs, contains symmetrically dimethylated arginines (sDMA) (Hebert, Shpargel et al. 2002). This modification mediates Coilin interaction with SMN and proper colocalization of gems and CBs (Clelland, Kinnear et al. 2009). The degree of colocalization of CBs and gems is variable during different stages of development and among different cells types.

Indeed, gems and CBs do not exist in all cell types in adults, but are present in all tissues during the embryonic period. In contrast to the other cell types, the number of gems/CBs within nuclei of motor neurons is higher in adults than embryos and the highest degree of colocalization of gems with CBs is also seen in mature lower motor neurons. Indeed, these two sub-nuclear compartments are not sometimes distinguishable from each other in mature motor neurons (Liu and Dreyfuss 1996, Young, Le et al. 2001). SMN is also localized to the nucleolus in some developing tissues suggesting a nucleolar role for SMN (Young, Le et al. 2001).

So far, several functions have been described for SMN:

1- Biogenesis of small nuclear ribonucleoproteins (snRNPs)
2- Assembly of other ribonucleoproteins (RNPs)
3- Regulation of gene transcription and translation
4- Inhibition of apoptosis

The role of SMN in biogenesis of small nuclear ribonucleoproteins (snRNPs)

pre-mRNAs of eukaryotic cells contain both exons and introns. And before entering the translation stage, they need to be edited through a highly coordinated process called RNA splicing (Konkel, Tilghman et al. 1978, Rabbitts 1978). RNA splicing is catalyzed inside the nucleus by macromolecules called small nuclear ribonucleoproteins (snRNPs) (Liautard, Sri Widada et al. 1981, Yang, Lerner et al. 1981, Steitz, Berg et al. 1982). Each snRNP complex contains one or two of the major snRNA molecules (e.g. U1, U2, U4, and U5). Each snRNA molecule binds to a set of seven RNA-binding proteins (including SmB/B′, SmD1, SmD2, SmD3, SmE, SmF, and SmG). This heptamer protein complex, also called the 'Sm core', is a very stable structure and has a very slow turnover. Since pre-mRNA splicing is an essential component for cell viability, biogenesis of snRNPs is considered as a housekeeping function in cells.

Indeed, it has been known for a long time that snRNPs are assembled in the cytoplasm before their translocation to the nucleus (Nyman, Hallman et al. 1986). But, it was only after the discovery of SMN that the details of snRNP assembly were revealed in detail. Briefly, after being transcribed in the nucleus, snRNAs are exported to the cytoplasm by PHAX (Ohno, Segref et al. 2000, Segref, Mattaj et al. 2001). Here, the SMN complex mediates the proper assembly of Sm core onto the Sm site of each snRNA (Kambach, Walke et al. 1999, Kambach, Walke et al. 1999). Each SMN complex consists of a SMN dimer and Gemin proteins (i.e. Gemin2-8) (Liu and Dreyfuss 1996, Liu, Fischer et al. 1997, Pellizzoni, Kataoka et al. 1998, Pellizzoni, Yong et al. 2002). SMN binds directly to methylated arginine tails of SmB/B′, SmD1, and SmD3 through its 'Tudor domain' (Friesen, Massenet et al. 2001). Sm core is transferred from the SMN complex to snRNAs in an ATP-dependent manner, and the 5′ cap of snRNP is hypermethylated. Together with the SMN complex, mature snRNPs are imported to the nucleus by snurportin and

beta importin to be integrated into the spliceosomal machinery (Plessel, Fischer et al. 1994, Raker, Plessel et al. 1996, Lauber, Plessel et al. 1997, Plessel, Luhrmann et al. 1997). The SMN complex also has an important role in ensuring that the Sm core is assembled onto the right snRNA (Pellizzoni, Yong et al. 2002).

SMN interacts with Sm proteins through its 'Tudor domain' and a clinically known point mutation within this domain decreases the affinity of SMN for Sm proteins, which might contribute to the pathogenesis of SMA (Buhler, Raker et al. 1999). Indeed, the assembly of snRNP complexes is severely impaired in SMN deficient cells and animals (Gabanella, Butchbach et al. 2007). However, it is suggested that the low levels of SMN only affects the biogenesis of a subset of snRNPs (Gabanella, Butchbach et al. 2007, Zhang, Lotti et al. 2008).

The role of SMN in assembly of ribonucleoproteins (RNPs)

Ribonucleoproteins (RNPs) are important RNA/protein complexes, which contribute to many aspects of cell biology. Considering the vast variety of both RNA molecules and RNA-binding proteins, the appropriate assembly of RNPs is of extreme importance. It is proposed that in addition to the spliceosomal snRNPs, SMN complexes play crucial roles in the assembly of some other RNPs like small nucleolar RNPs (snoRNPs) and RNA helicase A (RHA). RHA is involved in the transcription machinery, so it seems that SMN also plays a role in the regulation of gene transcription through this mechanism (Battle, Kasim et al. 2006). SMN also interacts with some heterogeneous nuclear ribonucleoproteins (hnRNPs). The hnRNP proteins are a family of proteins that play important roles in various steps of mRNA processing like pre-mRNA splicing, mRNA transport and mRNA translation, stability and degradation (Mourelatos, Abel et al. 2001).

The role of SMN in transcription and translation

It is reported that SMN has several roles in the regulation of gene transcription and translation. Strasswimmer et al. (1999) reported that SMN interacts with the nuclear transcription activator 'E2' of papillomavirus *in vitro* and *in vivo*. Overexpression of *SMN* increased E2-dependent transcriptional activity, while the mutant forms of SMN decreased E2 gene activity (Strasswimmer, Lorson et al. 1999). Using an *in vitro* translation system, Sanchez et al. (2013) showed that SMN interacts with ribosomes and represses their translational activity. Specifically, it was shown that the translation of CARM1 (an arginine methyltransferase enzyme) is regulated by SMN. CARM1 is upregulated in spinal cords of SMA mouse models and also cells isolated from SMA patients (Sanchez, Dury et al. 2013). A recent study also showed that SMN might have a role in the assembly of translational platforms associated with plasma membranes of fibroblasts. SMN is localized and interacts with caveolin-1, a membrane protein which mediates the anchoring of translation machinery to the cell membrane. Depletion of SMN resulted in reduction of membrane associated ribosomes and the failure of cultured fibroblasts to extend membrane protrusions (Gabanella, Pisani et al. 2016).

The role of SMN in inhibition of apoptosis

Both *in vitro* and *in vivo* studies have shown that SMN protects neurons from the apoptosis induced by viral infection. On the other hand, it has been suggested that two common mutant isoforms of SMN (including delta-7 SMN and SMN-Y272C) own proapoptotic activity (Kerr, Nery et al. 2000).

Motor neuron specific functions of SMN

It has been proposed that in motor neurons, SMN has several functions independent of snRNPs biogenesis. These functions include cell migration and differentiation, axonal growth,

and, maturation and maintenance of neuromuscular junctions (NMJs) (McWhorter, Monani et al. 2003, Briese, Esmaeili et al. 2005, Carrel, McWhorter et al. 2006, Giavazzi, Setola et al. 2006, Setola, Terao et al. 2007).

In primary cultures of motor neurons, SMN is present in several regions of the cytoplasm including outer nuclear pores, polyribosome complexes, axons, dendrites and growth cones (Fan and Simard 2002, Zhang, Xing et al. 2006). Within these areas, SMN is localized to granules containing Gemin proteins (but not any Sm proteins); live cell imaging has shown that SMN is actively transported to processes and growth cones along these granules (Zhang, Xing et al. 2006). Electron microscopy examination of mouse spinal cord also showed that SMN protein is present within processes of motor neurons *in vivo* (Pagliardini, Giavazzi et al. 2000).

It has also been showed that in motor neurons, SMN interacts with several mRNA binding proteins (mRBPs) including hnRNP R, KSRP, IMP1 and HuD. Some scientists proposed that these interactions are critical for the appropriate assembly of these mRBPs with their specific target mRNAs, and the axonal transport of these mRNAs. Depletion of SMN in motor neurons results in significant reduction of mRNA levels within their axonal projections (Rossoll, Kroning et al. 2002, Tadesse, Deschenes-Furry et al. 2008, Akten, Kye et al. 2011, Fallini, Zhang et al. 2011, Hubers, Valderrama-Carvajal et al. 2011). In accordance with this, cultured motor neurons isolated from a SMA mouse model have smaller growth cones and shorter processes, although do have normal survival (Rossoll, Jablonka et al. 2003, Zhang, Xing et al. 2006).

Regulation of actin is believed to be another motor neuron specific function of SMN. It has been shown that in neurons, *β-actin* mRNA is actively transported to processes and growth cones and its local translation within these areas is necessary for axonal outgrowth and synaptic differentiation and maintenance (Yao, Sasaki et al. 2006, Vogelaar, Gervasi et al. 2009,

Donnelly, Park et al. 2013). There are reports that in motor neurons, SMN mediates transport of *β-actin* mRNAs into distal axons and growth cones. It is also shown that some carriers of *β-actin* mRNA (e.g. hnRNP-R) interact with SMN protein. Suppression of hnRNP-R reduces the levels of *β-actin* mRNA in growth cones of cultured motor neurons and results in shorter axons (Rossoll, Kroning et al. 2002, Dombert, Sivadasan et al. 2014). Also in neurons, SMN interacts with profilin II, an actin-binding protein with a crucial role in actin dynamics. In spinal cord, the highest expression of profillin II is in the anterior horn regions (Giesemann, Rathke-Hartlieb et al. 1999, Sharma, Lambrechts et al. 2005).

Pathologic alterations due to depletion of SMN

Complete deletion of SMN from cells compromises their viability. Also, knocking out the *Smn* gene in mice is embryonically lethal. Several groups have conducted a tissue specific knock out of *Smn* to look at the consequences of selective SMN deletion in different tissues like skeletal muscles, CNS or liver. They showed that the total abolition of full length SMN in any of these tissues results in massive cell death (Frugier, Tiziano et al. 2000, Cifuentes-Diaz, Frugier et al. 2001, Vitte, Davoult et al. 2004). On the other hand, the depletion of SMN to very low levels is not lethal but results in SMA phenotype in human and other animals. The amount of FL-SMN in fibroblasts isolated from SMA patients is moderately decreased and inversely correlates with the severity of SMA. Also, the number of gems is significantly reduced in fibroblasts isolated from SMA patients, and the number of gems also correlates inversely with the severity of SMA. It is reported that the levels of FL-SMN is about 10-fold reduced in spinal cords of SMA patients (Coovert, Le et al. 1997). It is believed that a level of 20-25% of FL-SMN is a critical threshold for the development of the SMA phenotype in human and mouse (Simic, Mladinov et al. 2008,

Bowerman, Murray et al. 2012). In accordance with these observations, introducing at least two copies of the *SMN2* gene to *Smn* knockout mice rescues them from embryonic lethality. These mice show severe SMA phenotype if the *SMN2* copy numbers is low, and mild or no phenotype if the *SMN2* copy numbers are high. (Monani, Sendtner et al. 2000).

The main question here is how the insufficiency of such an important housekeeping protein results in a disease with dominant neuromuscular pathologies. Some scientists proposed that there is a cell specific requirement for SMN protein (Park, Maeno-Hikichi et al. 2010). Indeed, targeted depletion of FL-SMN in motor neurons showed that it is sufficient to reproduce a SMA like disorder in mouse, however, with a less severe phenotype than universal depletion of FL-SMN. (Park, Maeno-Hikichi et al. 2010). In a reciprocal study, the restoration of FL-SMN just in motor neurons of a mouse model of SMA improved the number and function of motor units, but was not enough to prolong the life span of the affected animals. Interestingly, replacement of FL-SMN in both motor neurons and glial cells in these mice improved their survival dramatically (McGovern, Iyer et al. 2015). So it seems that although motor neurons are primary targets of SMN deficiency, the involvement of other cell types also contribute to the severity of the SMA phenotype.

An important issue in SMA is to find which functions of SMN are impaired. Based on the different functions of SMN, two major theories have emerged for SMA pathogenesis. The first theory relies on the function of SMN in the assembly of spliceosomal machinery and claims that SMA is a general splicing disease which involves not only motor neurons but also other tissues. In accordance to this theory, it is shown that severe depletion of SMN in mouse results in pathologic reduction of the repertoire of snRNAs and widespread disruption of mRNA editing in several tissues beside motor neurons. Gabanella et al. found that the expression levels of Gemin

proteins and the snRNP assembly activity were severely impaired in the spinal cords of severe SMA mice. They showed that both Gemin proteins levels and snRNP assembly activity correlated inversely with the severity of phenotype in spinal cords of different mouse models of SMA. snRNP assembly activity was also affected in other tissues but to a lower extent (Gabanella, Butchbach et al. 2007). It is postulated that due to the large size of motor neurons and their high demand of energy these cells are among the most susceptible cells to these pathologic changes (Pellizzoni, Yong et al. 2002, Wan, Battle et al. 2005, Winkler, Eggert et al. 2005, Gabanella, Butchbach et al. 2007, Zhang, Lotti et al. 2008). The major pitfall for this theory is the fact that only a few mis-splicing events have been reported so far in SMA.

The second theory proposes that beside the role in snRNP assembly, SMN also has tissue-specific functions. Based on this theory, the susceptibility of certain cell types to low levels of SMN comes from the compromise of biologic processes which depend heavily on cell specific functions of SMN. This theory is supported by the localization of SMN to other RNPs within the cytoplasm and neurites of motor neurons (Fan and Simard 2002, McWhorter, Monani et al. 2003, Rossoll, Jablonka et al. 2003, Carrel, McWhorter et al. 2006). Based on this theory, low levels of SMN leads to impaired neurite outgrowth and synaptogenesis of motor neurons. These conditions inhibit the full differentiation of MNs and their integration into their natural circuits. The undifferentiated MNs will continue to migrate ectopically. The ectopic MNs activate astrocytes and they form glial bundles within ventral roots of spinal cord (Simic 2008, Simic, Mladinov et al. 2008).

As it was mentioned before, most of the products of *SMN2* gene are translated to SMN protein lacking exon 7 (i.e. Δ7-SMN). Some scientists debated if this isoform of SMN has any contribution to the pathologies observed in SMA. Indeed, it is shown that Δ7-SMN is an unstable

protein (Le, Coovert et al. 2000). Also, Δ7-SMN does not function as a dominant-negative protein for FL-SMN since it is able to form gems, though at much lower rates (in contrast to Δ7-SMN, SMN lacking both exon 5 and 7 is not able to form gems) (Le, Coovert et al. 2000). In addition, mice carrying high copy numbers of the *SMN2* gene, and therefore producing high amounts of Δ7-SMN, show no obvious pathology (Monani, Sendtner et al. 2000).

Pathologic changes of motor units in SMA

A motor unit consists of a lower motor neuron and the myofibers innervated by that motor neuron. Pathologic changes involving motor units (including degeneration of motor neurons and atrophy of skeletal muscles) are the hallmarks of SMA (Bromberg and Swoboda 2002).

Post-mortem examination of SMA patients shows extensive pathologic changes within anterior horns of their spinal cords. The pathologic changes of spinal cord in SMA were described first by Guido Werdnig (1891) as a 'neuropathologic tetrad' including: 1) loss of motor neurons, 2) empty cell beds within ventral horn regions of spinal cord, 3) formation of glial bundles within ventral roots of spinal cord, and 4) heterotopic motor neurons. As it can be postulated from the symmetrical involvement of skeletal muscles, the motor neuron loss in SMA patients happens within both ventral horns of the spinal cord. The majority of surviving motor neurons show abnormal morphology (e.g. chromatolytic morphology) and localization (e.g. heterotopic MNs with no neurite extensions), some motor neurons have a necrotic or apoptotic appearance (about 2-3% of remaining MNs). And, only 10-20% of motor neurons (depending on the severity of the disease) show normal morphology and localization in SMA patients (Simic, Mladinov et al. 2008).

Weakness and atrophy of skeletal muscles are the major clinical findings in the examinations of SMA patients. Increasing evidence is pointing out that beside degeneration of motor neurons, intrinsic defects also aggravate the pathologic changes of skeletal muscles in the course of SMA. For example, depletion of SMN in differentiating C2C12 myoblasts resulted in decreased proliferation and abnormal fusion of these cells (Shafey, Cote et al. 2005). Cultured myoblasts isolated from SMA patients or myoblasts isolated from *Smn*$^{2B/-}$ mice showed significant reduction in the levels of myogenic regulatory factors under normal and differentiating conditions (Arnold, Gueye et al. 2004, Boyer, Deguise et al. 2014).

Several studies have reported a delayed myogenic program and increased immature myofibers in different mouse models of SMA (Martinez-Hernandez, Soler-Botija et al. 2009, Dachs, Hereu et al. 2011, Lee, Mikesh et al. 2011, Boyer, Deguise et al. 2014). For example it is shown that embryonic isoforms of myosin heavy chain (MHC) and acetylcholine receptor (AChR) are aberrantly expressed after birth in skeletal muscles of the 'delta 7 SMA' mice (Kong, Wang et al. 2009, Lee, Mikesh et al. 2011). Altogether, it seems that the development of skeletal muscles is impaired during the course of SMA.

There is also some evidence that mature myofibers might be affected by the lower levels of SMN in a cell autonomous manner (Rajendra, Gonsalvez et al. 2007, Walker, Rajendra et al. 2008). It is shown that in the normal skeletal and cardiac myofibers, the SMN complex including SMN, Gemins and Unrip (but not Sm proteins) are localised to the Z-discs in skeletal and cardiac muscle (Walker, Rajendra et al. 2008). In addition, SMN also interacts with α-actinin and contributes to stabilization of actin filaments in myofibers (Rajendra, Gonsalvez et al. 2007). In accordance with these findings, skeletal muscles from mouse models of SMA show pathologic defects involving Z-disc structure and function (Walker, Rajendra et al. 2008).

Using the cre-loxP system, Cifuentes-Diaz et al. deleted exon 7 of mouse *Smn* gene specifically in the skeletal myofibers (Cifuentes-Diaz, Frugier et al. 2001). The $Smn^{\Delta 7/\Delta 7}$ mice showed a muscle dystrophy phenotype, paralysis and died prematurely. In another study, Martinez et al. restored mouse *Smn* function specifically in skeletal myofibers of 'delta 7 SMA' mice. They observed significant improvement in survival, weight gain, and motor behavior (but not the number of motor neurons) of these mice. The authors concluded that SMN might own some cell specific functions within skeletal myofibers which are impaired in SMA (Martinez, Kong et al. 2012). In one study, Iyer et al. deleted both alleles of the *Smn* gene selectively in skeletal muscles of mice which carry two alleles of human *SMN2*. The authors did not observe any pathologic change within skeletal muscles of these mice. However, their approach was capable of decreasing FL-SMN about 70% in skeletal muscles (Iyer, McGovern et al. 2015). So, it seems that the remaining FL-SMN protein (about 30%) is above the threshold required for induction of any pathology in skeletal myofibers. It would have been a good idea if the authors had repeated their observations using mice which carry only one allele of human *SMN2* and had investigated if the amount of FL-SMN protein produced by only one *SMN2* gene is still enough to prevent pathology in myofibers lacking the functional *Smn* gene.

Pathologic changes of neuromuscular junctions (NMJs) in SMA

The original descriptions of the pathologic changes in SMA (i.e. degeneration of motor neurons and atrophy of skeletal muscles) were mainly based on the examinations which were carried out on the post-mortem samples. After the discovery of *SMN* genes and especially with the generation of animal models of SMA, scientists could investigate pathologic events at earlier stages of the disease (Table 1.2).

In different mouse models of SMA, it is shown that neuromuscular junctions (NMJs) are developed normally during the embryonic period. After birth and before any obvious pathologic change within the skeletal muscles or spinal cords of these mice, several pathologic changes occur within their NMJs. Also, the degree of the NMJ pathology increases with the progress of the SMA phenotype in these mice (McGovern, Gavrilina et al. 2008, Murray, Lee et al. 2010). In a chronological order, these pathologic changes include accumulation of neurofilaments within pre-synaptic areas of NMJs, reduced size and delayed maturation of motor endplates (MEPs), and at the end stages of the disease, denervation and degeneration of MEPs (Murray, Lee et al. 2010). In addition, axonal projections of motor neurons undergo degenerative changes before degeneration of lower motor neurons themselves (Cifuentes-Diaz, Frugier et al. 2001). These observations confirm that SMA is a neurodegenerative disorder characterized by progressive degeneration of NMJs and consequent denervation of skeletal myofibers (Murray, Comley et al. 2008).

Also, electrophysiological studies revealed several functional abnormalities in NMJs before the onset of the SMA phenotype in mouse. These pathologies include decreased evoked endplate currents (EPCs), reduced quantal content (QC), and decreased probability of vesicle release (Kong, Wang et al. 2009). Other abnormalities within NMJs include reduced number of mitochondria, and abnormal calcium homeostasis (Torres-Benito, Neher et al. 2011). Also, postsynaptic areas of NMJs show some abnormalities in mouse models of SMA. These abnormalities include delayed switch of the fetal acetylcholine receptor (gamma subunit) to the adult AChR isoform (epsilon subunit) and reduced size and abnormal organization of AChR clusters (Kong, Wang et al. 2009, Torres-Benito, Neher et al. 2011). Similar pathologic changes

of NMJs were also obserevd in a Drosophila model of SMA (Chan, Miguel-Aliaga et al. 2003, Timmerman and Sanyal 2012).

Pathologic involvement of NMJs is also reported during pre-symptomatic stages of SMA in human. Martínez-Hernández et al. studied samples of human embryos which were aborted due to discovery of homozygote *SMN1* mutations in prenatal genetic tests. They observed several NMJ pathologic changes including accumulation of neurofilaments and aberrant vesicles within motor nerve terminals. These changes were only present in the embryos with low copy numbers of the *SMN2* gene. The authors concluded that in severe forms of SMA, the pathologic changes of NMJs start during embryonic life (Martinez-Hernandez, Soler-Botija et al. 2009, Martinez-Hernandez, Bernal et al. 2013).

Based on this evidence, some researchers suggest that SMA is a synaptopathy in nature, and SMN is critical for normal homeostasis and function of neuromuscular junctions (Donlin-Asp, Bassell et al. 2016). It is worth noting that SMN protein is shown to be localized to the axonal end terminals of cultured motor neurons (Pagliardini, Giavazzi et al. 2000, Jablonka, Bandilla et al. 2001). Some researchers also proposed that the maintenance of NMJs is impaired in SMA mice due to defective axonal transport (Jablonka, Wiese et al. 2004). In support of this, it has been shown that the levels of polymerized tubulin are reduced in sciatic nerves from a mouse model of SMA (Wen, Lin et al. 2010).

Type of pathology	embryonic	pre-symptomatic	early symptomatic	late symptomatic
accumulation of neurofilaments	-	+/-	+	++
reduced size of motor endplates	-	-	+	++
denervation	-	-	+/-	+

Table 1.2. Pathologic changes of neuromuscular junctions in SMA.

NMJs show several degenerative changes during the course of SMA. The severity of NMJs' pathologic changes increases as the disease progresses. The table is based on the results of the study on 'delta7 SMA' mice by Murray et al. (2008).

Pathologic changes of central synapses in SMA

There is convincing evidence that central nervous system tissues and especially central synapses are affected during the course of SMA. Extensive muscle weakness and atrophy are the main findings in SMA; these symptoms were initially assumed to happen due to widespread denervation of NMJs. However, further studies showed that (at least in mouse models of SMA) most NMJs remain innervated until the very end stages of the disease (Kong, Wang et al. 2009). To justify the severity of muscle atrophy and weakness in SMA, some researchers proposed that beside the function of NMJs, the neural circuits are also compromised within the central nervous system (Ling, Lin et al. 2010). Neural circuits within the spinal cord govern the performance of motor neurons extensively. Indeed, motor neurons like any other type of neurons are parts of complex neural networks within the central nervous system and receive massive inputs from spinal neural circuits, descending pathways, and sensory neurons.

Impairments of sensory-motor circuits have been reported in spinal cords of ‘delta 7 SMA’ mice. It is shown that excitatory synaptic inputs onto lower motor neurons are significantly reduced in these mice. Interestingly, this phenomenon occurs in a period prior to any motor neuron loss in these mice (Ling, Lin et al. 2010, Mentis, Blivis et al. 2011). In one study, selective depletion of SMN in motor neurons also resulted in reduction of sensory inputs on them (Park, Maeno-Hikichi et al. 2010).

Some studies also proposed the involvement of brain in SMA. *Smn* is highly expressed in central nervous system tissues of mouse embryo. After birth, the expression of *Smn* remains high in several regions of the mouse brain (e.g. hippocampus and retina). It is reported that the overall neuronal population is reduced within some areas of the brain in severe SMA mice (Liu, Shafey et al. 2010, Wishart, Huang et al. 2010, Liu, Beauvais et al. 2011). Liu et al. reported that severe *Smn* depletion in mouse leads to cell death and pathological foci within its telencephalon during

development (Liu, Shafey et al. 2010). Also, several pathologic changes within the retina and optic nerve have been reported in these mice (including abnormal synaptogenesis and neurofilament accumulation within the neurites of retinal neurons) (Liu, Beauvais et al. 2011). Wishart et al. reported impaired neurogenesis and reduced cell density within the hippocampus of the 'severe SMA' mice. Proteomic analysis on the hippocampus of these mice revealed extensive alterations in the levels of proteins regulating cellular proliferation, migration and development (Wishart, Huang et al. 2010). In a follow up study, the same experiment was repeated on the synaptosome fractions isolated from hippocampus of 'severe SMA' mice. The results showed that synapses within hippocampus of SMA mouse undergo molecular alterations at a pre-symptomatic period (Wishart, Mutsaers et al. 2014).

Despite the above mentioned findings in mouse, little attention has been paid to pathologic changes of the brain in SMA patients. In one study, a 6 year old girl affected by type I SMA had some lesions within her thalamus accompanied with widespread abnormal patterns in her electroencephalography (EEG) (Ito, Kumada et al. 2004). Also, post-mortem examination of brains of type I SMA patients revealed degenerative lesions within the lateral formation of their thalami (Shishikura, Hara et al. 1983).

Pathologic changes of peripheral neuronal tissues in SMA

Deficits of peripheral sensory nerves are reported in SMA patients (Rudnik-Schoneborn, Goebel et al. 2003). Recently, Yonekawa et al. examined peripheral nerve conduction in patients with confirmed SMA. The authors showed that sensory nerve conduction velocities (SCVs) are decreased in some type I SMA patients, but no sensory deficit was observed in SMA type II patients (Yonekawa, Komaki et al. 2013).

There are also reports showing that the enteric nervous system (ENS) is also impaired in mouse models of SMA; this probably explains some of the gastrointestinal complications of SMA patients (Gombash, Cowley et al. 2015).

Pathologic changes of non-neuronal tissues in SMA

There is increasing evidence that non-neural tissues are also affected by the depletion of SMN (including heart, pancreas, liver, spleen, intestine, lungs and blood vessels). Indeed, in SMA, the involvement of other systems (in addition to the neuromuscular system) may contribute to the severity of the disease. Based on these observations, scientists now postulate that SMA is indeed a multisystem disorder (Liu, Shafey et al. 2010, Shababi, Habibi et al. 2010, Wishart, Huang et al. 2010, Hua, Sahashi et al. 2011, Liu, Beauvais et al. 2011, Bowerman, Swoboda et al. 2012, Shababi, Habibi et al. 2012, Somers, Stencel et al. 2012, Schreml, Riessland et al. 2013, Bowerman, Michalski et al. 2014, Deguise, De Repentigny et al. 2017).

Signalling pathways affected in SMA

After more than two decades since the discovery of the *SMN* gene, it is still not known which defective signalling pathways and impaired cellular functions cause SMA. Though SMN is well known for its function in the biogenesis of RNA splicing machinery, only few mis-splicing events have been reported so far in the context of SMA disease. On the other hand, it seems that pathways that are not directly involved in RNA splicing and metabolism are affected widely in the course of the disease. Some examples are pathways involved in actin dynamics (Giesemann, Rathke-Hartlieb et al. 1999, Bowerman, Shafey et al. 2007, Oprea, Krober et al. 2008, Stratigopoulos, Lanzano et al. 2010, Bernal, Also-Rallo et al. 2011, Nolle, Zeug et al. 2011, Caraballo-Miralles, Cardona-Rossinyol et al. 2012, Hao le, Wolman et al. 2012), PTEN/PI3K/AKT pathway (Ning, Drepper et al. 2010) and the ubiquitin–proteasome system

(UPS) (Aghamaleky Sarvestany, Hunter et al. 2014, Powis, Mutsaers et al. 2014, Wishart, Mutsaers et al. 2014). Also, there are some SMA related disorders that occur due to mutations in genes which do not have any known role in RNA metabolism. These include congenital autosomal dominant SMA due to mutations in the *Bicadual D2* (*BICD2*) gene, and X-linked infantile SMA due to mutations in the *ubiquitin-like modifier activating enzyme 1*(*UBA1*) gene (Ramser, Ahearn et al. 2008, Neveling, Martinez-Carrera et al. 2013).

It seems that several proteins involved in actin dynamics are affected by the depletion of SMN. SMN protein has several proline-rich motifs within its C-terminus regions. These types of motifs are known to interact with profilin proteins (Reinhard, Giehl et al. 1995). Profilins are small proteins which regulate the polymerisation of actin (Carlsson, Nystrom et al. 1977). Giesemann et al. showed that SMN interacts with profilin IIa (a neuron specific isoform of profilin) in both the cytoplasm and the nucleus of motor neurons (Giesemann, Rathke-Hartlieb et al. 1999). Bowerman et al. also observed that SMN depletion in cultured PC12 cells resulted in an increase in expression and also availability of profilin IIa. The authors also showed that the higher activity of profilin IIa mediates the aberrant activation of the Rho/Rho kinase (ROCK) pathway, which results in defective actin dynamics and impaired neuritogenesis (Bowerman, Shafey et al. 2007). In a follow up study, the same group showed increased expression of profilin IIa in $Smn^{2B/-}$ mice. Interestingly, the expression of Plastin 3 was upregulated upon deletion of profilin II in these mice (Bowerman, Anderson et al. 2009). The authors concluded that in SMA, actin dynamics is probably perturbed in all neurons; however due to possession of big synapses, motor neurons are among the most sensitive neurons to SMN depletion (Bowerman, Anderson et al. 2009).

Wishart et al. conducted proteomics analysis on the synaptosome fractions prepared from hippocampus of 'severe SMA' mice at PND1 (i.e. within a pre-symptomatic period) (Wishart, Mutsaers et al. 2014). The authors reported that 52 out of 150 proteins identified in mass spectrometry (MS) were differentially induced in synaptosome fractions from 'severe SMA' mice (with more than 20% change). Functional clustering analyses revealed that several canonical pathways are perturbed in these mice including oxidative phosphorylation, protein ubiquitination, glycolysis and gluconeogenesis, purine metabolism and PI3K/AKT signaling. The authors further showed that splicing of *UBA1* pre-mRNA is dysregulated in 'severe SMA' mice resulting in low levels of UBA1 and subsequent accumulation of beta catenin as a downstream target of UBA1. Interestingly, the pharmaceutical inhibition of beta catenin rescued the SMA phenotype in a zebrafish model of SMA (Wishart, Mutsaers et al. 2014).

Effect of genetic background on the severity of SMA phenotype

It is not unusual that some patients with neuromuscular disorders (NMDs) share the same genetic mutations but present with different ages at onset, severity of the disease, and clinical manifestations. For example, several cases of 'discordant NMD families' (i.e. siblings who share an identical genetic mutation but show variable neuromuscular phenotypes) have been reported so far (Novelli, Gennarelli et al. 1995, Cudkowicz, McKenna-Yasek et al. 1997, Al-Chalabi, Andersen et al. 1998, Zatz, Vainzof et al. 2000, Michaelides, Chen et al. 2007, Felbecker, Camu et al. 2010, Kalman, Leonard et al. 2011, Vainzof, Feitosa et al. 2016). There are also some rare reports of some siblings of NMD patients who carry the same NMD causative mutation but show no neuromuscular phenotype during their life (Al-Chalabi, Andersen et al. 1998, Oprea, Krober et al. 2008). Studying discordant NMD families, scientists provided evidence that minor genetic

differences among children of these families are most probably responsible for variability in their NMD phenotypes (Lupski, Garcia et al. 1991, Tawil, Storvick et al. 1993, Abbadi, Philippe et al. 1994, Oprea, Krober et al. 2008). For example, there have been several cases of female monozygotic twins who showed discordant clinical manifestations of Duchenne muscular dystrophy due to the inactivation of opposite X-chromosome (Richards, Watkins et al. 1990). Some studies also suggested chromosomal rearrangement events as the reason for discordance of clinical manifestations in twins with genetic forms of muscular dystrophies (Tawil, Storvick et al. 1993). Also, in some SMA discordant families, female siblings do not show any SMA phenotype despite having the same *SMN1/SMN2* genotype. It has been shown that an X-chromosome related gene (Plastin 3) modifies the SMA phenotype in these cases (Oprea, Krober et al. 2008).

Generation of animal models of NMDs in different genetic backgrounds confirmed the above mentioned observations. It has been shown that when a known NMD genetic mutation is introduced to different mouse genetic strains, it results in different phenotypic outcomes (Table 1.3) (Monani, Sendtner et al. 2000, Heiman-Patterson, Deitch et al. 2005, Le, Pham et al. 2005, Heiman-Patterson, Sher et al. 2011, Hatzipetros, Bogdanik et al. 2014, Coley, Bogdanik et al. 2016). In one study, Heimann-Patterson et al. (2011), introduced a clinically relevant mutant of *human superoxide dismutase 1* gene (i.e. *G93A-hSOD1Tg*) into several strains of mice and showed the survival of the transgenic mice varies among different strains (Heiman-Patterson, Sher et al. 2011). Similar observations have been reported for mouse models of SMA (Table 1.4). When generating the 'severe SMA' mouse model, Monani et al. found that all of the 'severe SMA' pups with a BL6 background die before birth. On the other hand, 'severe SMA' mice with a FVB background showed a median survival of 5 days. Le et al. also reported that about 50% of

‘delta7’ pups with a BL6 background die before birth, while ‘delta 7 SMA’ pups with the FVB background have a median survival of 10 days. Surprisingly, ‘Taiwanese model’ mice showed a longer survival in BL6 background than FVB background. It is not clear how ‘Taiwanese model’ mice behave differently from ‘severe SMA’ and ‘delta7 SMA’ mice in BL6 and FVB genetic backgrounds; however, the different type of mutation introduced in mouse *Smn* in these animal models could be a potential explanation.

Disease	Mouse model	Strains with shorter survival	Strains with longer survival
ALS	G93A-hSOD1Tg	BL6, BL10, BALB/c	ALR, SJL or C3H
Muscular Dystrophy	γ-sarcoglycan KO	129T2/SvEmsJ	DBA/2J
Duchenne Muscular Dystrophy	*mdx*	C57BL/10ScSn	DBA/2J

Table 1.3. The effect of genetic background on the severity of neuromuscular disorders. Generation of NMD models in different strains of mouse results in different phenotype severity. The table is based on the studies by Heiman-Patterson et al. (2011), Heydemann, et al. (2005), Coley, et al. (2015).

SMA mouse model	median survival in BL6 background	median survival in FVB background	genotype
Severe SMA	all die before birth	5 days	*Smn*$^{-/-}$, tg*SMN2*
delta7 SMA	1 day	10 days	*Smn*$^{-/-}$, tg*SMN2*, tg*Δ7SMN2*
Taiwanese	15 days	10 days	*Smn*$^{\Delta 7/\Delta 7}$, tg*SMN2*

Table 1.4. The effect of genetic background in the severity of spinal muscular atrophy. Generation of different models of SMA in different strains of mouse results in different phenotype severity. The table is based on the studies by Monani et al. (2000), Le, et al. (2005), Ackermann, et al. (2013).

Modifier genes of SMA phenotype

A modifier gene alters the phenotypic outcome of a disorder caused by a primary mutation in another gene. Modifier genes might change any aspect of the primary genetic disease including the age at onset, survival, severity and clinical manifestations (Wirth, Garbes et al. 2013, Lamar and McNally 2014). Some modifier genes may act on several NMDs. For example, *PGC1 alpha* can modify ALS, Parkinson's and Huntington's disease (Eschbach, Schwalenstocker et al. 2013, Weydt, Soyal et al. 2014). This shows that different types of NMDs share common molecular pathways, and that these pathways could be targeted to develop new therapeutic strategies. The modifier genes can also be used as biomarkers for the prognosis of NMDs and also for the prediction of a patient's response to medical treatments. Therefore, discovering the modifier genes has been an important goal of many NMDs studies.

Several strategies can be used to discover modifier genes including linkage analysis of family data, association study of case-control data and genome-wide screening (Genin, Feingold et al. 2008). Also other high throughput screening methods have been used for the screening of modifier genes. *Plastin 3* was identified as a modifier of SMA, using an unbiased transcriptomics approach (i.e. RNA sequencing) on some discordant SMA families (Oprea, Krober et al. 2008). Modifiers can be identified through studying both human populations and animal models. While they may not be fully representative of exact disease mechanisms in human, congenic animal models have some advantages including less genetic variability, a more controlled environment and less expensive collection of required samples (Wirth, Garbes et al. 2013, Lamar and McNally 2014).

SMN2

Although most of the products of the *SMN2* gene are devoid of exon7, this gene does produce a low amount of FL-SMN. So, in the absence of functional *SMN1*, *SMN2* is the main source of SMN protein inside the cells. As mentioned before, the level of SMN protein correlates inversely with the severity of SMA (Lorson, Hahnen et al. 1999, Monani, Lorson et al. 1999). The fact that the copy number of *SMN2* is widely variable among human individuals makes it the most predominant determining factor in the severity of the disease. Indeed, most of the variability observed in the phenotype among SMA patients - including different types of the disease - is due to the different copy numbers of *SMN2*. Most type I SMA patients carry only two copies of the *SMN2* gene, while type II SMA patients in general have three *SMN2* copies, type III SMA patients have four *SMN2* copies and type IV SMA patients have usually four to six copies of the *SMN2* gene (Feldkotter, Schwarzer et al. 2002, Mailman, Heinz et al. 2002, Wirth, Brichta et al. 2006). Animal studies also confirmed these findings; it has been shown that *Smn* knockout mice, which harbor only one copy of *SMN2* do not survive after birth, while 2 copies of *SMN2* extend the survival of these animals up to 8 days. Interestingly, 8 copies of *SMN2* rescue the *Smn* knockout mice completely without any motor neuron loss and muscle atrophy (Hsieh-Li, Chang et al. 2000, Monani, Sendtner et al. 2000). Not surprisingly, there is a consensus among researchers that *SMN2* is the most important modifier gene in SMA.

Plastin 3

Besides the *SMN2* gene as a modifier for SMA, there are several genes identified that modify the SMA phenotype independent of SMN levels. Interestingly, some of these modifiers are related to actin dynamics (Oprea, Krober et al. 2008, Bowerman, Beauvais et al. 2010, Bowerman, Murray et al. 2012).

Plastin proteins are a family of actin-cross-linking and actin-bundling proteins (Zu, Shigesada et al. 1990). *Plastin 3* or *T-Plastin* (also known as *T-Fimbrin*) is a ubiquitously expressed gene located on chromosome Xq23 (Lin, Aebersold et al. 1988). Plastin 3 contributes to the assembly and stabilization of actin bundles in a calcium dependent manner (Hanein, Volkmann et al. 1998, Volkmann, DeRosier et al. 2001).

Studying SMA-discordant families, Oprea et al. found that *Plastin 3* is differentially induced in peripheral lymphoblasts of unaffected *SMN1*-deleted female siblings. They observed that Plastin 3 interacts with SMN protein both *in vitro* and *in vivo*. They also showed that *Plastin 3* rescues the axonogenesis defects in primary motor neuron cultures and animal models of SMA (Oprea, Krober et al. 2008). Overexpression of *Plastin 3* in animal models of SMA also rescued myofiber atrophy, NMJ pathology and motor deficits associated with depletion of SMN in these animals (Hao le, Wolman et al. 2012, Ackermann, Krober et al. 2013). However, *Plastin 3* was not able to improve NMJ function in 'severe SMA' mice and did not increase the survival of these animals (McGovern, Massoni-Laporte et al. 2015). Follow up clinical studies also suggested that *Plastin 3* expression may not always modify the SMA phenotype in human. In fact it seems that the beneficial effects of *Plastin 3* in SMA depend on the age, puberty state and sex of the patients and also the severity of the disease. It seems that postpubertal female patients with type II or III SMA gain the most from *Plastin 3* function (Stratigopoulos, Lanzano et al. 2010, Bernal, Also-Rallo et al. 2011, Yanyan, Yujin et al. 2014, Yener, Topaloglu et al. 2016).

In a more detailed study, Hosseinibarkooie et al. showed that *Plastin 3* could rescue completely 'Taiwanese SMA' mice which were pre-treated with suboptimal doses of *SMN* antisense oligonucleotide (ASO). Endocytosis is a key function for the recovery and recycling of released synaptic vesicles. The authors also showed that endocytosis is decreased within NMJs

of these mice and overexpression of *Plastin 3* could restore the level of endocytosis to the normal levels. The authors concluded that the modifying effects of *Plastin 3* in SMA depend on the severity of the phenotype and occur mainly through improving the function of NMJs (Hosseinibarkooie, Peters et al. 2016).

RhoA

Ras homologue A (RHOA) is a gene located on chromosome 3p21 in human (Cannizzaro, Madaule et al. 1990). Rho A is a small GTPase protein which acts mainly as a regulator of actin dynamics. Active Rho A activates its downstream kinase ROCK which upon activation, phosphorylates LIM kinase and other proteins. Consequent phosphorylation of cofilin by LIM kinase inhibits its actin depolymerization activity (Maekawa, Ishizaki et al. 1999).

The activity of *RhoA* and its downstream kinase, '*Rho kinase'* (ROCK), is aberrantly increased in Smn-depleted neuronal cells and tissues. And, pharmacological inhibition of ROCK in $Smn^{2B/-}$ mice resulted in longer survival, increased myofiber size and improved maturation of NMJs. However, inhibition of ROCK increased neither the levels of SMN protein nor the number of motor neurons in spinal cords of these mice. So it seems that inhibition of ROCK rescues the SMA phenotype in an SMN independent manner (Bowerman, Beauvais et al. 2010, Bowerman, Murray et al. 2012).

Rationale

Pathologic alterations of NMJs have been extensively studied in SMA. However, it seems that synapses within central nervous system tissues are also affected during the course of SMA. *Smn* is widely expressed in the CNS in a specific spatiotemporal order, and *Smn* deficient mouse embryos have cell death and pathological foci within their cortices (Liu et al., 2010). A recent study on 'severe SMA' mice showed widespread perturbations in proteomics of synapses of the hippocampus of these mice before the onset of the SMA phenotype (Wishart et al., 2014). Synapses within spinal cord are also affected in SMA and excitatory synaptic inputs on motor neurons are reduced in a period prior to any motor neuron loss. Several other studies also showed impaired function of central neural circuits in fly and mouse models of SMA. The $Smn^{2B/-}$ mouse shows a relatively long pre-symptomatic period (Bowerman, Beauvais et al. 2010). This provides a unique opportunity to explore aberrant molecular events preceding the SMA phenotype in more detail. Through studying alterations in proteomics of central synapses in $Smn^{2B/-}$ mice at pre- and early- symptomatic stages, our goal is to identify novel therapeutic targets for the treatment of SMA.

The effect of genetic background on the severity of neuromuscular disorders has been recognized previously. This effect has been attributed to the function of modifier genes on the phenotype caused by a primary mutation in the causative gene (Montagutelli, 2000). Initial characterization of 'severe SMA' and 'delta 7 SMA' mice confirmed the effect of the mouse genetic background on the severity of the disease. A fraction of $Smn^{2B/-}$ mice on a hybrid BL6xCD1 genetic background showed a considerable long survival. Considering the effect of genetic background in other mouse models of SMA, we decided to backcross the Smn^{2B} allele

into two different mouse strains (FVB and C57BL/6) and characterize the congenic *Smn*$^{2B/-}$ mice resulting from this exercise.

Hypothesis

Part 1- Here we hypothesize that in *Smn*$^{2B/-}$ mice central synapses undergo molecular pathologic changes.

Part 2- Here we hypothesize that congenic *Smn*$^{2B/-}$ mice will show a less variable phenotype than *Smn*$^{2B/-}$ mice with a mixed background.

Aims and Goals

1- 1- To study the number and morphology of neurons within the central nervous system of *Smn*$^{2B/-}$ mice.
1- 2- To study the number of synaptic vesicles within the central nervous system of *Smn*$^{2B/-}$ mice.
1- 3- To study the proteomic alterations within central synapses of *Smn*$^{2B/-}$ mice.
2-1 - To generate congenic *Smn*$^{2B/-}$ mice in both the FVB and C57BL/6 mouse backgrounds.

2- 2-To characterize and compare congenic *Smn*$^{2B/-}$ mice in both the FVB and C57BL/6 mouse backgrounds.

Chapter 2 : Materials and Methods

Mouse maintenance and handling

C57BL/6 (will be mentioned as BL6 in this monograph afterwards) and FVB *Smn*$^{+/-}$ mice and BL6 and FVB *wild type* mice were purchased from the Jackson Laboratory as follows: FVB/NJ (#001800), C57BL/6J (#000664), B6.129P2(Cg)-Smn1<tm1Msd>/J (# 010921), and FVB.129P2-Smn1<tm1Msd>/J (# 006214) (Bar Harbor, Maine, USA). *Smn*$^{2B/2B}$ mice were previously generated in our laboratory and had been maintained on a BL6 x CD1 hybrid background (Bowerman, Beauvais et al. 2010). All animals were handled according to institutional guidelines (Animal Care and Veterinary Services, University of Ottawa). The humane endpoints included severe dehydration, hypothermia or dragging of the hind limbs.

Generation of congenic *Smn*$^{2B/2B}$ in FVB and BL6 genetic backgrounds

In order to generate two congenic strains, *Smn*$^{2B/2B}$ mice on the hybrid background were backcrossed to *FVB* and BL6 *wild type* mice. At each subsequent generation, male pups were genotyped for the *Smn*^{2B} allele (using the following primers: 5'-AAC TCC GGG TCC TCC TTC CT-3' and 5'-TTT GGC AGA CTT TAG CAG GGC-3') and male *Smn*$^{2B/+}$ mice were mated to *wild type* female mice with the relevant genetic background. The backcrossing was continued to the tenth generation of *Smn*$^{2B/+}$ mice and fully congenic *Smn*$^{2B/2B}$ mice were attained by mating *Smn*$^{2B/+}$ female and male mice with the same genetic background.

Characterization of SMA phenotype in congenic *Smn*$^{2B/-}$ mice

Congenic *Smn*$^{2B/2B}$ mice with either FVB or BL6 backgrounds were generated by mating *Smn*$^{2B/+}$ female and male mice (from the same genetic background) at the sixth generation of backcrossing. To generate congenic *Smn*$^{2B/-}$ mice, *Smn*$^{2B/2B}$ mice were mated with *Smn*$^{+/-}$ mice of the relevant genetic background. Since *Smn*$^{2B/+}$ mice show no SMA phenotype (Bowerman, Murray et al. 2012), they were used as the normal controls unless otherwise indicated.

Measuring survival and growth of *Smn*$^{2B/-}$ mice

All of the breeding cages were inspected for new litters, death or any humane endpoints on a daily basis and any new event was recorded. Each individual pup was identified by tattooing. Using a Scout Pro digital mini-scale (Ohaus Corp, NJ), daily weight of each pup was measured and recorded. The scale was calibrated automatically every day upon initializing. All the pups were genotyped in the first litters of each breeding cage. The mice which were euthanized due to the humane endpoints were excluded from the study.

Evaluation of muscle strength of mice

Based on the guidelines of Treat-NMD, 'inverted mesh grip test' (protocol number SMA-M.2.1.002) and 'tube test' (protocol number SMA-M.2.2.001) were used to evaluate muscle strength of the mice (Sumner 2010, Sumner 2011). Briefly 'inverted mesh grip test' was performed by placing one pup on a plastic mesh (with 1 mm^2 grids) mounted tightly on a plastic frame. Then the mesh and the frame were inverted and mounted slowly on a cage with 80 cm height and soft beddings on the bottom. Using a digital chronometer, the 'latency to fall' times were measured up to a maximum of 60 sec (which was considered as 100% success or the goal achievement). The test was repeated for five rounds for all the pups in each session. The 'inverted mesh grip test' was performed starting at postnatal day 13 (PND13) and was repeated every other day until PND25.

'Tube test' (also known as 'hind limb suspension test') was performed using a metal tube with 6.5 cm diameter, 20 cm height and about 1 mm wall thickness and soft beddings on the bottom. One mouse was hung downward and inside the tube with its hind limbs over the rim of the tube. Using a digital chronometer, the 'latency to fall' times were measured up to a maximum amount of 60 sec or until the mouse came out of the tube (which were considered as 100%

success or the goal achievement). The test was repeated for five rounds for all the pups in each cage in each session. The 'hind limb suspension test' was performed starting at PND7 and was repeated every other day until PND25.

Measurement of mouse myofiber cross-sectional areas

Using a CO_2 chamber and cervical dislocation, mice were euthanized and both hind limbs were surgically removed off the body. The skin of the hind limbs was removed to expose the muscles. Tibialis anterior (TA) muscles were carefully dissected. Using a liquid nitrogen-isopentane bath, freshly dissected muscles were mounted immediately in Optimal Cutting Temperature (OCT) compound (Tissue-Tek). A Leica CM1850 cryostat machine was used to section (10 µm) TA muscles at their biggest diameters; sections were mounted on microscope slides and were air dried at room temperature. The sectioned TA muscles were stained using hematoxylin and eosin (H&E) technique. High quality images were prepared from several microscopic fields of each stained sample using a Zeiss Ax10 microscope equipped with an Axiocam MRC camera (Plan-APOCHROMAT 40X/0.95 Ph3 lens). Using ImageJ software, the cross-sectional areas of 300-400 myofibers were measured in each section.

Measurement of the number of mouse spinal motor neurons

Using a CO_2 chamber and cervical dislocation, mice were euthanized and the entire spines were surgically removed . Using the last rib as a marker, the lumbar spinal cords were dissected under the level of T12, and incubated immediately in 4% paraformaldehyde/PBS overnight at 4°C. Fixed spinal cords were incubated in 30% sucrose/PBS for 24 h and then mounted in OCT using a liquid nitrogen-isopentane bath. Using a Leica CM1850 cryostat machine, an initial 0.5 mm of each lumbar spinal cord was trimmed. Then from each sample, six transverse sections with an interval of 100 µm were mounted on one microscope slide (spanning

a longitudinal segment of about 500 µm of each mouse lumbar spinal cord at the level of L1-L2). The samples were air dried at room temperature and then permeabilized in 0.3% TritonX-100/PBS for 30 min. The sections were incubated with 1X Power Block blocking reagent (BioGenex, Fremont, CA) for 10 min at room temperature. Then, the sections were incubated with a goat anti-ChAT antibody (EMD Millipore, Darmstadt, Germany) for 48 h at 4°C, and then were incubated with Alexa Fluor 555 donkey anti-goat IgG (Life Technologies, Carlsbad, California) for 2 h at room temperature. After several washings in PBST, samples were incubated with 4',6-diamidino-2-phenylindole (DAPI) for labelling of nuclei. High quality images were prepared from both ventral horn areas of all mouse spinal cord sections using a Zeiss Ax10 microscope (Plan-APOCHROMAT 20X/0.8 Ph2 lens) equipped with an Axiocam HRM camera. Images were then quantified for the number of motor neurons (ChAT and DAPI positive neurons) using ImageJ software.

Evaluation of pathologic changes within mouse neuromuscular junctions

Mice were euthanized using a CO_2 chamber and cervical dislocation, and the anterior part of the thoracoabdominal wall was cut off each mouse body. The tissues were incubated immediately in 2% PFA/PBS for 10 min at room temperature and washed several times with PBS. Mouse transverse abdominal muscles (TVAs) were dissected out from the fixed tissues and immunostained for neurofilament-M (NFM) and motor endplates (MEP) as described before (Murray, Gillingwater et al. 2014). Briefly, TVA muscles were first incubated in 0.3% Triton X-100/PBS for 30 min, and then with 1X Power Block for 10 min at room temperature (BioGenex, Fremont, CA). Mouse TVA muscles were incubated with a mouse anti-neurofilament-M antibody and a mouse anti-SV2 antibody (Developmental Studies Hybridoma Bank, Iowa City, IA) overnight at 4°C, and after washing several times with PBST, TVA muscles were incubated

with Alexa Fluor 488 goat anti-mouse IgG (Life Technologies, Carlsbad, California) for 1 h at room temperature. MEPs were counterstained with tetramethylrhodamine (TRITC) conjugated alpha-bungarotoxin (Life Technologies, Carlsbad, California). Using Dako Fluorescent mounting media, mouse TVA muscles were mounted on microscope slides. High quality z-stack images were prepared from several microscopic fields of each sample using a confocal LSM510 Zeiss microscope (Plan-APOCHROMAT 63X/1.4 oil DIC). The motor endplate (MEP) areas and the grade of presynaptic swelling of NMJs were quantified using ImageJ software.

Measurement of protein expression levels

Western blotting techniques were used to quantify the protein expression levels in mouse lumbar spinal cord samples and synaptosome preparations. Briefly, samples were homogenized and incubated in RIPA buffer (Cell Signalling Technology) for 10 min on ice. Protein concentration of homogenates was measured using a Pierce™ BCA Protein Assay Kit (Thermo Fisher Scientific) and 10 µg total protein from each sample was incubated with Laemmli loading buffer at 95°C for 5 min. Samples were cooled at room temperature and loaded on 10-12% SDS-polyacrylamide gels and separated by electrophoresis. Gels were then blotted onto Immobilon-FL membranes (EMD Millipore). Before blocking, the blotted membranes were stained for total protein using Sypro Ruby staining reagent (Life Technologies) and scanned by a Chemidoc-IT imager (UVP) (Supplementary Figure 4.1) . Then, the following primary antibodies were used to probe the membranes: mouse anti-SMN (BD Bioscience), mouse anti-β-actin, and rabbit anti-Pls3 (Genetex). Membranes then were incubated with IRDye fluorescent conjugated (LiCOR) or HRP conjugated secondary antibodies (Jackson Laboratories) and were developed using an Odyssey CLx scanning machine or chemiluminescence western blotting substrate (Thermo

Scientific Pierce), respectively. The images were quantified using Image Studio 4.0 (LiCOR) or ImageJ software. Total protein of each lane was used to normalize the signals within that lane.

Measuring density of hippocampus pyramidal neurons

Nissl staining technique was used to determine the density of pyramidal neurons within the CA1 region of the mouse hippocampus. Briefly, the mice were euthanized by CO_2 and their brains were dissected immediately. Mouse brains were rinsed in PBS once and fixed in 4% paraformaldehyde (PFA) in PBS at 4°C overnight. Then, the fixed brains were incubated in 30% sucrose in PBS (at 4°C overnight), and mounted in OCT. Using a Leica CM1850 cryostat, coronal sections of mouse brains (with 10 µm thickness) were prepared on microscope slides, spanning both proximal and distal regions of the hippocampus. The slides were air dried and stained at room temperature as follows. Samples were incubated in Hemo-D (15 min), then rehydrated in decreasing ethanol concentrations (95%, 70% and 50%; 1 min each) and ddH2O (1 min). The samples were stained in 0.1% cresyl violet solution (5-10 min) and washed immediately with ddH2O and dehydrated in increasing ethanol concentrations (50%, 75%, 95% and 100% 1 min each) and Hemo-D (5 min). The slides were then air dried shortly and mounted using Paramount mounting reagent. Using a Zeiss Ax10 microscope equipped with an Axiocam MRC camera (Plan-APOCHROMAT 20X/0.95 Ph3 lens) images were taken from CA1 regions of each section. Using ImageJ software, CA1 pyramidal neurons of both proximal and distal hippocampus (2-3 fields each) were counted; the areas of each field were determined and used to calculate the density of neurons.

Measuring spine density of hippocampus pyramidal neurons

Golgi-Cox staining technique was used to determine the density of pyramidal neurons within the CA1 region of mouse hippocampus. Briefly, the mice were euthanized and their brains

were dissected immediately. Mouse brains were rinsed in ddH2O once and incubated in Golgi-Cox solution (1% K2Cr2O7, 1% HgCl2 and 0.8% K2CrO4) and kept in the dark at room temperature (Golgi-Cox solutions were replaced with fresh ones after 24 h). Mouse brains remained in Golgi-Cox solutions for 14 days in the dark and were then rinsed in ddH2O once and incubated in 40% sucrose in ddH2O (at 4°C overnight, dark). Impregnated mouse brains were rinsed in ddH2O once and then 'snap frozen' in isopentane liquid nitrogen bath. Using a Leica CM1850 cryostat (Leica Biosciences, Germany), coronal sections of mouse brains with 100 µm thickness were prepared on glass microscope slides, spanning both proximal and distal regions of the hippocampus. The slides were air dried and stained in the dark at room temperature as follows. Samples were incubated in ddH2O (1 min), then in 30% ammonium hydroxide (NH4OH) (30 min), then in ddH2O (1 min), and then in Kodac Rapid Fixer solution (diluted 5 times, 30 min). The samples were washed in ddH2O (1 min) and then dehydrated in increasing ethanol concentrations (50%, 75% and 95%; 1 min each, then in 100% ethanol; 5 min), then in CHE reagent (1/3 chloroform, 1/3 HemoDe and 1/3 100% ethanol; 15 min) and Hemo-D (15 min). The slides were then air dried shortly and mounted using Paramount mounting reagent. Using a Zeiss Ax10 microscope equipped with an Axiocam MRC camera (Plan-APOCHROMAT 40X/0.95 Ph3 lens) Z-stack images were taken from the CA1 region of the hippocampus. Using ImageJ software, the numbers of spines on the 2^{nd} and 3^{rd} branches of the basal processes of CA1 pyramidal neurons of both proximal and distal hippocampus (6 fields each) were counted; the length of each branch was determined and used to calculate the density of dendritic spines.

Measuring density of synaptic inputs on motor neurons

Immunofluorescent staining techniques were used to determine the density of synaptic inputs on motor neurons within anterior horns of mouse lumbar spinal cords. Briefly, the mice were euthanized and their lumbar spinal cords were dissected under the level of T12 (using the last rib as a marker). Mouse spinal cords were rinsed in PBS once and fixed in 4% paraformaldehyde (PFA) in PBS (at 4°C overnight), and incubated in 30% sucrose in PBS (at 4°C overnight), then mounted in OCT. Using a cryostat (Leica Biosciences, Germany), an initial 500 µm of each spinal cord was trimmed. Then, transverse sections of mouse spinal cord (with 10 µm thickness) were prepared on glass microscope slides. The slides were air dried and stained at room temperature as follows. Samples were permeabilized in 0.3% TritonX-100 in PBS for 30 min, then blocked in 1X Power Block (BioGenex, Fremont, CA) for 10 min at room temperature. First, the synapses were labeled by a mouse anti-SV2 antibody (Developmental Studies Hybridoma Bank, Iowa) using Vector MOM Immunodetection Kit (Vector laboratories, CA) according to manufacturer recommendations. Then, sections were incubated with a goat anti-ChAT antibody (EMD Millipore, Darmstadt, Germany) in 1% BSA and 0.3% TritonX-100 in PBS for 48 h at 4°C. Samples were incubated with Alexa Fluor 555 donkey anti-goat IgG (Life Technologies, Carlsbad, California) for 2 h at room temperature. Nuclei were counterstained with 4',6-diamidino-2-phenylindole (DAPI). Images were taken using a confocal LSM510 Zeiss microscope (Plan-APOCHROMAT 63X/1.4 oil DIC). The number of labeled synapses on the periphery of each motor neuron was quantified using ImageJ software. The total length of periphery of each motor neuron was used to calculate the density of synaptic input on motor neurons.

Preparation of synaptosome fractions

Based on a methods described by Dunkley et al. (2008), non-continuous Percoll gradients were used to achieve highly pure and enriched synaptosome fractions from mouse spinal cords and cortices (Dunkley, Jarvie et al. 2008). Briefly, mice were euthanized and their cortices and spinal cords were dissected immediately. The samples were rinsed in ddH2O and were immediately homogenized in 6 ml of a sucrose buffer (containing 320 mM sucrose, 5 mM Tris HCl pH 7.5 and 0.1 mM EDTA) using a 7 ml dounce tissue grinder (10 strokes loose and 10 strokes tight pestles). The homogenates were centrifuged at 1,100 g (10 min at 4°C) and the supernatants were transferred to new tubes and were centrifuged at 20,000 g (10 min at 4°C). The supernatants were discarded and the pellets were resuspended in 2 ml of gradient medium (GM) buffer (containing 250 mM sucrose, 5 mM Tris HCl pH 7.5 and 0.1 mM EDTA) and loaded gently on the top of the non-continuous Percoll gradients (prepared according to Table 2.1). The gradient tubes were centrifuged at 45,000 g (5 min at maximum speed, 4°C) using a fixed angle 70.1 Ti rotor (Beckman). The 3^{rd} and 4^{th} fraction of each tube was aspirated carefully using a pasteur pipette and transferred to new tubes and diluted 10 times by GM buffer and centrifuged at 45,000 g (5 min at maximum speed, 4°C). The supernatants were discarded and the pellets were resuspended in 2 ml of GM buffer and transferred to microcentrifuge tubes and centrifuged in a benchtop machine at maximum speed (5 min at maximum speed, 4°C). The retrieved pellets were considered as synaptosome fractions and were used for further analysis.

Gradient	GM buffer (ml)	SIP* (ml)
3%	12.85	0.466
10%	11.85	1.46
15%	11.06	2.26
23%	9.93	3.4

Table 2.1. Preparation of different percentages of non-continuous Percoll gradient. *Stock solutions of Isometric Percoll (SIP) are prepared by adding 9 volumes of Percoll to 1 volume of 2.5 M sucrose.

Electron microscopy (EM) imaging of synaptosomes

Transmission electron microscopy (TEM) was used to determine the integrity and quality of prepared synaptosomes. Briefly, fresh synaptosome fractions prepared from mouse cortices and spinal cords were incubated with Karnovsky's fixative buffer (4% paraformaldehyde, 2% glutaraldehyde and 0.1 M sodium cacodylate in PBS, pH 7.4) for at least 1 h at room temperature. Samples were centrifuged at 20,000 g for 1 min and the pellets were washed three times in 0.1 M sodium cacodylate buffer for 10 min. Samples were post-fixed with 1% osmium tetroxide in 0.1 M sodium cacodylate buffer for 2 h and washed three times in distilled water for 5 min. After the last wash, the pellets were dehydrated in increasing concentrations of ethanol (50%, 75% and90%; 15 min each), then were washed for 10 min in ethanol/acetone (50:50) solution followed by centrifugation at 20,000 g for 1 min, and then were washed for 15 min in

100% acetone followed by centrifugation at 20,000 g for 1 min. The samples were infiltrated first in 30% spurr resin/acetone overnight, then in 50% spurr resin/acetone for 6h and then in fresh 100% spurr resin overnight (all infiltration steps were performed on a rotator at low speed). Synaptosomes were embedded in fresh liquid spurr resin and then polymerized overnight at 70ºC. The specimens were sectioned using an ultramicrotome (at 80 nm thickness), the ultrathin sections were collected onto 200-mesh copper grids and stained using 2% aqueous uranyl acetate and then Reynold's lead citrate. Several electron micrographs were prepared from the stained sections using a transmission electron microscope (Hitachi 7100) at 10,000x and 100,000x magnifications, and then were visually examined for ultrastructural analysis.

Mass Spectrometry analysis of synaptosomes

Label-free quantitative mass spectrometry proteomics was performed on synaptosome fractions as follow. Synaptosome fractions prepared from the mouse spinal cords were solubilised in 6x SDS loading dye. Samples from three biological replicates of *Smn*$^{2B/-}$ mice and their control littermates were separated on SDS-PAGE gels, then digested using mass spectrometry grade trypsin (Promega). For quantification purposes, 1 µL of a 750 fmol/µL stock solution of Hi3 peptide standards (Waters) was added to each sample prior to mass spectrometry analysis.

Liquid chromatography–mass spectrometry (LC-MS) technique was used to determine the proteomics profile of each sample using a nano Acquity UPLC system and a SYNAPT G2-Si mass spectrometer (Waters). Analysis of data was performed using Progenesis QI (Nonlinear Dynamics) for peptide identification within a Mus musculus subset of the UniprotKB/SwissProt database. Analysis parameters included a maximum protein mass of 250 kDa, a minimum of

seven fragment ion matches per protein, a minimum of three fragment ion matches per peptide, a maximum of two missed cleavages (trypsin), a minimum of two matched peptides per protein and a false-discovery rate of 1% using a decoy database. Three technical replicates for each of the biological replicates were analyzed separately (72 total measurements). Quantitative analysis was performed using the three most abundant peptides per protein normalized to the six Hi3 internal peptides (50 fmol on column).

Data analysis and presentation

Prism 6 GraphPad software (San Diego, CA) was used to analyze data. The statistical tests used for each analysis are specified in the corresponding results section. All data are presented as mean ± standard error of the mean (SEM).

Chapter 3 - Results

3. 1- Characterization of proteomic alterations in the central synapses of *Smn*$^{2B/-}$ mouse model

3.1.1. The gross morphology, total area and cell density of the hippocampus is not altered in *Smn*$^{2B/-}$ mice

Wishart et al. studied the morphology of hippocampus in 'severe SMA' mice and reported no anomaly at a pre-symptomatic stage (PND1). However, the total hippocampal areas and the density of hippocampal neurons were reduced at a post-symptomatic stage in these mice (PND5) (Wishart, Huang et al. 2010). We investigated hippocampus morphology in *Smn*$^{2B/-}$ mice at PND16 using Nissl stained coronal sections of mouse brains. PND16 is considered as a post-symptomatic stage in *Smn*$^{2B/-}$ mice (Bowerman, Beauvais et al. 2010). We studied proximal regions as well as distal regions of the hippocampus and found no gross morphological abnormality (Figure 3.1.1A and B). The quantification of the cross-sectional areas of mouse hippocampus showed no significant difference in the size of hippocampus in *Smn*$^{2B/-}$ mice (1.88 ± 0.14 mm^2) compared to their control littermates (1.95 ± 0.22 mm^2) at PND 16 (n=3; unpaired t test, p> 0.05) (Figure 3.1.1C). We also analyzed neuronal densities within proximal and distal CA1 regions of mouse hippocampus in *Smn*$^{2B/-}$ mice. Our quantification revealed no significant difference in the neural density in *Smn*$^{2B/-}$ mice (133.6 ± 14.94 neurons/mm^2) compared to their control littermates (120.8 ± 8.65 neurons/mm2) (n=3; unpaired t test p>0.05) (Figure 3.1.1D). In conclusion, we did not find any gross morphological abnormality, altered size or reduced neural density in hippocampus of *Smn*$^{2B/-}$ mice at PND16.

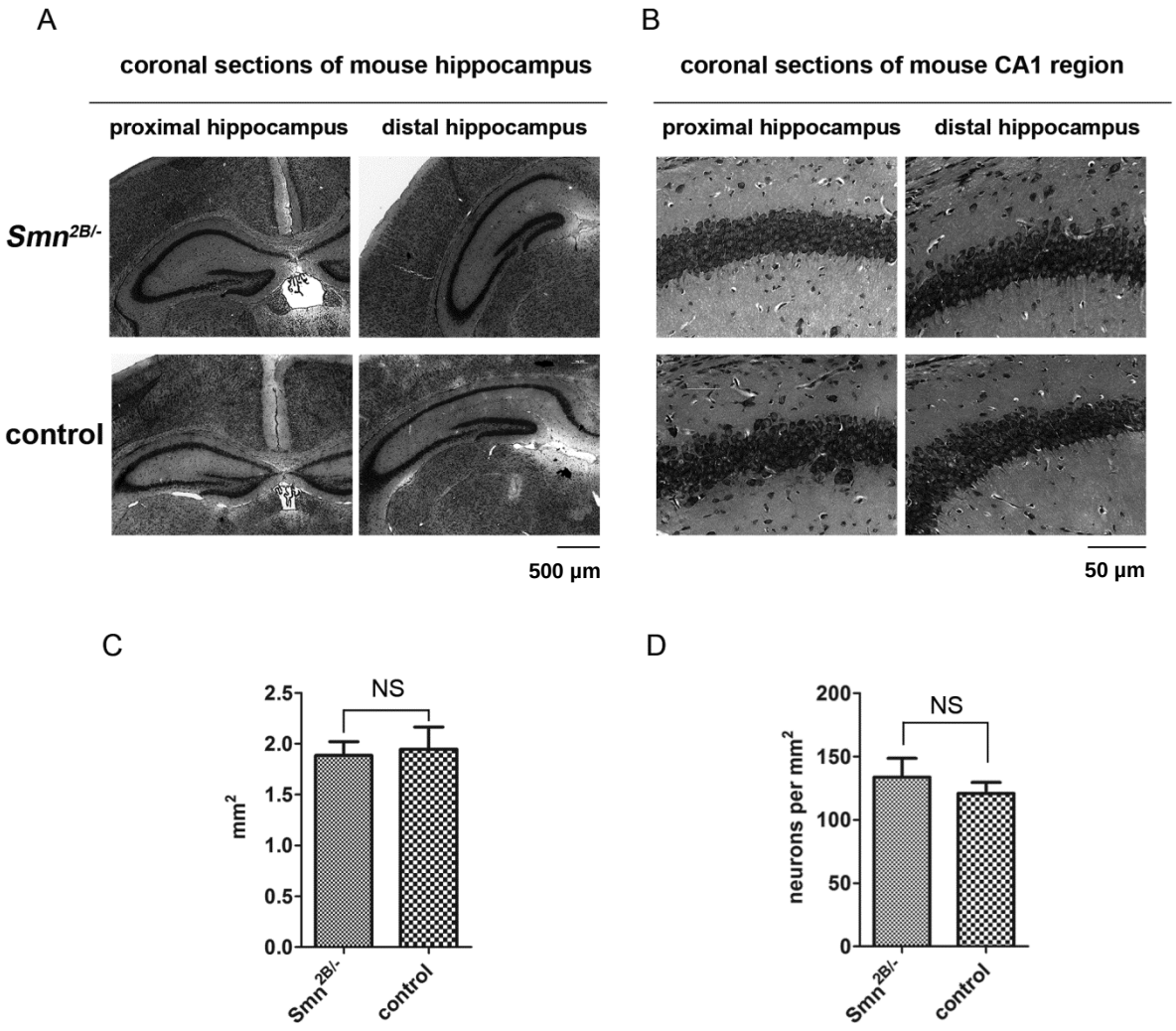

Figure 3.1.1. At PND16, the morphology and neuronal density of the hippocampus is not altered in *Smn*$^{2B/-}$ mice. A) Representative images of Nissl stained coronal sections of PND16 mouse brains. We did not observe any obvious abnormality within either proximal or distal parts of the hippocampus of *Smn*$^{2B/-}$ mice. B) High magnification images of coronal sections of CA1 region of mouse hippocampus. C) Cross-sectional areas of hippocampus of *Smn*$^{2B/-}$ mice were not significantly different from their controls (n=3; unpaired t test, P >0.05). D) Quantification of neuronal density of CA1 regions of hippocampus did not show any alteration in *Smn*$^{2B/-}$ mice compared to their normal controls (n=3; unpaired t test, P >0.05).

3.1.2. The morphology and spine density of dendrites of hippocampal neurons are not altered in *Smn*$^{2B/-}$ mice

We investigated if there is any abnormality in the morphology of dendritic trees and dendritic spine densities of the pyramidal neurons within hippocampus of *Smn*$^{2B/-}$ mice. To visualize the dendritic trees of pyramidal neurons, we utilized Golgi-Cox staining technique on the brains of *Smn*$^{2B/-}$ mice and their controls at PND11 (the pre-symptomatic stage) and PND16 (the post-symptomatic stage) (Figure 3.1.2). We did not observe any gross morphological abnormality of dendritic trees of pyramidal neurons in hippocampus of *Smn*$^{2B/-}$ mice compared to their control littermates at PND11 or PND16 (Figure 3.1.2A). We also quantified the density of spines on the 2nd and 3rd dendritic branches of pyramidal neurons within proximal and distal CA1 regions of mouse hippocampus. Our quantification revealed that there was no significant alteration in the spine densities of the 2nd or the 3rd dendritic branches of basal projections of hippocampal neurons of *Smn*$^{2B/-}$ mice comparing to their control littermates at PND11 (0.18±0.01 vs. 0.19±0.02 spine/µm for the 2nd and 0.22±0.01 vs. 0.23±0.03 for the 3rd dendritic branches) (n=3; unpaired t test p>0.05) (Figure 3.1.2B and C). Also at PND16, the spine densities of the 2nd or the 3rd dendritic branches of basal projections of hippocampal neurons of *Smn*$^{2B/-}$ mice were not significantly different from their control littermates (0.33±0.02 vs. 0.38±0.02 spine/µm for the 2nd and 0.42±0.02 vs. 0.44±0.04 for the 3rd dendritic branches) (n=3; unpaired t test p>0.05) (Figure 3.1.2D and E). Therefore, the arborisation of the dendritic trees of pyramidal neurons of hippocampus looks to be normal in *Smn*$^{2B/-}$ mice (Figure 3.1.2).

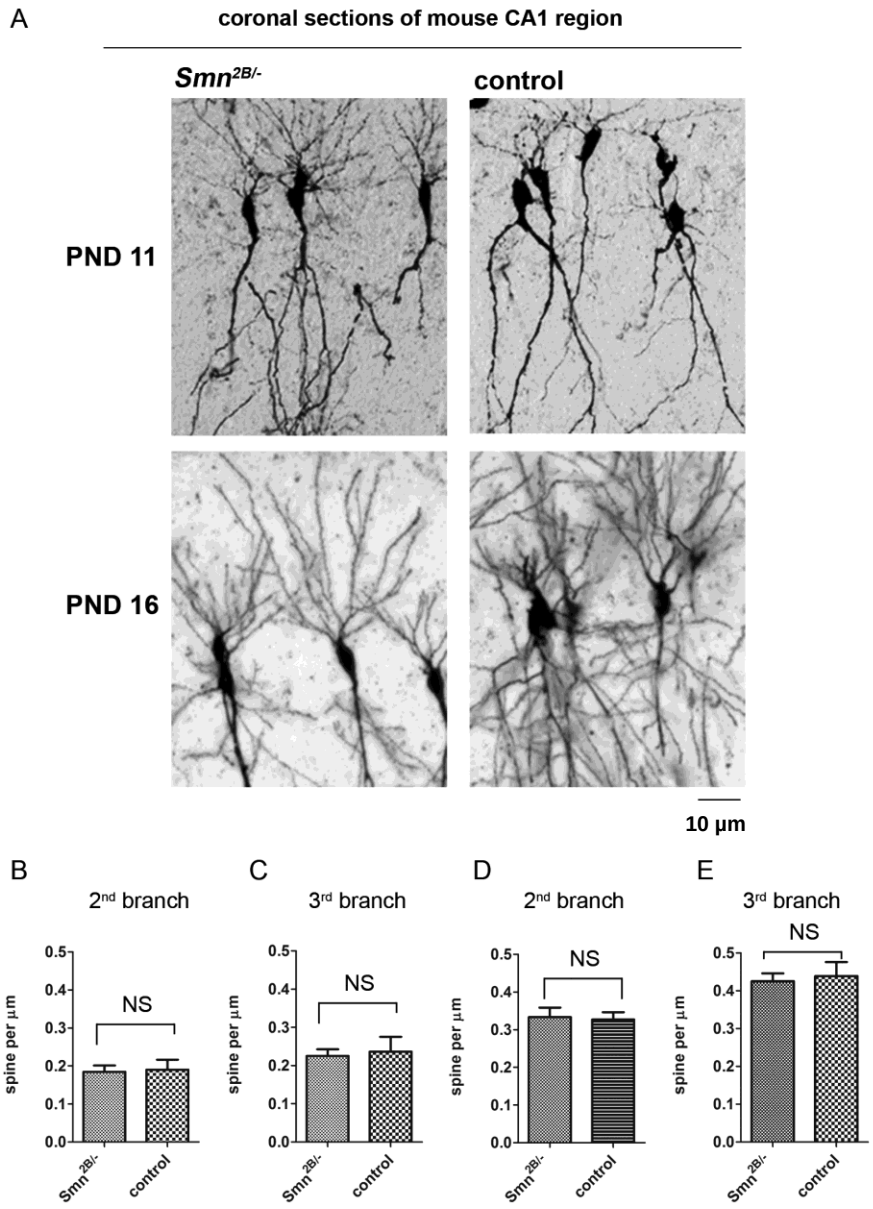

Figure 3.1.2. The morphology of dendritic tree and spine density of hippocampal neurons are not altered in *Smn*$^{2B/-}$ mice. A) Representative images of Golgi-cox stained coronal sections of PND11 and PND16 mice brains. No obvious abnormality was observed in the morphology of dendritic trees of hippocampal neurons at either PND11 or PND16 in *Smn*$^{2B/-}$ mice. The spine density of 2nd dendritic branches (B and D) or 3rd dendritic branches (C and E) was not significantly altered in *Smn*$^{2B/-}$ mice at either PND11 (B and C) or PND16 (D and E) (n=3; unpaired t test, P >0.05) (Samples were prepared by M. Eshraghi and microscopic imaging was done by S. Cummings).

3.1.3. The density of synaptic inputs onto lower motor neurons of *Smn*$^{2B/-}$ mice showed modest increase in number at a pre-symptomatic stage but no change was observed at post-symptomatic stages.

It has been reported that the total number of synaptic inputs onto spinal motor neurons is not reduced in the 'delta 7 SMA' mice until the very end stages of the disease (i.e. PND14) (Ling, Lin et al. 2010). We also investigated if the number of synaptic inputs onto spinal motor neurons had been altered in *Smn*$^{2B/-}$ mice at various ages: PND11 (pre-symptomatic stage), PND16 and PND21 (post-symptomatic stages). This was done by immunofluorescent staining on horizontal sections prepared from mouse lumbar spinal cords using antibodies against synaptic vesicle glycoprotein 2 (SV2, to delineate synapses) and choline acetyltransferase (ChAT, to delineate lower motor neurons) (Figure 3.1.3). Studying several images prepared from each mouse spinal cord, we did not observe any gross morphological abnormality in the pattern and distribution of synaptic inputs onto motor neurons of *Smn*$^{2B/-}$ mice (Figure 3.1.3A). Using Image J software, we quantified the number of synapses adjacent to soma and proximal dendrites of the motor neurons (less than 1 µm apart). We also measured the periphery of each motor neuron and used it to calculate the density of synaptic inputs on each motor neuron. Our quantification revealed that there is a modest increase in the density of synaptic inputs on spinal motor neurons of *Smn*$^{2B/-}$ mice at PND11 (n=3; two way ANOVA, $p < 0.01$ was considered significant) (Figure 3.1.3B). However, at the later stages of the disease (i.e. PND16 and PND 21), there was no significant alteration in the density of synaptic inputs on spinal motor neurons between *Smn*$^{2B/-}$ mice (n=3; two way ANOVA, $p > 0.05$ was considered significant). Thus, synaptic inputs onto motor neurons are not reduced in *Smn*$^{2B/-}$ mice.

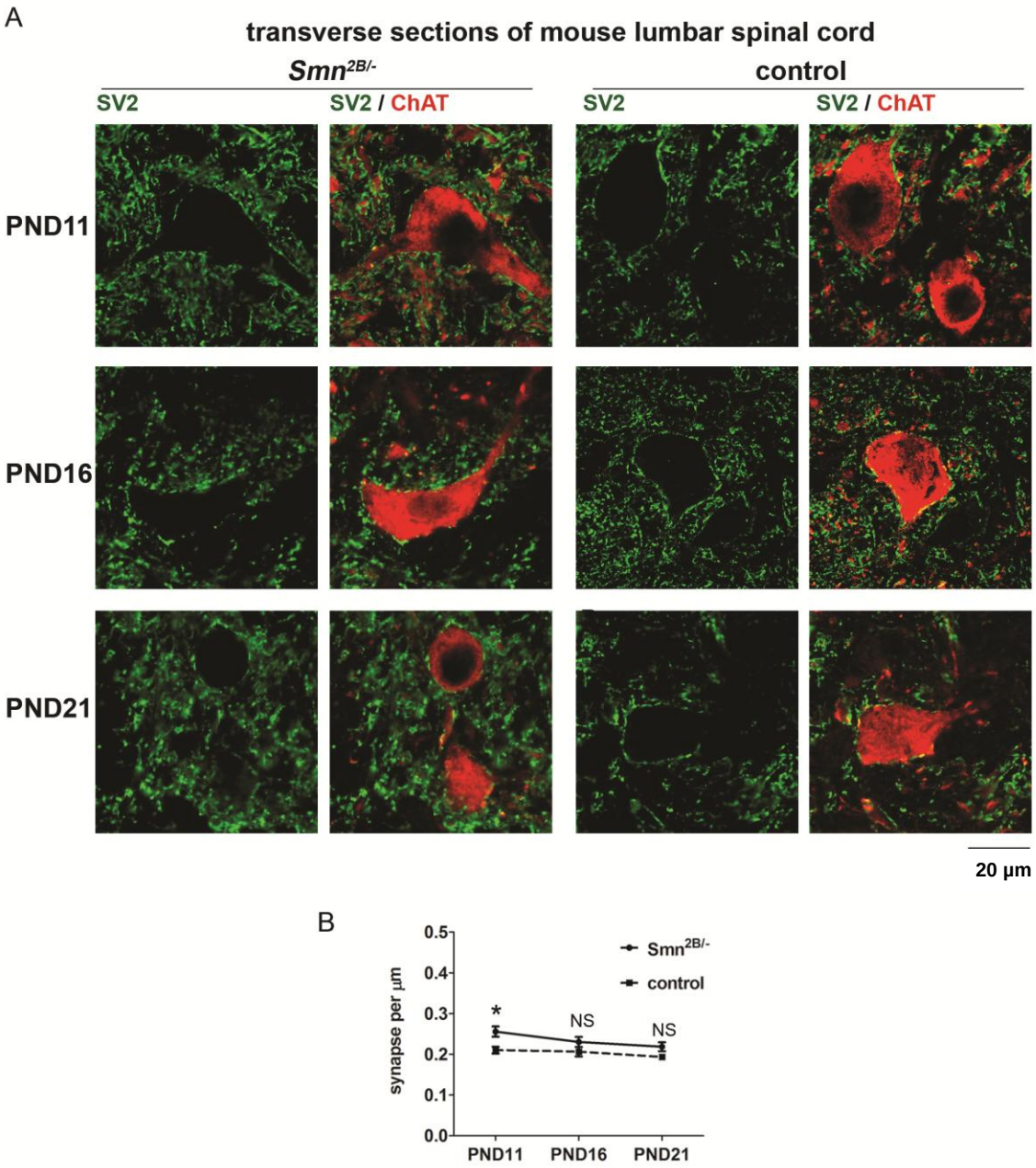

Figure 3.1.3. *Smn*$^{2B/-}$ mice do not show any decrease in the density of synaptic inputs onto lower motor neurons.

A) Representative images of immunofluorescence stained transverse sections of mouse lumbar spinal cords (green represents SV2 staining and red represents ChAT staining). B) Quantification of the density of SV2 labeled synapses adjacent to the periphery of motor neurons showed small increase at PND11 but no significant alterations at PND16 and PND21 (n=3; two way ANOVA, $p<0.05$ was considered significant). * indicates statistically different from the control.

3.1.4 Synaptosome fractions prepared from mouse cortices and spinal cords showed high purity and quality

We initiated this project to decipher perturbations of molecular signaling pathways within central synapses at a time prior to the onset of any neurological phenotype in *Smn*$^{2B/-}$ mice. Several techniques for the isolation of crude or pure synaptosome fractions have been described before. Presynaptic areas are specialized parts of cytoplasm of neurons; they contain huge protein complexes and vesicles. Upon mechanical homogenization of CNS tissues under isotonic conditions, presynaptic areas are severed from axonal terminals and reseal to form organelle-like sacs known as synaptosomes. Postsynaptic areas (including postsynaptic densities) also remain attached to the synaptosomes (Dunkley, Jarvie et al. 1986). At this stage, it is possible to isolate synaptosomes from other cell organelles based on their densities. This can be achieved using differential centrifugation or gradient ultra-centrifugation. However, CNS tissues are heterogeneous and any homogenate from them is highly contaminated by materials from other cell types especially myelin and its associated proteins. To overcome this problem, we followed a conservative method (Dunkley, Jarvie et al. 2008, Westmark, Westmark et al. 2011), which included both differential centrifugation and a non-continuous Percoll gradient ultra-centrifugation (please refer to Materials and Methods for details). At the end of the ultra-centrifugation, Percoll gradients yield five distinct fractions, here labeled as F1 to F5. Based on the literature, fractions F3 and F4 contain synaptosomes and together are used as the synaptosome preparation (Dunkley, Jarvie et al. 2008). We prepared synaptosomes from mouse brain and spinal cord at PND14 and used immunoblotting techniques to investigate the purity and enrichment of synaptosome fractions (Figure 3.1.4).

As shown in Figure 3.1.4, fractions F3 and F4 (from both brain and spinal cord) showed minimum reactivity with antibodies against histone H3 as a marker for nucleus, myelin basic protein (MBP) as a marker for myelin, or glial fibrillary acidic protein (GFAP) as a marker for astrocytes. We also used antibodies against synaptic markers to investigate the enrichment of these synaptosome fractions. Fractions F3 and F4 showed stronger signals than other fractions when antibodies against synaptic vesicle glycoprotein 2 (SV2), synaptophysin and postsynaptic density protein 95 (PSD-95) were used to probe the membranes. These results confirmed good purity and enrichment of our synaptosome fractions. Fractions F3 and F4 also reacted with antibodies against cytochrome c oxidase 4 (COX4) and succinate dehydrogenase A (SDHA) as the marker for mitochondria (Figure 3.1.4). This confirms the existence of intra-synaptic mitochondria within retrieved synaptosomes. However, the strongest reaction with these two antibodies was in fraction F5; it has been previously shown that this fraction includes extra-synaptic mitochondria (Dunkley, Jarvie et al. 2008). Using electron microscopy (EM), we also investigated the quality of the synaptosome fractions prepared from mouse cortices and spinal cords through electron microscopy (EM) (Figure 3.1.5). Here we combined fractions F3 and F4 as our synaptosome preparation. EM showed a good integrity of synaptosome membranes and presence of synaptic vesicles and mitochondria inside the synaptosome sacs (Figure 3.1.5A; arrow head and asterisk respectively), indicating the isolation of healthy and viable synaptosomes. Together, these results confirmed that our synaptosome fractions have good quality and high enrichment of central synapses from mouse CNS tissues.

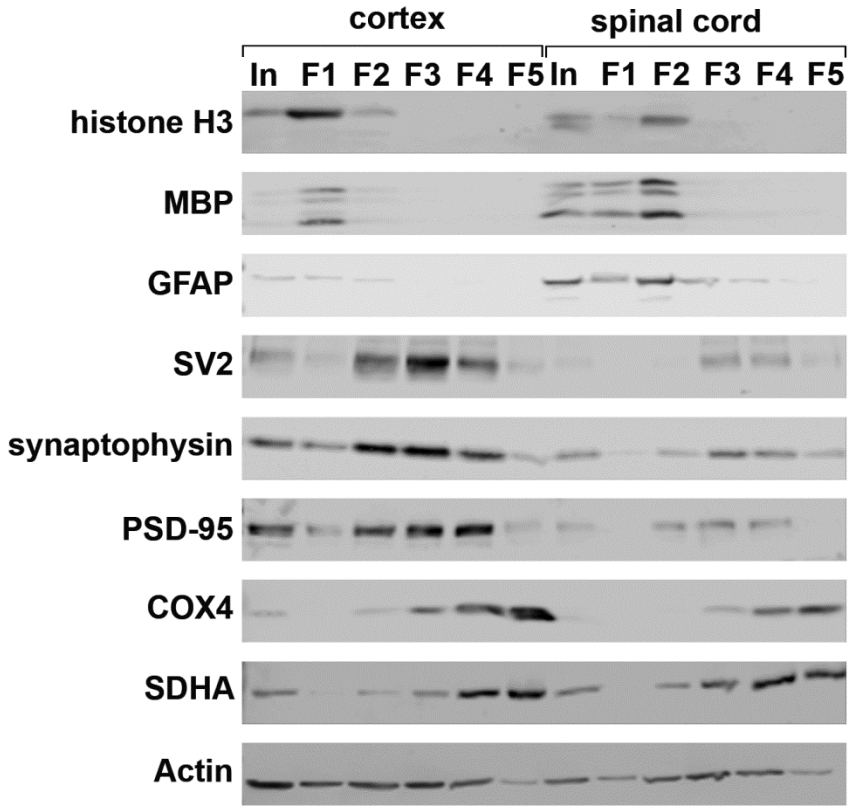

Figure 3.1.4. Synaptosomal fractions prepared from mouse cortex and spinal cord show good purity and enrichment. Using a Percoll non-continuous gradient, homogenates of mouse cortex and spinal cord were fractionated to five distinct fractions (F1-F5, In = input). Equal amounts of total protein were used from the input and each fraction to perform western blot analysis. Probing of the membranes with different antibodies showed a good purity and enrichment of synaptosomes within fractions F3 and F4 from mouse cortex and spinal cord. Histone H3 was used as a marker for nucleus; MBP and GFAP as markers for myelin andglia ; SV2, synaptophysin and PSD-95 as markers for synapses, and Cox4 and SDHA as markers for mitochondria. Please note that fractions F3 and F4 react with the antibodies specific for mitochondria protein. This indicates that the retrieved synaptosomes contain intra-synaptic mitochondria. However, fraction F5 showed the highest reaction with mitochondria markers; it has been shown that this fraction contains extra-synaptic mitochondria.

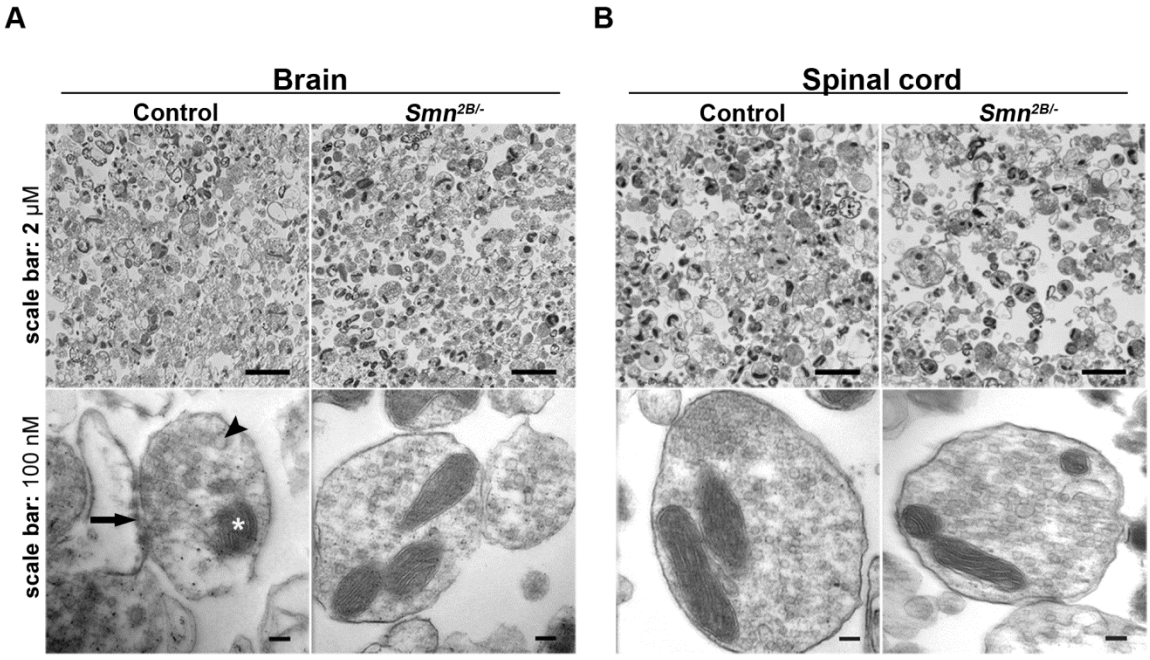

Figure 3.1.5. Synaptosome fractions prepared from cortices and spinal cords of *wt* and *Smn*$^{2B/-}$ mice show good membrane integrity and quality. Electron microscopic imaging on synaptosome fractions prepared from mouse cortex (A) and spinal cord (B) confirmed the integrity of the membrane of retrieved synaptosomes in *wt* and *Smn*$^{2B/-}$ mice. Note the synaptosome sacs contain synaptic vesicles and intra-synaptic mitochondria (arrow head and astrix respectively). Also some synaptosomes are still attached to the post-synaptic densities (arrow). (Synaptosome fractions were prepared by M. Eshraghi and EM imaging was done by Y. De Repentigny).

3.1.5. Quantitative mass spectrometry analysis of synaptosome fractions revealed widespread changes in protein levels within the synaptosomes prepared from spinal cords of *Smn*$^{2B/-}$ mice at a presymptomatic stage

Using crude synaptosome preparations, Wishart et al. showed widespread alterations in the proteome of synapses in the hippocampus of 'delta7 SMA' mice at a pre-symptomatic stage (Wishart, Mutsaers et al. 2014). After confirming high purity and quality of the synaptosomes, we also performed a proteomic analysis of the synaptosome samples prepared from spinal cords of *Smn*$^{2B/-}$ mice at a pre-symptomatic stage (PND11). We selected mouse spinal cords as the source of our synaptosome preparations because synapses within spinal cord of 'delta7 SMA' mice undergo pathologic alterations during pre-symptomatic stages (Mentis, Blivis et al. 2011). We prepared synaptosome fractions from spinal cords of four male *Smn*$^{2B/-}$ mice and four male control littermates at PND11; shown as a pre-symptomatic stage in *Smn*$^{2B/-}$ mice with BL6 background (Eshraghi, McFall et al. 2016).

Unbiased quantitative mass spectrometry (MS) techniques were used to determine the proteomics profile of *Smn*$^{2B/-}$ mice and their control littermates (n=3; ANOVA, $p < 0.05$ was considered significantly different from the controls) (for details please refer to Materials and Methods). Comparative analysis of MS results revealed widespread and consistent perturbations in the proteome of synaptosome preparations from PND11 *Smn*$^{2B/-}$ mice. From over 2,300 unique proteins identified by MS, the levels of 361 proteins were significantly altered more than 30% (i.e. a fold change of less than 0.7 or more than 1.3 of the controls) in synaptosomes isolated from *Smn*$^{2B/-}$ mice (49 proteins had lower levels, and 312 protein had higher levels in *Smn*$^{2B/-}$ mice than the controls) (Figure 3.1.6 and Supplementary Tables 4.1 and 4.2; only the proteins with significant alterations are shown).

To decipher which canonical molecular pathways are affected within synapses of spinal cords of *Smn*$^{2B/-}$ mice, we used the online program DAVID and conducted functional cluster analysis of the proteins that showed significant alterations within the MS results (Table 3.1.1). Our analysis revealed that the 'oxidative phosphorylation' pathway was dysregulated in synapses of spinal cords of *Smn*$^{2B/-}$ mice with the highest score. This was of special interest because we had previously shown that impairment of the 'oxidative phosphorylation' pathway correlates with vulnerability of motor neurons in *Smn*$^{2B/-}$ mice (Murray, Beauvais et al. 2015). In our analysis, pathways related to other neurodegenerative conditions (e.g. Parkinson's disease, Huntington's disease, and Alzheimer's disease) were also affected in *Smn*$^{2B/-}$ mice with high scores. 'Ribosome' was another pathway identified as altered in our analysis. We had shown before that genes involved in 'ribosome and RNA binding' are dysregulated in vulnerable motor neurons of *Smn*$^{2B/-}$ mice (Murray, Beauvais et al. 2015).

Also, our functional cluster analysis suggested that some important metabolic pathways were affected within synapses of spinal cords of *Smn*$^{2B/-}$ mice (Table 3.1.1). These included 'branched-chain amino acids' (BCAAs) metabolism, 'pyruvate' metabolism, 'fatty acid' (FA) metabolism, and 'glycolysis/gluconeogenesis' pathways. Interestingly, these metabolic pathways are also affected in other neuromuscular diseases like ALS (Carunchio, Curcio et al. 2010, Gray, Tompkins et al. 2014, Ngo and Steyn 2015, Ioannides, Ngo et al. 2016). Some pathways specific for synaptic functions were also affected in synaptosomes isolated from *Smn*$^{2B/-}$ mice. These included 'soluble NSF attachment protein receptors' (SNAREs) and 'long-term potentiation' pathways. Our analysis also showed that pathways involved in regulation of actin cytoskeleton and 'endocytosis' are also affected in synapses of spinal cords of *Smn*$^{2B/-}$ mice (Table 3.1.1).

Altogether our results showed that the proteome of central synapses is altered in *Smn*$^{2B/-}$ mice at a presymptomatic period. Since several pathways suggested by functional cluster analysis

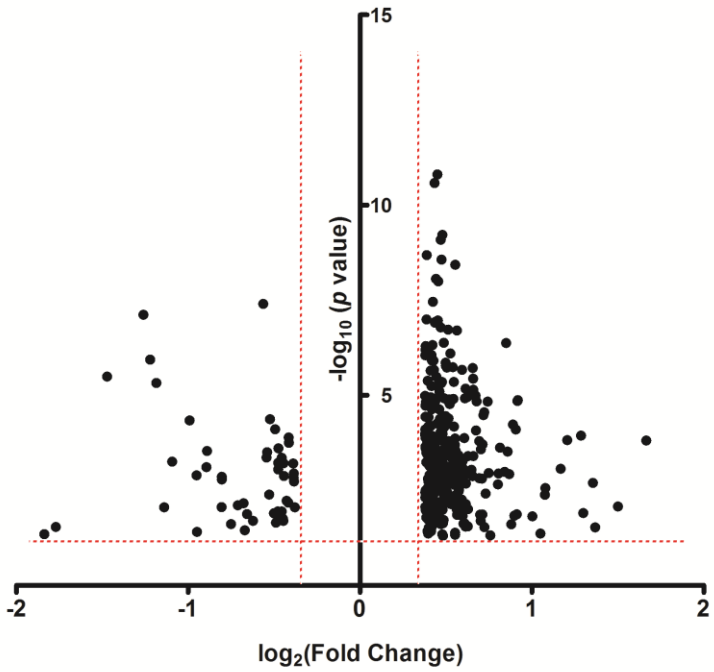

Figure 3.1.6. Volcano graph representing the proteins with more than 30% change in synaptosomes isolated from spinal cords of *Smn*$^{2B/-}$ mice. Unbiased proteomic analysis of synaptosome fractions from spinal cords of *Smn*$^{2B/-}$ mice (compared to their control littermates) revealed that from more than 2,300 unique proteins identified by mass spectrometry (not shown here), the levels of 361 proteins were changed more than 30% in *Smn*$^{2B/-}$ mice (n=3; ANOVA, $p<0.05$) (each black dot represents one protein). From these, the levels of 49 proteins were decreased with a fold change less than 0.7 (black dots to the left side of Y axis), and the levels of 313 proteins were increased with a fold change more than 1.3 (black dots to the right side of Y axis). X axis represents the $\log_2$ amount of fold change of each protein and Y axis represents the $-\log_{10}$ of *p* value of the ANOVA test performed for the alterations of each protein. A complete list of altered proteins in synapses of spinal cords of *Smn*$^{2B/-}$ mice is presented in Supplementary Tables 4.1 and 4.2.

pathway	proteins with more than 30% change in *Smn*$^{2B/-}$ mice	*p* value
Oxidative phosphorylation *	↑Atp6v1e2, ↑Atp6ap1, ↑Ndufa9, ↑Ndufs1, ↓Ndufs4, ↓Cox7a2l	1.14×10^{-31}
Parkinson's disease ¶	↑Ndufa9, ↑Ndufs1, ↑Slc25a31, ↓Ndufs4, ↓Cox7a2l	3.76×10^{-27}
Huntington's disease ¶	↑Ndufa9, ↑Ndufs1, ↑Cltc, ↑Dctn1, ↑Gnaq, ↑Slc25a31, ↓Ndufs4, ↓Cox7a2l	8.36×10^{-25}
Alzheimer's disease ¶	↑Ndufa9, ↑Ndufs1, ↑App, ↑Gnaq, ↑Ppp3ca, ↑Ppp3cb, ↓Ndufs4, ↓Cox7a2l	2.75×10^{-24}
Ribosome #	↑Rpl10a, ↑Rpl7, ↑RplP0, ↓Rpl12, ↓Rpl36	2.64×10^{-21}
branched-chain amino acids #	↑Dbt, ↑Abat, ↑Echs1, ↑Pcca, ↑Ivd, ↑Hadh	2.39×10^{-24}
pyruvate metabolism *	↑Acat1, ↑Acss1, ↑Aldh1b1, ↑Aldh2, ↑Grhpr, ↑Haghl, ↑Pck2	2.02×10^{-11}
fatty acid metabolism *	↑Acat1, ↑Acsl1, ↑Acsl3, ↑Acsl6, ↑Aldh1b1, ↑Aldh2, ↑Echs1, ↑Hadh, ↓Acaa1b	2.34×10^{-9}
glycolysis/gluconeogenesis *	↑Acss1, ↑Aldh1b1, ↑Aldh2, ↑Eno3, ↑Hk1, ↑Pck2, ↑Pfkp, ↑Pgk2	1.59×10^{-7}
SNARE in vesicular transport ₴	↑Stx8, ↑Vti1b, ↓Vamp3	4.2×10^{-7}
long-term potentiation ₴	↑Gnaq, ↑Ppp1cc, ↑Prkacb, ↑Ppp1r1a, ↑Ppp3ca, ↑Ppp3cb, ↓Rap1b, ↓Kras	1.25×10^{-6}
regulation of actin cytoskeleton₳	↑Msn,↑Tmsb4x, ↓Actn3, ↓Cfl1, ↓Cfl2, ↓Fgf1, ↓Ppp1cc, ↓Kras	2.08×10^{-5}
endocytosis ₳	↑Agap3, ↑Rab11fip5, ↑Rab5b, ↑Cltc, ↑Asap2, ↑Hspa1, ↑Nedd4, ↓Arfgap1	6.54×10^{-4}

Table 3.1.1. Several molecular signaling pathways are affected within synapses of spinal cords of *Smn*$^{2B/-}$ mice.

Functional cluster analysis of the proteins with more than 30% alterations in synaptosome fractions prepared from spinal cords of *Smn*$^{2B/-}$ mice revealed that several canonical pathways are dysregulated in these mice. Interestingly, *Smn*$^{2B/-}$ mouse model shares alterations in its synaptic proteomics with several other neurodegenerative conditions. Also, actin dynamism is affected in central synapses of *Smn*$^{2B/-}$ mice (↑ indicates increased levels, ↓ indicates decreased levels, * indicates pathways involved in energy metabolism, ¶ indicates pathways involved in neurodegenration, # indicates pathways involved in protein metabolism, ₴ indicates pathways involved in synaptic transmission, ₳ indicates pathways involved in regulation of actin cytoskeleton and vesicle trafficking).

3.1.6. The levels of some proteins involved in the regulation of actin cytoskeleton are altered in synaptosomes isolated from spinal cords of *Smn*$^{2B/-}$ mice at a presymptomatic stage

Impaired regulation of actin cytoskeleton has been proposed as one of the primary molecular defects in SMA (Tisdale and Pellizzoni 2015). The results from our proteomics analysis also showed that several proteins involved in the regulation of actin cytoskeleton are dysregulated in the synapses of spinal cords of *Smn*$^{2B/-}$ mice (Table 3.1.1). Using immunoblotting techniques, we measured the levels of these proteins (Figure 3.1.7). We found that the levels of α-actinin and KRAS were reduced and, the levels of Moesin were increased in synaptosomes isolated from spinal cords of PND11 *Smn*$^{2B/-}$ mice, confirming the results from the MS analysis (n=3; paired t test, $p < 0.05$). We did not observe any significant difference in the levels of FGF1, Cofilin1 and Cofilin2 in synaptosomes isolated from spinal cords of PND11 *Smn*$^{2B/-}$ mice; although, a decreasing trend was observed in the levels of Cofilin1 (n=3; paired t test, $p >0.05$) (Figure 3.1.7B).

We also looked at the levels of some other actin binding proteins which have a role in actin dynamics (i.e. assembly/disassembly of actin filaments) in the synaptosomes isolated from spinal cords of PND11 *Smn*$^{2B/-}$ mice (Figure 3.1.8). We observed that that the levels of Plastin 3 and Arp2 were reduced in synaptosomes isolated from spinal cords of PND11 *Smn*$^{2B/-}$ mice (n=3; paired t test, $p < 0.05$).

A

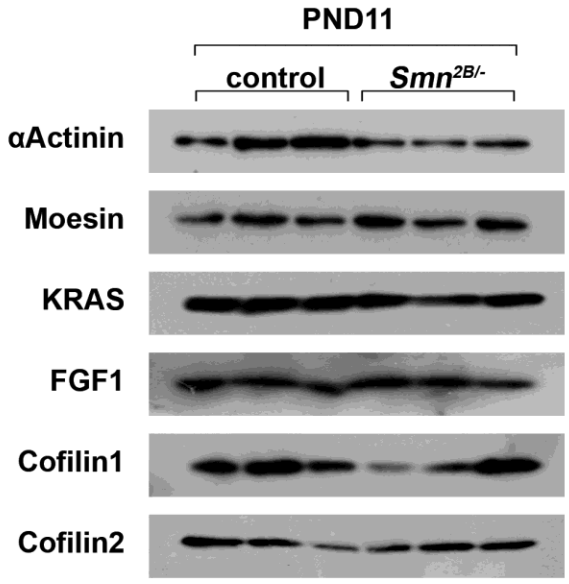
PND11
control
Smn2B/-
αActinin
Moesin
KRAS
FGF1
Cofilin1
Cofilin2

B

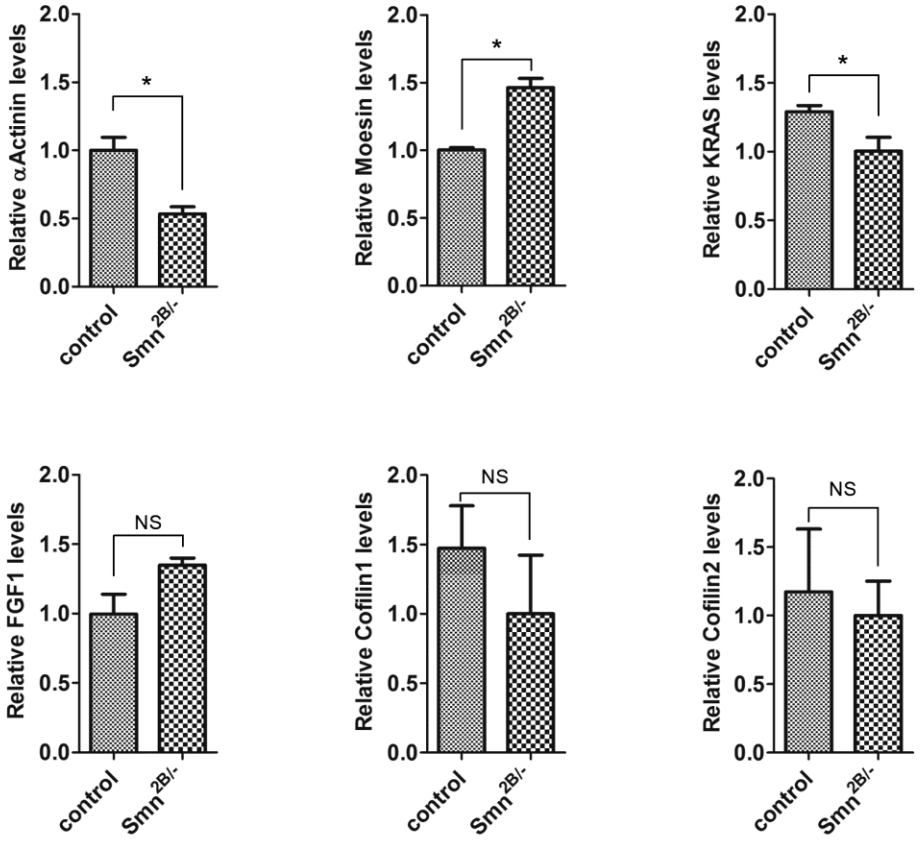
Relative αActinin levels
Relative Moesin levels
Relative KRAS levels
Relative FGF1 levels
Relative Cofilin1 levels
Relative Cofilin2 levels
2.0
1.5
1.0
0.5
0.0
*
NS
control
Smn2B/-

Figure 3.1.7. The levels of some proteins involved in the regulation of actin cytoskeleton are altered within synapses of spinal cords of *Smn*$^{2B/-}$ mice at a presymptomatic stage.

A) Representative images of immunoblotting experiments on synaptosome fractions prepared from spinal cords of *Smn*$^{2B/-}$ mice and their control littermates at PND11. B) Quantification of immunoblotting images showed decrease of the levels of α-actinin and KRAS while the levels of Moesin are increased in synapses of spinal cord of *Smn*$^{2B/-}$ mice at PND11 (n=3; paired t test, $p < 0.05$ was considered as significant). * indicates statistically different.

A

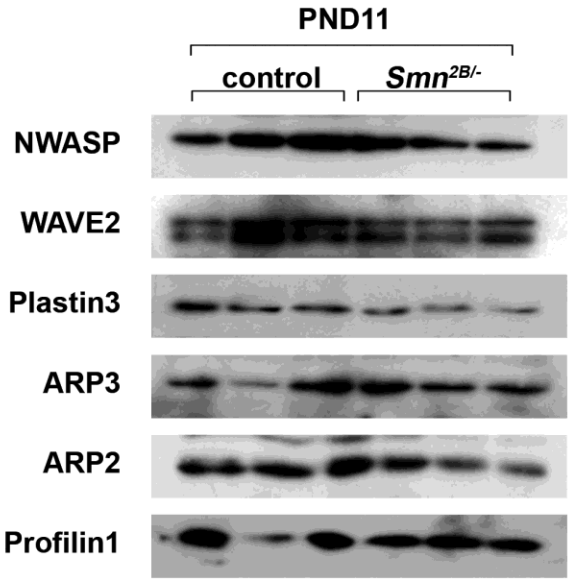
PND11
control
Smn2B/-
NWASP
WAVE2
Plastin3
ARP3
ARP2
Profilin1

B

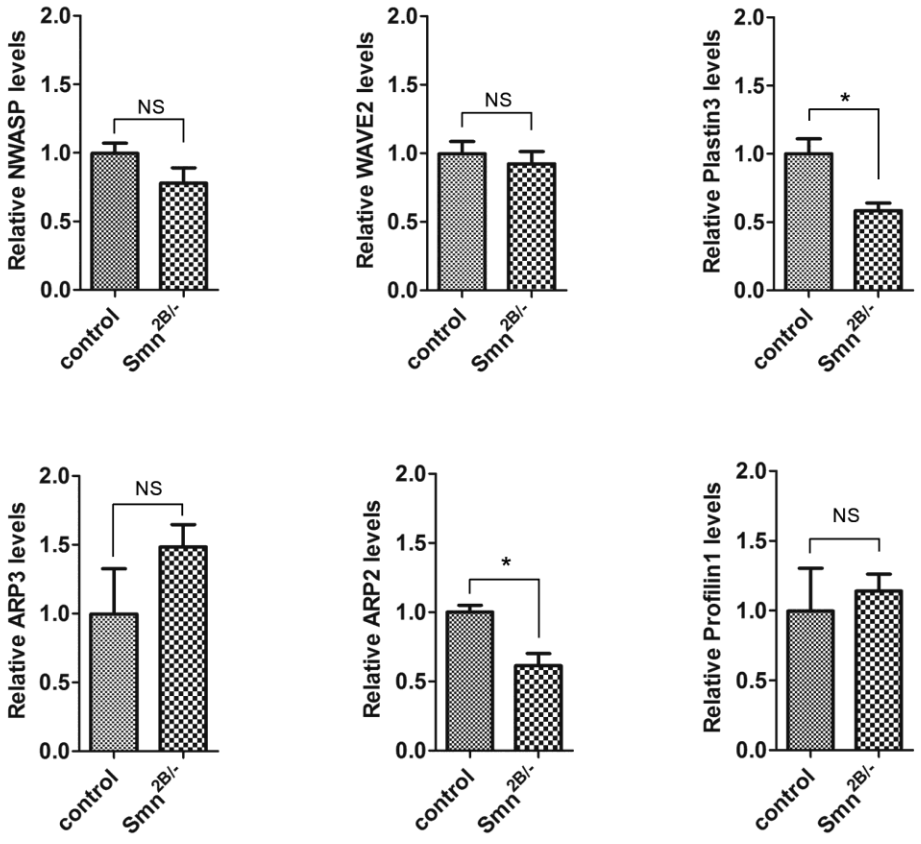
Relative NWASP levels
NS
Relative WAVE2 levels
NS
Relative Plastin3 levels
*
Relative ARP3 levels
NS
Relative ARP2 levels
*
Relative Profilin1 levels
NS
2.0
1.5
1.0
0.5
0.0
control
Smn2B/-

Figure 3.1.8. The levels of some actin binding proteins are altered within synapses of spinal cords of *Smn*$^{2B/-}$ mice at a presymptomatic stage.
A) Representative images of immunoblotting experiments on synaptosome fractions prepared from spinal cords of *Smn*$^{2B/-}$ mice and their control littermates at PND11. B) Quantification of immunoblotting images showed decrease of the levels of Plastin 3 and ARP2 (while the levels of other actin binding proteins are not changed) in synapses of spinal cord of *Smn*$^{2B/-}$ mice at PND11 (n=3; paired t test, $p < 0.05$ was considered as significant). * indicates statistically different.

3.1.7. Synaptic proteins are dysregulated within synapses of spinal cords and cortices of *Smn$^{2B/-}$* mice

The results from the proteomics experiment suggested that the functions of synapses within spinal cords maybe dysregulated in *Smn$^{2B/-}$* mice. To investigate this phenomenon in more depth, we looked at the levels of some pre-synaptic proteins in synaptosome fractions prepared from spinal cords of *Smn$^{2B/-}$* mice at PND11 and PND16 using immunoblotting techniques (Figure 3.1.9). At PND11, we did not find any alteration in the levels of most pre-synaptic proteins (including SV2, synaptotagmin, synaptophysin, SNAP25). This indicates that probably the number of synapses and synaptic vesicles were not changed within spinal cords of *Smn$^{2B/-}$* mice at this age. However, the level of amphiphysin (a protein involved in synaptic vesicle endocytosis) was substantially higher in synapses of spinal cords of *Smn$^{2B/-}$* mice at PND 11 (n=3; paired t test, $p < 0.05$). At PND16, the levels of a few pre-synaptic proteins (including SV2 and synaptotagmin) are increased in synapses of spinal cords of *Smn$^{2B/-}$* mice. Interestingly, at this age the levels of amphiphysin within synapses of spinal cords of *Smn$^{2B/-}$* mice were decreased (n=3; paired t test, $p < 0.05$) (Figure 3.1.9B).

We repeated these experiments using synaptosome fractions prepared from cortices of PND11 and PND16 *Smn$^{2B/-}$* mice (Figure 3.1.10). We observed an almost similar pattern of changes in the levels of pre-synaptic proteins in synapses of cortices of *Smn$^{2B/-}$* mice; at PND11 amphiphysin was increased, and at PND16, SV2 and synaptophysin showed upregulation while amphiphysin was significantly reduced (n=3; paired t test, $p < 0.05$). Our results showed that presynaptic proteins in central synapses of *Smn$^{2B/-}$* mice were dysregulated mainly at a symptomatic stage but not at a pre-symptomatic period. However, amphiphysin levels changed in a specific manner in synapses of both spinal cords and cortices of *Smn$^{2B/-}$* mice at both pre-

symptomatic and symptomatic periods. This suggests a specific role for amphiphysin in the biology of SMA.

The activity of ERK1/2-synapsin pathway has an important role in synapse formation and function (Giachello, Fiumara et al. 2010). We investigated the activity of this pathway within synaptosome fractions of mouse spinal cords by looking at the relative levels of phosphorylated ERK1/2 and synapsin at PND 11 and PND16 (Supplementary Figure 4.2). Our analysis did not show any alteration in the relative levels of phospho-ERK1/2 or phospho-synapsin (n=3; paired t test, $p > 0.05$) (Supplementary Figure 4.2B). This suggests that the ERK1/2-synapsin pathway is not aberrantly activated within synapses of spinal cords of $Smn^{2B/-}$ mice.

A

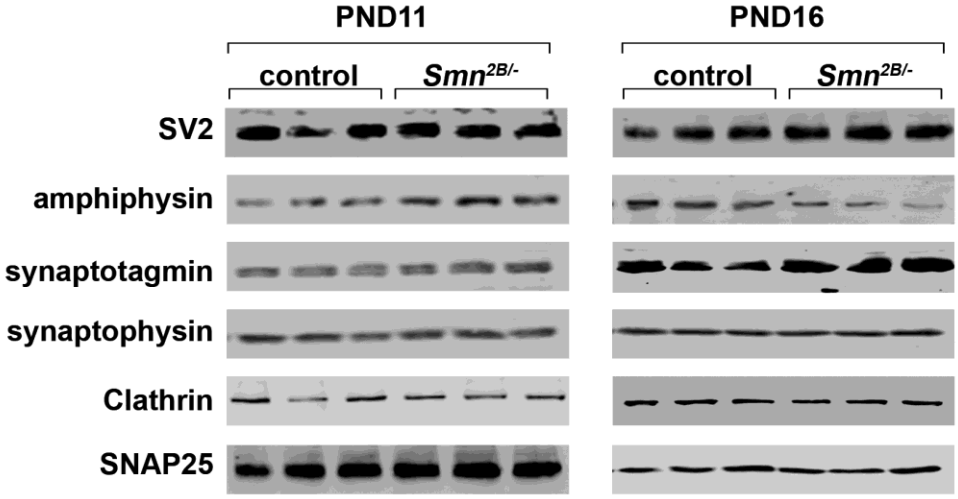
PND11
PND16
control
Smn2B/-
control
Smn2B/-
SV2
amphiphysin
synaptotagmin
synaptophysin
Clathrin
SNAP25

B

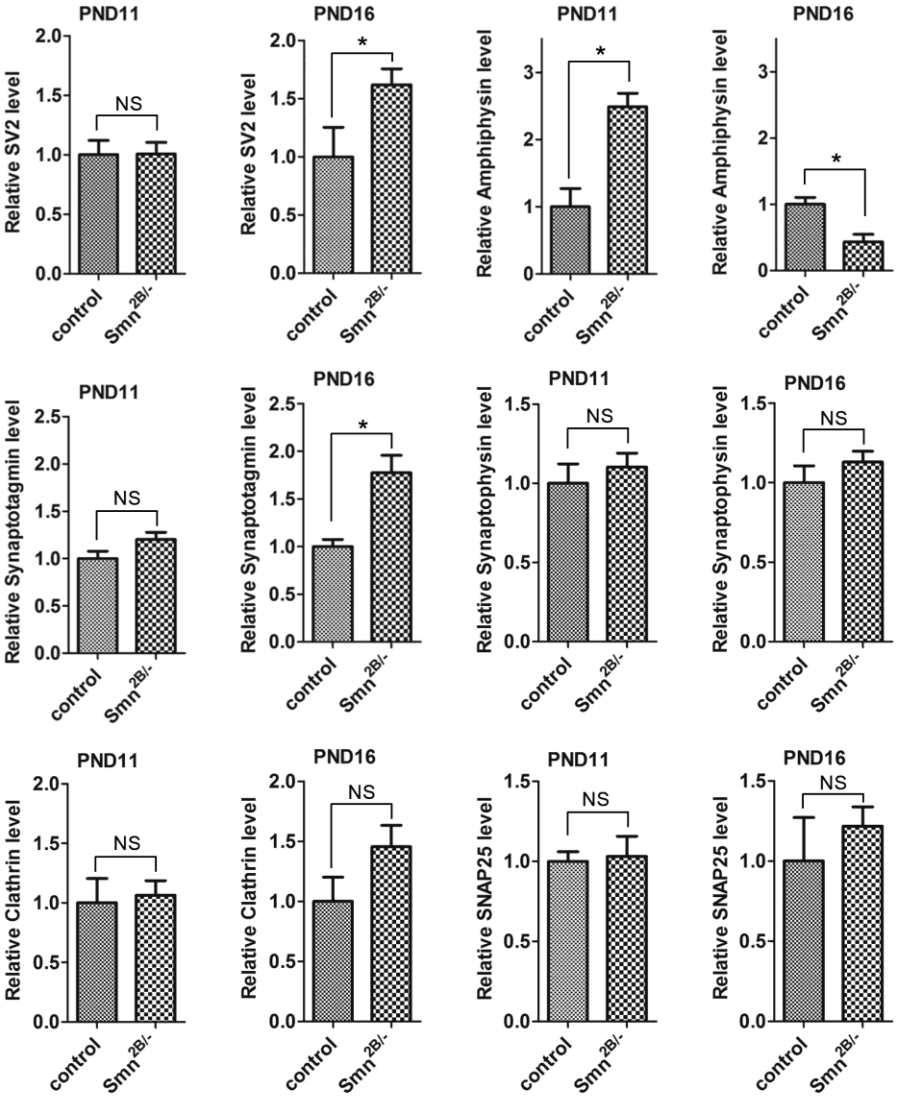
PND11
PND16
PND11
PND16
Relative SV2 level
Relative SV2 level
Relative Amphiphysin level
Relative Amphiphysin level
NS
*
*
*
control
Smn2B/-
PND11
PND16
PND11
PND16
Relative Synaptotagmin level
Relative Synaptotagmin level
Relative Synaptophysin level
Relative Synaptophysin level
NS
*
NS
NS
PND11
PND16
PND11
PND16
Relative Clathrin level
Relative Clathrin level
Relative SNAP25 level
Relative SNAP25 level
NS
NS
NS
NS

Figure 3.1.9. The levels of some pre-synaptic proteins are altered within synapses of spinal cords of *Smn*$^{2B/-}$ mice.
A) Representative images of immunoblotting experiments on synaptosome fractions prepared from spinal cords of *Smn*$^{2B/-}$ mice and their control littermates at PND11 and PND16. B) Quantification of immunoblotting images showed alteration of the levels of some synaptic proteins at PND16 (i.e. symptomatic stage). However, at PND11 only the level of amphiphysin is altered in synapses of spinal cord of *Smn*$^{2B/-}$ mice. In contrast to SV2 and synaptotagmin, the level of amphiphysin is decreased at PND16 while its level shows a remarkable increase at PND11 (i.e. pre-symptomatic stage).

A

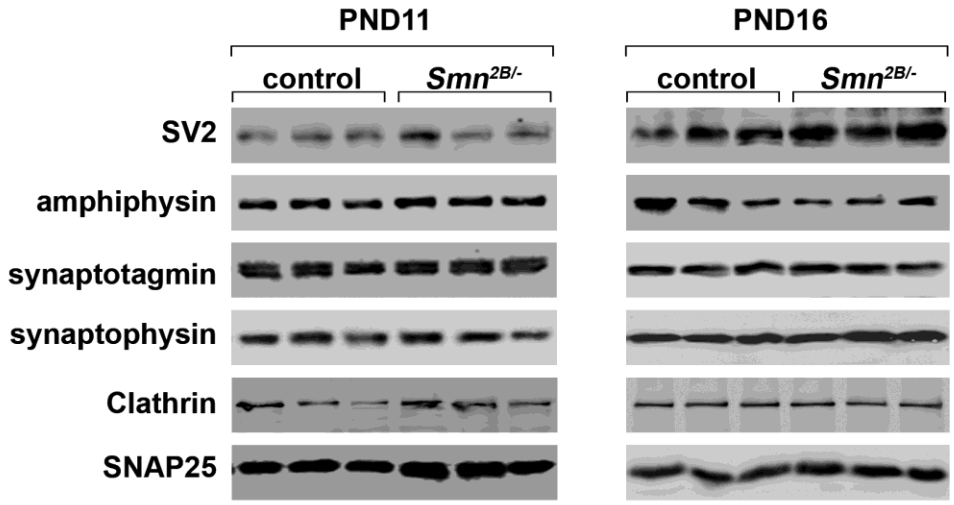
PND11
PND16
control
Smn2B/-
control
Smn2B/-
SV2
amphiphysin
synaptotagmin
synaptophysin
Clathrin
SNAP25

B

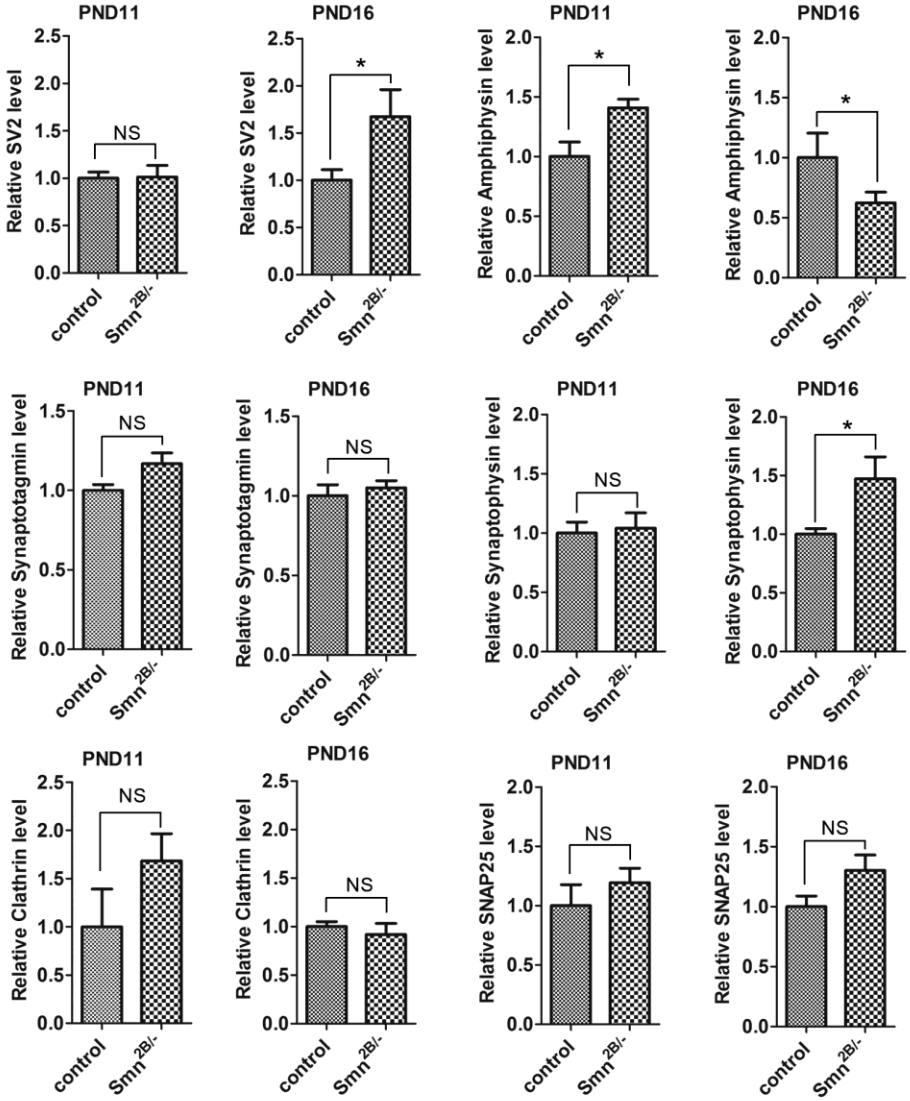
PND11
PND16
PND11
PND16
Relative SV2 level
Relative SV2 level
Relative Amphiphysin level
Relative Amphiphysin level
NS
*
*
*
control
Smn2B/-
PND11
PND16
PND11
PND16
Relative Synaptotagmin level
Relative Synaptotagmin level
Relative Synaptophysin level
Relative Synaptophysin level
NS
NS
NS
*
PND11
PND16
PND11
PND16
Relative Clathrin level
Relative Clathrin level
Relative SNAP25 level
Relative SNAP25 level
NS
NS
NS
NS

Figure 3.1.10. The levels of some pre-synaptic proteins are altered within synapses of cortex of *Smn*$^{2B/-}$ mice. A) Representative images of immunoblotting experiments on synaptosome fractions prepared from cortices of *Smn*$^{2B/-}$ mice and their control littermates at PND11 and PND16. B) Quantification of immunoblotting images showed alteration of the levels of some synaptic proteins at PND16 (i.e. symptomatic stage). At PND11, the level of amphiphysin is increased in synapses of spinal cords of *Smn*$^{2B/-}$ mice. And like spinal cord of *Smn*$^{2B/-}$ mouse (Figure 3.7), SV2 and synaptophysin are increased at PND16 while the level of amphiphysin is decreased at PND16 (i.e. pre-symptomatic stage).

3. 2- Effect of genetic background on the phenotype of the *Smn*$^{2B/-}$ mouse model of spinal muscular atrophy

This part is adapted from:

Eshraghi M, McFall E, Gibeault S, Kothary R. Effect of genetic background on the phenotype of the Smn2B/- mouse model of spinal muscular atrophy. Hum Mol Genet. 2016 Oct 15; 25(20):4494-4506. doi: 10.1093/hmg/ddw278. PubMed PMID: 28172892.

3.2.1. BL6 *Smn*$^{2B/-}$ mice have a longer life span than FVB *Smn*$^{2B/-}$ mice

Previously, we showed that *Smn*$^{2B/-}$ mice in a mixed background recapitulate an SMA-like phenotype, with a median survival of 28 days while a small fraction (about 10%) survive for more than 100 days (Bowerman, Beauvais et al. 2010, Bowerman, Murray et al. 2012, Bowerman, Murray et al. 2012). Here, we assessed the survival of congenic *Smn*$^{2B/-}$ mice in either BL6 or FVB backgrounds. For this study, we set up breeder cages and mated congenic *Smn*$^{2B/2B}$ mice (from the 6th generation of backcrossing) to congenic *Smn*$^{+/-}$ mice of the same relevant background. We monitored the offspring on a daily basis for survival and weight. The mice that did not show any phenotype after postnatal day (PND) 21 were genotyped to rule out the presence of any *Smn*$^{2B/-}$ mice within this group. Kaplan-Meier analysis revealed that BL6 *Smn*$^{2B/-}$ mice had a median survival of 25 days (range of 19 to 35 days, n=19) and FVB *Smn*$^{2B/-}$ mice had a median survival of 19 days (range of 17 to 21 days, n=22) (Fig. 3.2.1A). There was a significant difference in median survival between BL6 *Smn*$^{2B/-}$ and FVB *Smn*$^{2B/-}$ mice (Gehan-Breslow-Wilcoxon Test, $p<0.0001$).

Since breeding cages with FVB background had larger litter sizes (average of 9.1±2.4 pups for FVB *vs.* 6.2±2.1 pups for BL6, $p<0.05$), we tested whether this correlated with the shorter life span in the FVB background. We plotted the survival of each *Smn*$^{2B/-}$ mouse versus the size of the correspondent litter (Figure 3.2.1B). As shown, there was no correlation between litter size and the length of survival for *Smn*$^{2B/-}$ mice in the FVB background ($R^2= 0.03055$, $p>0.05$). To our surprise, within the BL6 *Smn*$^{2B/-}$ mice, there was a positive correlation between litter size and increased survival ($R^2= 0.3419$, $p<0.01$).

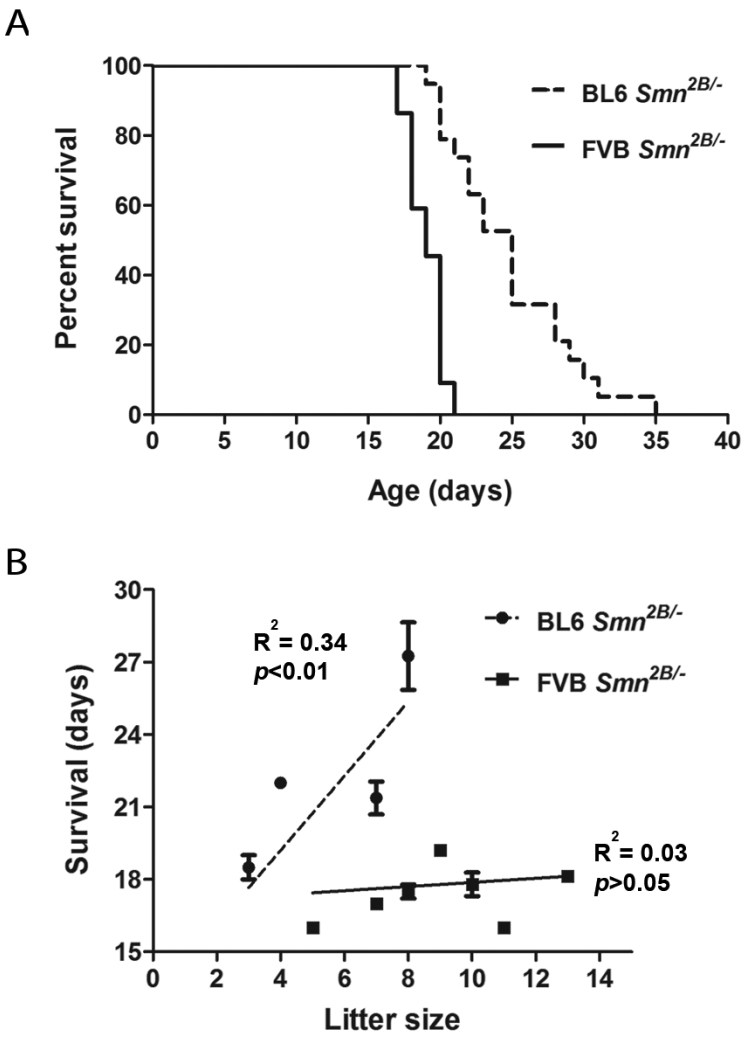

Figure 3.2.1. BL6 *Smn*$^{2B/-}$ mice have a longer life span than FVB *Smn*$^{2B/-}$ mice.

A) Kaplan-Meier survival curve showing that BL6 *Smn*$^{2B/-}$ mice have a median survival of 25 days (n=19) while FVB *Smn*$^{2B/-}$ mice have a median survival of 19 days (n=22). The difference in survival was significant between the two strains (Gehan-Breslow-Wilcoxon Test, $p<0.0001$). No death was observed in control littermates (not shown). B) The shorter life span of FVB *Smn*$^{2B/-}$ mice is not due to larger litter sizes in this strain. In the FVB strain (solid line), there was no correlation between the size of the litters and survival of *Smn*$^{2B/-}$ mice (Goodness of Fit test, $R^2=0.03$ $p>0.05$). Interestingly, the bigger litter size in the BL6 strain (dashed line) correlated with longer survival of *Smn*$^{2B/-}$ mice (Goodness of Fit test, $R^2=0.34$ $p<0.01$).

3.2.2. FVB *Smn*$^{2B/-}$ mice lose weight more rapidly than BL6 *Smn*$^{2B/-}$ mice

Starting on day three after birth, body weights for mice were measured on a daily basis. The average weight of *Smn*$^{2B/-}$ mice is significantly lower than control mice after PND11 for FVB and after PND12 for BL6 (two way ANOVA, $p<0.05$) (Figure 3.2.2A and B). After PND15 the average weight of *Smn*$^{2B/-}$ mice starts to decrease in both backgrounds. To investigate if the rate of weight loss is different between the two backgrounds, we calculated the weight of each *Smn*$^{2B/-}$ mouse at each time point as a percentage of the average weight of the relevant control mice at that time point (Figure 3.2.2C). Beginning at PND16, FVB *Smn*$^{2B/-}$ mice lost weight continuously and reached 50% of the average weight of controls at PND18. By comparison, the weight loss rate is lower for BL6 *Smn*$^{2B/-}$ mice, which reached 50% of the average weight of controls at PND22.

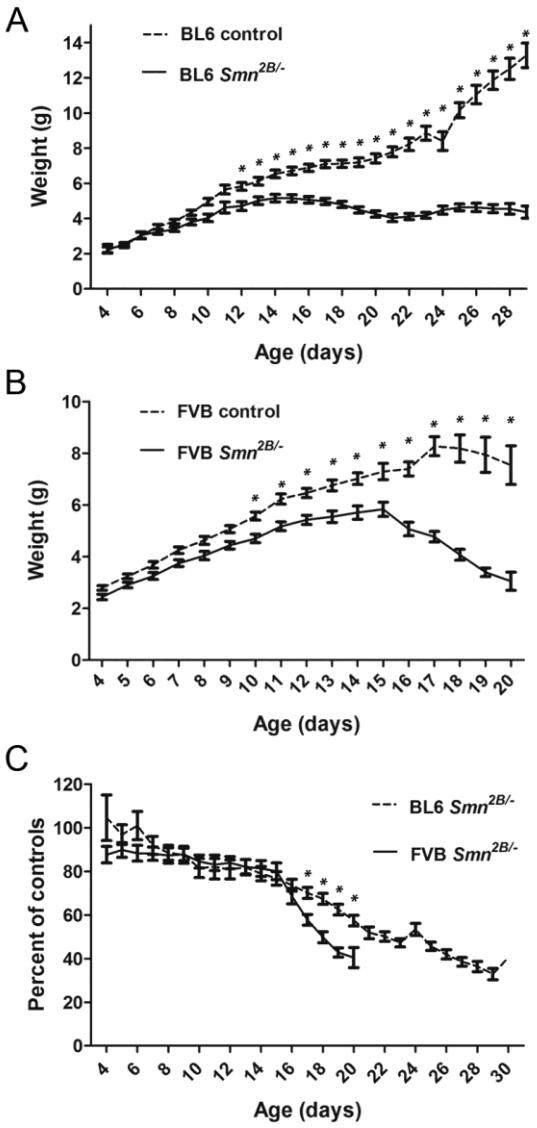

Figure 3.2.2. FVB *Smn*$^{2B/-}$ mice lose weight more rapidly than BL6 *Smn*$^{2B/-}$ mice.

A and B) Analysis of daily weights showed that *Smn*$^{2B/-}$ mice are smaller than their control littermates after PND12 in the BL6 background (n=19) (A), and after PND10 in the FVB background (n=22) (B), (two way ANOVA, $p<0.05$). C) Comparing daily weights of BL6 and FVB *Smn*$^{2B/-}$ mice (represented as a percentage of the average of the weight of the control littermates) showed that after PND15, FVB *Smn*$^{2B/-}$ mice lose weight at a faster pace than BL6 *Smn*$^{2B/-}$ mice (two way ANOVA, $p<0.05$). * indicates significant difference between *Smn*$^{2B/-}$ mice and their control littermates in A and B, and between BL6 and FVB *Smn*$^{2B/-}$ mice in C.

3.2.3. Muscle strength is reduced earlier in FVB *Smn*$^{2B/-}$ mice than in BL6 *Smn*$^{2B/-}$ mice

Progressive muscle weakness and atrophy are clinical hallmarks of SMA (Pearn 1978). In SMA model mice, muscle strength is also reduced early in the course of the disease (Boyer, Murray et al. 2013). To evaluate the muscle strength in *Smn*$^{2B/-}$ mice, we used two standard motor tests recommended by Treat-NMD: 'inverted mesh grip test' and 'hind limb suspension test' (Sumner 2010, Sumner 2011). Inverted mesh grip test evaluates the strength of all mouse limbs by suspending the animal from an inverted mesh. We found that PND13 is the first time that pups are able to suspend from the inverted mesh (data not shown). After PND13, the average latency to fall for BL6 control mice was increased continuously and reached 100% of the goal (i.e. 60 sec) at PND23 (repeated measures ANOVA, $p<0.05$) (Figure 3.2.3A). This trend was also the same for FVB control mice however the test was only performed until P21 (70% of the goal) due to the lower maximum survival of FVB *Smn*$^{2B/-}$ mice (Figure 3.2.3B). The latency to fall for *Smn*$^{2B/-}$ mice in both backgrounds was not significantly different relative to controls at PND13 (repeated measures ANOVA, $p>0.05$). However, the difference in hang time between *Smn*$^{2B/-}$ mice and their control littermates did reach significance at PND17 for the BL6 background and at PND15 in the FVB background (two way ANOVA, $p<0.05$) (Figure 3.2.3A and B).

In the hind limb suspension test (also known as the tube test), the average time to fall for both BL6 and FVB control mice was unchanged until PND13 (repeated measures ANOVA, $p>0.05$) and then increased at PND15 and reached 100% of the goal (60 sec) at PND17 (repeated measures ANOVA, $p<0.05$) (Figure 3.2.3C and D). By comparison, hanging time started to decrease significantly at PND13 for BL6 *Smn*$^{2B/-}$ mice and at PND11 for FVB *Smn*$^{2B/-}$ mice (repeated measures ANOVA, $p<0.05$) (Figure 3.2.3C and D). The difference between *Smn*$^{2B/-}$

mice and their control littermates was significant at PND15 for both BL6 and FVB lines (two way ANOVA, $p<0.05$). Thus, collectively these results indicate that muscle weakness occurs at an earlier age in FVB than in BL6 *Smn*$^{2B/-}$ mice.

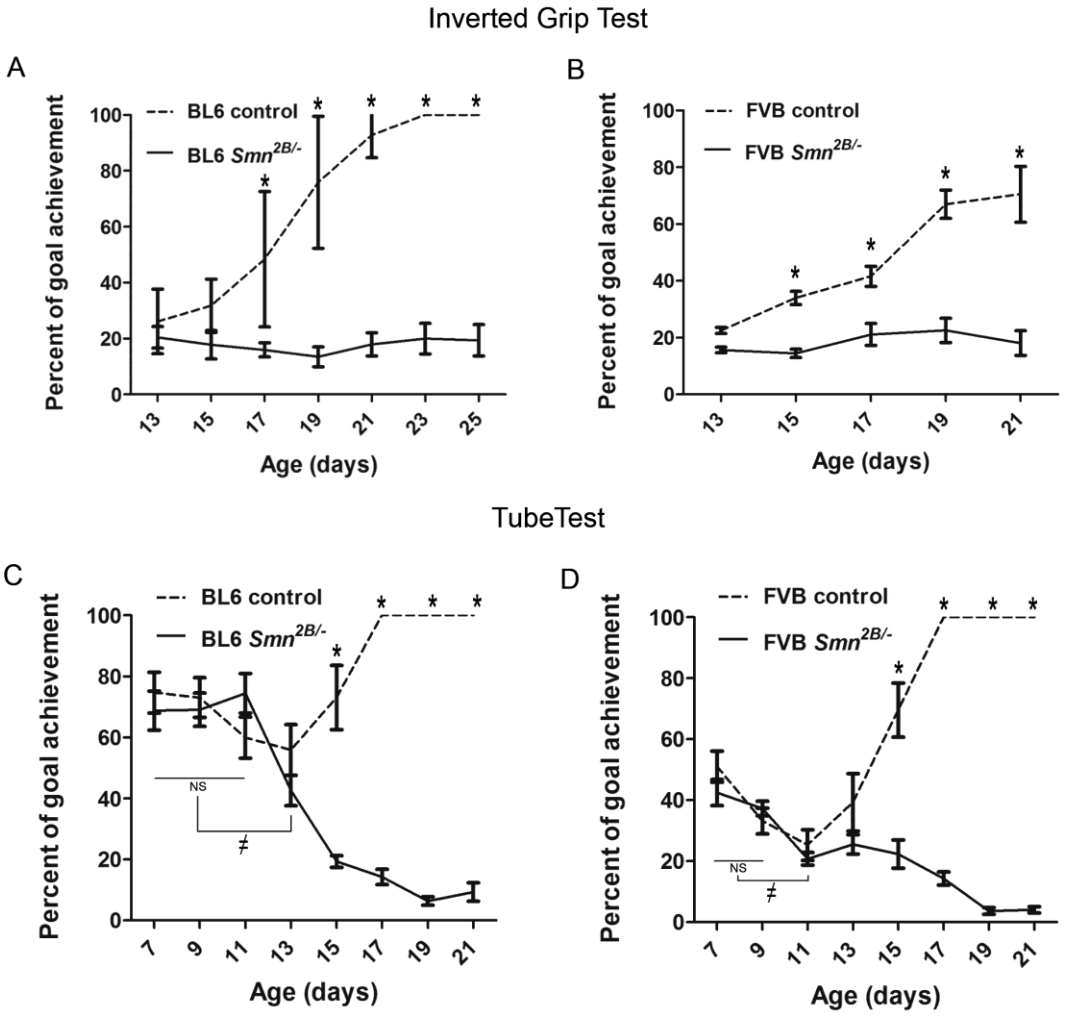
Inverted Grip Test
A
B
BL6 control
BL6 Smn2B/-
FVB control
FVB Smn2B/-
Percent of goal achievement
Age (days)
TubeTest
C
D
NS
≠

Figure 3.2.3. Muscle weakness occurs at earlier ages in FVB *Smn*$^{2B/-}$ mice than in BL6 *Smn*$^{2B/-}$ mice.

A and B) Analysis of the results from inverted mesh grip tests showing that *Smn*$^{2B/-}$ mice had a shorter latency to fall than their control littermates after PND17 in BL6 *Smn*$^{2B/-}$ mice (A) and after PND15 in FVB *Smn*$^{2B/-}$ mice (B), (two way ANOVA, $p<0.05$). There were no significant changes in latency to fall times of *Smn*$^{2B/-}$ mice (solid lines) of both strains during the test period (repeated measures ANOVA, $p>0.05$). C and D) Analysis of hind limb suspension test (also known as tube test) revealed that *Smn*$^{2B/-}$ mice suspended from their hind limbs had a shorter latency than their control littermates after PND15 in both strains. The latency to fall time of FVB *Smn*$^{2B/-}$ mice was significantly shorter at PND11 than earlier ages (D, ≠ on the solid line). In BL6 *Smn*$^{2B/-}$ mice the latency to fall time was shorter at PND13 than earlier ages (C, ≠ on the solid line) (repeated measures ANOVA, $p<0.05$). The goal was set as 60 seconds for the inverted grip test (A and B), and as 60 seconds or climbing out of the tube for the tube test (C and D). * indicates significant difference between *Smn*$^{2B/-}$ mice and their control littermates.

3.2.4. Muscle fiber cross-sectional area is reduced earlier in FVB *Smn*$^{2B/-}$ mice than in BL6 *Smn*$^{2B/-}$ mice

Previously we showed that average myofiber area is remarkably reduced in mixed background *Smn*$^{2B/-}$ mice at PND21 (Bowerman, Beauvais et al. 2010, Bowerman, Murray et al. 2012). Here, we investigated myofiber caliber in the tibialis anterior (TA) skeletal muscle at earlier time points in the congenic *Smn*$^{2B/-}$ mice (Figure 3.2.4). The fraction of small myofibers (200-350 μm^2) was not increased in BL6 *Smn*$^{2B/-}$ mice at PND11 (two way ANOVA, $p>0.05$) but is significantly higher at PND16 compared to the control littermates (two way ANOVA, $p<0.05$) (Figure 3.2.4C). In contrast, the fraction of small myofibers was significantly increased in FVB *Smn*$^{2B/-}$ mice at both PND11 and PND16 relative to control pups (two way ANOVA, $p<0.05$) (Figure 3.2.4D). We further analyzed the average myofiber cross-sectional area and found that it is reduced significantly at PND11 in FVB *Smn*$^{2B/-}$ mice and continues to be smaller at PND16 (Mann Whitney test, $p<0.05$) (Table 1). In BL6 *Smn*$^{2B/-}$ mice however, the average myofiber area is not decreased at PND11 but reduced significantly at PND16 (Mann Whitney test, $p<0.05$). We also found that at PND16 myofiber atrophy is more severe in FVB than BL6 *Smn*$^{2B/-}$ mice (54.6±16.8% vs. 72.4±18.42% of the average of myofiber areas of controls respectively, $p<0.05$).

We further investigated myofiber atrophy at an earlier age (PND9) in FVB *Smn*$^{2B/-}$ mice (Supplementary Figure 4.3) to study a pre-phenotypic time point. Although the fraction of small myofibers (250 μm^2) was slightly increased (Supplementary Figure 4.3B), the average myofiber cross-sectional area was not significantly different from the control littermates (Mann Whitney test, $p>0.05$) (Supplementary Figure 4.3C). This might indicate that PND9 is an early stage of myofiber atrophy in FVB *Smn*$^{2B/-}$ mice.

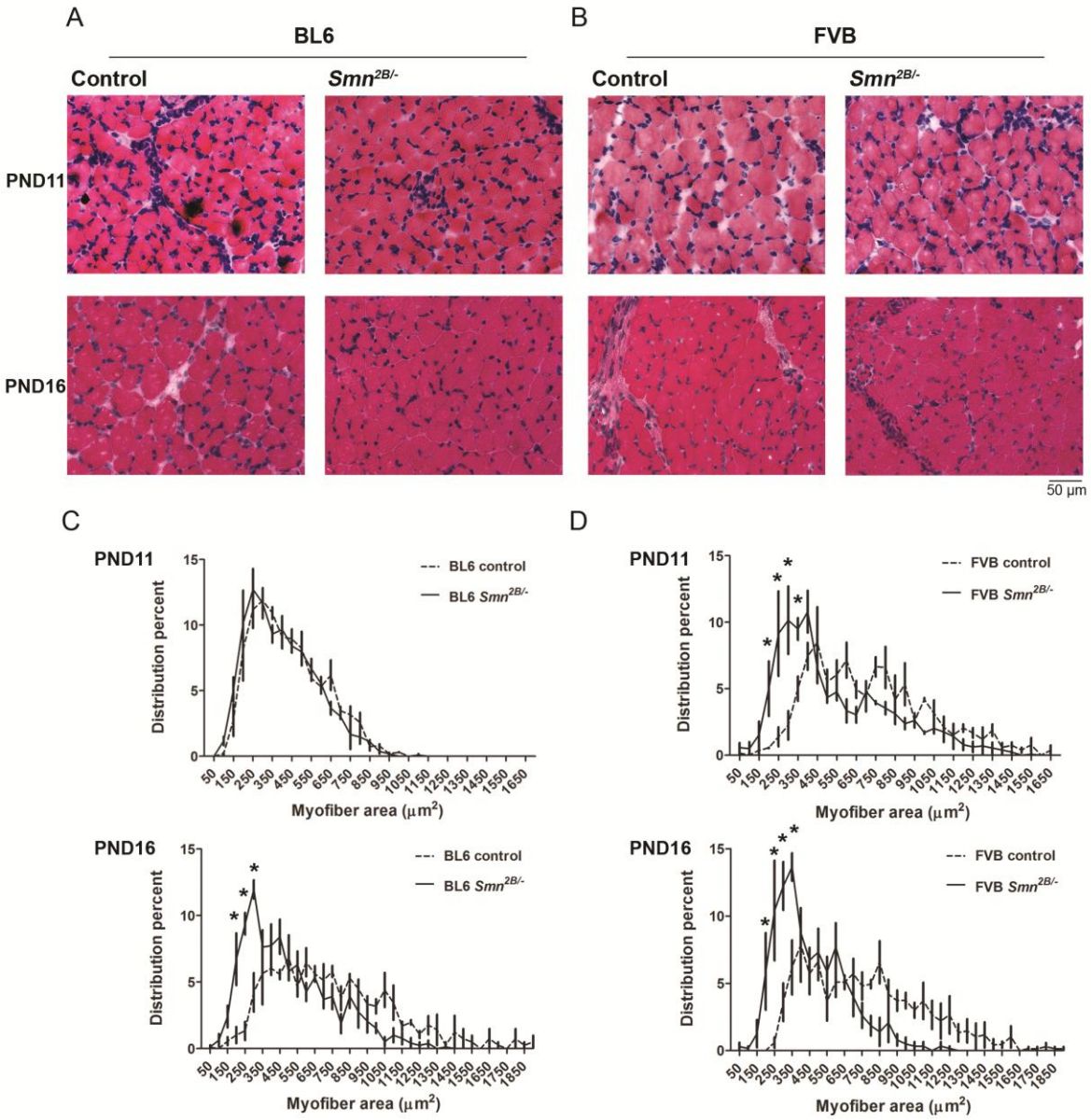
A
BL6
Control
Smn2B/-
PND11
PND16
B
FVB
Control
Smn2B/-
50 µm
C
PND11
BL6 control
BL6 Smn2B/-
Distribution percent
Myofiber area (µm2)
PND16
BL6 control
BL6 Smn2B/-
Distribution percent
Myofiber area (µm2)
D
PND11
FVB control
FVB Smn2B/-
Distribution percent
Myofiber area (µm2)
PND16
FVB control
FVB Smn2B/-
Distribution percent
Myofiber area (µm2)

Figure 3.2.4. Muscle fiber cross-sectional area is reduced earlier in FVB *Smn*$^{2B/-}$ mice than in BL6 *Smn*$^{2B/-}$ mice.

A and B) Representative images of H&E stained TA muscles from BL6 mice (A) and FVB mice (B) at PND11 and PND16. C and D) Quantification and analysis of myofiber cross-sectional areas showed that at PND11 there was no difference in the distribution of myofibers of BL6 *Smn*$^{2B/-}$ mice (n=3, two way ANOVA, $p>0.05$). However, at PND11 there is a higher percentage of small caliber myofibers in FVB *Smn*$^{2B/-}$ mice compared to their control littermates, and at PND16, the fractions of smaller myofibers are significantly higher in both BL6 and FVB *Smn*$^{2B/-}$ mice (n=3, two way ANOVA, $p<0.05$). * indicates significant difference between *Smn*$^{2B/-}$ mice and their control littermates.

3.2.5. Motor neuron loss happens earlier in FVB *Smn*$^{2B/-}$ mice than in BL6 *Smn*$^{2B/-}$ mice

We investigated motor neuron (MN) loss in lumbar spinal cords of congenic *Smn*$^{2B/-}$ mice by choline acetyltransferase (ChAT) immunostaining (Figure 3.2.5). We counted MN cell bodies in spinal cord sections from the *Smn*$^{2B/-}$ mice at different time points. At PND11 there is no difference in the number of motor neurons (MNs) between BL6 *Smn*$^{2B/-}$ mice and their control littermates (Figure 3.2.5A and C). At PND16 and PND19 however, a decrease in the number of MNs in BL6 *Smn*$^{2B/-}$ mice was observed when compared to control littermates (Figure 3.2.5A and C). Since muscle atrophy began earlier in FVB *Smn*$^{2B/-}$ mice, we counted the number of MNs in these mice at earlier time points. There was no decrease in the number of MNs at PND9 (Figure 3.2.5B and D). However, at PND11 and PND16, the number of MNs was reduced in FVB *Smn*$^{2B/-}$ mice compared to control littermates (Figure3.2.5B and D). To compare the pattern of MN loss between FVB and BL6 *Smn*$^{2B/-}$ mice, we calculated the fraction of MNs in these mice as a percentage of the average MN number of their corresponding control littermates. Although the rate of MN loss was similar in both backgrounds, this pathology began at least two days earlier in FVB *Smn*$^{2B/-}$ mice (Figure3.2.5E).

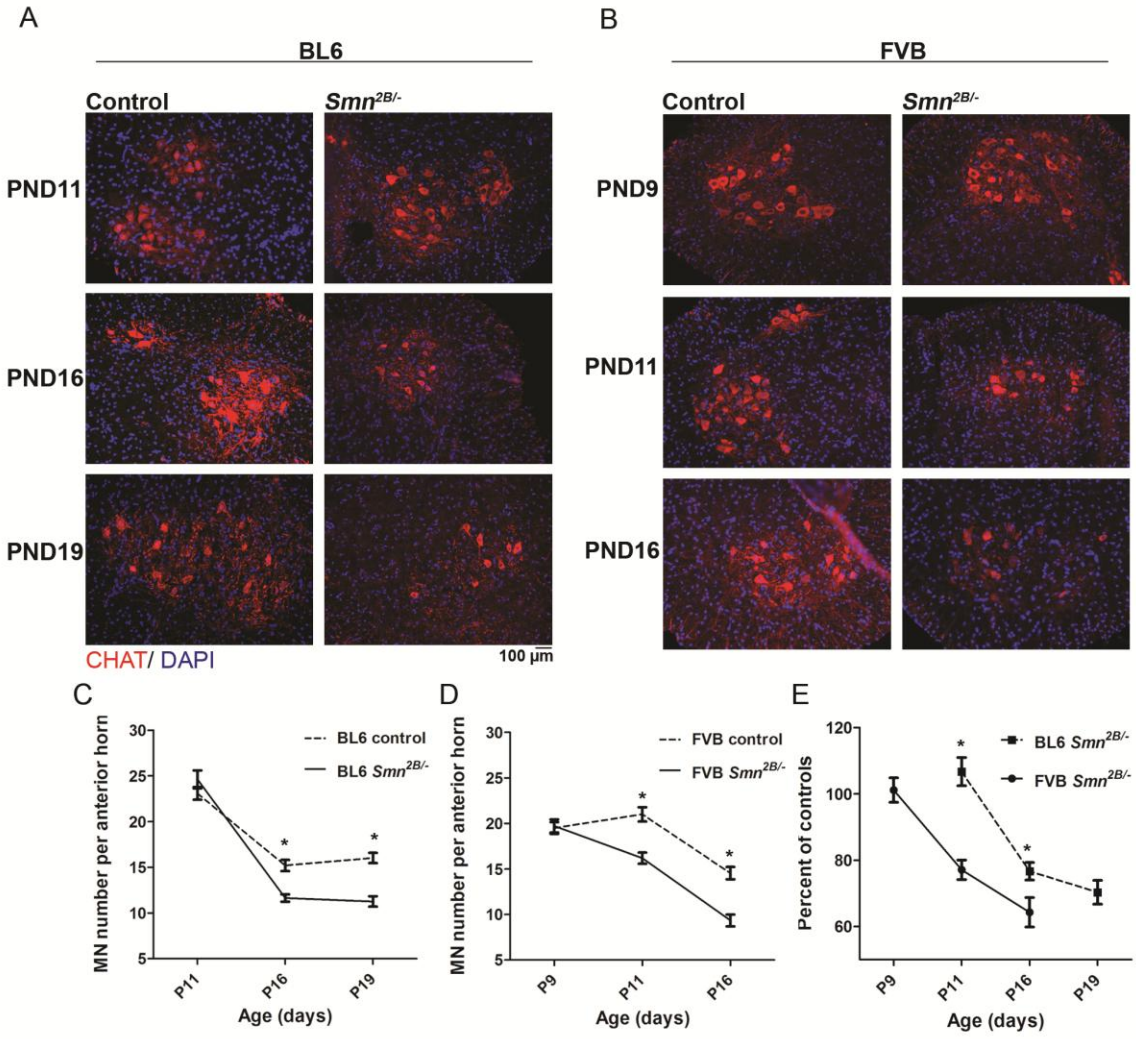
A
BL6
Control
Smn2B/-
PND11
PND16
PND19
CHAT/ DAPI
100 µm
B
FVB
Control
Smn2B/-
PND9
PND11
PND16
C
MN number per anterior horn
BL6 control
BL6 Smn2B/-
P11
P16
P19
Age (days)
D
MN number per anterior horn
FVB control
FVB Smn2B/-
P9
P11
P16
Age (days)
E
Percent of controls
BL6 Smn2B/-
FVB Smn2B/-
P9
P11
P16
P19
Age (days)

Figure 3.2.5. Motor neuron loss occurs at an earlier age in FVB *Smn*$^{2B/-}$ mice than in BL6 *Smn*$^{2B/-}$ mice.

A and B) Representative immunofluorescent images of the anterior horn regions of spinal cords from BL6 mice (A) at PND11, PND16 and PND19, and FVB mice (B) at PND9, PND11 and PND16 (red is ChAT staining and blue is DAPI staining). C) No motor neuron loss was observed in lumbar spinal cords of BL6 *Smn*$^{2B/-}$ mice at PND11. However, at PND16 and PND19 the number of motor neurons was significantly decreased in BL6 *Smn*$^{2B/-}$ mice compared to their control littermates (n=3, two way ANOVA, $p<0.05$). D) Motor neuron loss was not observed at PND9 in FVB *Smn*$^{2B/-}$ mice. However the number of motor neurons was significantly decreased in FVB *Smn*$^{2B/-}$ mice at PND11 and PND16, compared to their control littermates (n=3, two way ANOVA, $p<0.05$). E) The graph represents the number of motor neurons in sections from *Smn*$^{2B/-}$ mice as a percentage of the average number of motor neurons in sections from control mice for each time point. Motor neuron loss occurs earlier in FVB *Smn*$^{2B/-}$ mice than in BL6 *Smn*$^{2B/-}$ mice. * indicates significant difference between *Smn*$^{2B/-}$ mice and their control littermates in C and D, and between BL6 and FVB *Smn*$^{2B/-}$ mice in E.

3.2.6. Neuromuscular junction pathology occurs at an earlier age in FVB *Smn*$^{2B/-}$ mice than in BL6 *Smn*$^{2B/-}$ mice

NMJs are the primary sites of pathologic changes in SMA (Kariya, Park et al. 2008, Murray, Comley et al. 2008, Murray, Lee et al. 2010). These changes include pre-synaptic swelling due to accumulation of neurofilaments and reduced size of motor endplates (MEPs). Previous work has shown that NMJs undergo these changes prior to any obvious phenotype in SMA model mice. To investigate pre-synaptic swelling, mouse transverse abdominis (TVA) muscles were immunostained for neurofilament (NF-M) and synaptic vesicle 2 (SV2) (Figure3.2.6A and B). We used an established classification system for the severity of NMJ pre-synaptic swelling based on morphology (grade 1: normal, no pre-synaptic swelling; grade 2: swollen, pre-synaptic terminal arborization is thickened; grade 3: spheroid accumulations over the NMJ; grade 4: spheroid covers MEPs). At PND11, only FVB *Smn*$^{2B/-}$ mice show NMJ presynaptic swellings (Figure3.2.6C). At PND16, both BL6 and FVB *Smn*$^{2B/-}$ mice show NMJ pre-synaptic swelling (Figure3.2.6D). Interestingly, at this age FVB *Smn*$^{2B/-}$ mice show higher degrees of NMJ pre-synaptic swelling, reaching grade 4, relative to BL6 *Smn*$^{2B/-}$ mice that have only progressed to grade 3 (Figure3.2.6D).

We also investigated the post-synaptic NMJ abnormalities by labeling TVA muscles with a conjugated alpha-bungarotoxin and quantifying the size of the MEP areas at both PND11 and PND16. The average size of MEPs of BL6 *Smn*$^{2B/-}$ mice is not changed at PND11 (168.6 μm^2 *vs.* 183.3 μm^2 in controls, $p>0.05$), but significantly decreased at PND16 (142.6 μm^2 *vs.* 197.1 μm^2 in controls, $p<0.01$) (Figure3.2.6E). In contrast, the average size of MEPs is significantly decreased in FVB *Smn*$^{2B/-}$ mice at both PND11 and PND16 (127.2 μm^2 *vs.* 170.5 μm^2 at PND11 and 142.6 μm^2 *vs.* 197.1 μm^2 at PND16, $p<0.01$ for both) (Figure3.2.6F).

We also looked at NMJ morphology in FVB *Smn*$^{2B/-}$ mice at an earlier age (i.e. PND9) (Supplementary Figure 4.4). Although we did not find any difference in the average size of MEPs (Supplementary Figure 4.4B), we observed that FVB *Smn*$^{2B/-}$ mice show mild NMJ pre-synaptic swelling at PND9 (Supplementary Figure 4.4C).

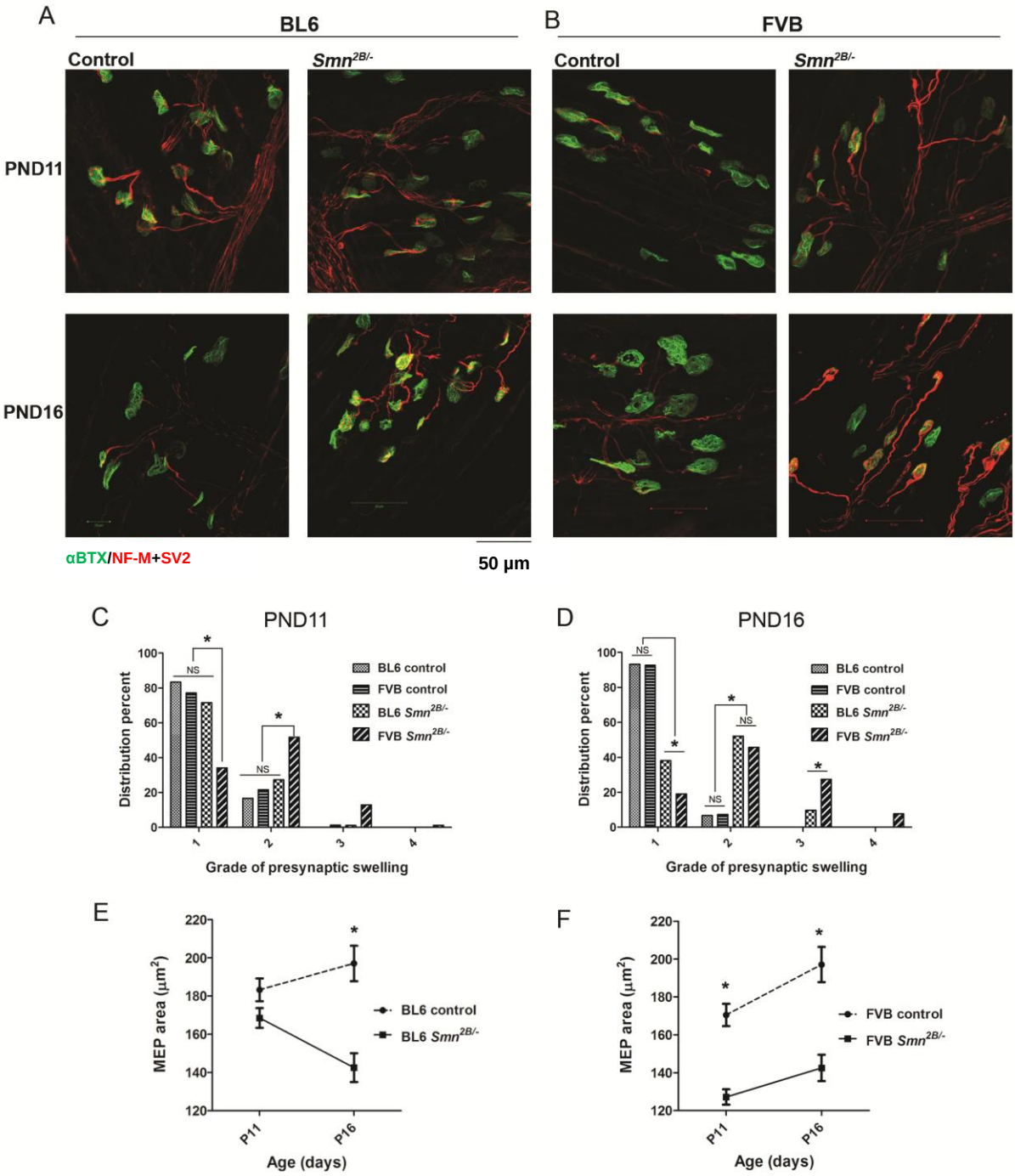
A
BL6
B
FVB
Control
Smn2B/-
Control
Smn2B/-
PND11
PND16
αBTX/NF-M+SV2
50 μm
C
PND11
D
PND16
Distribution percent
Grade of presynaptic swelling
NS
*
BL6 control
FVB control
BL6 Smn2B/-
FVB Smn2B/-
E
F
MEP area (μm2)
Age (days)
P11
P16

Figure 3.2.6. NMJ pathology occurs earlier in FVB *Smn*$^{2B/-}$ mice than in BL6 *Smn*$^{2B/-}$ mice.

A and B) Representative images of TVA muscles from BL6 mice (A) and FVB mice (B) at PND11 and PND16 stained for neurofilament-M (red) and motor endplates (α-BTX, green). C) At PND11, only FVB *Smn*$^{2B/-}$ mice show accumulation of neurofilaments within their NMJs (showing higher degrees of presynaptic swelling). D) At PND16, both BL6 and FVB *Smn*$^{2B/-}$ mice show accumulation of neurofilaments within presynaptic areas of their NMJs, however the degree of presynaptic swellings is higher in FVB *Smn*$^{2B/-}$ mice (n=3, two way ANOVA, $p<0.05$). E) Motor endplate size is significantly reduced in BL6 *Smn*$^{2B/-}$ mice at PND16 but not at PND11. F) Motor endplate size is significantly reduced in FVB *Smn*$^{2B/-}$ mice at both PND11 and PND16 (n=3, two way ANOVA, $p<0.05$). * in E and F indicates significant difference between *Smn*$^{2B/-}$ mice and their control littermates.

3.2.7. Smn protein levels are not differentially regulated in BL6 vs. FVB *Smn*$^{2B/-}$ mice

We evaluated the level of Smn protein in spinal cords at two different time points – PND5 and PND9. Total protein staining was used to normalize the immunoblot signals (data not shown). Our analysis revealed no significant difference in the level of Smn between FVB and BL6 *Smn*$^{2B/-}$ mice at both PND5 and at PND9 (13.0±1.0% *vs.* 10.4±2.1% of their normal controls, $p>0.05$) (Figure 3.2.7A and B). We also compared the expression of Smn between FVB *Smn*$^{2B/-}$ mice and FVB severe SMA mice (Supplementary Figure 4.5). At PND1 the level of Smn protein in spinal cords of FVB *Smn*$^{2B/-}$ mice is significantly higher than FVB severe SMA mice, confirming that the less severe phenotype in *Smn*$^{2B/-}$ mice is due to slightly higher Smn levels in these animals.

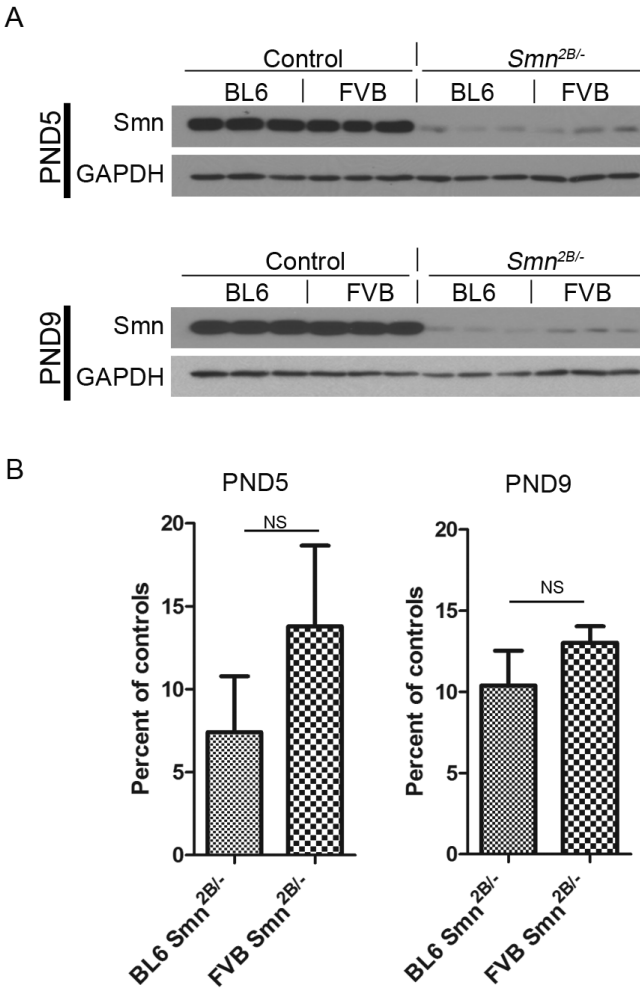

Figure 3.2.7. Smn protein levels are not differentially regulated in BL6 *vs.* FVB *Smn*$^{2B/-}$ mice.

A) Immunoblot analysis of lumbar spinal cord extracts of PND5 and PND9 mice using antibodies against Smn and GAPDH. B) Quantification revealed no difference in Smn protein between BL6 and FVB *Smn*$^{2B/-}$ mice (n=3, unpaired t test, $p>0.05$). NS = not significant.

3.2.8. Expression of some actin regulating proteins is altered in BL6 vs. FVB *Smn*$^{2B/-}$ mice

We evaluated the levels of three different proteins that are important in the regulation of the actin cytoskeleton and that could be involved in determining the severity of disease. To determine if there is any difference in expression in the *Smn*$^{2B/-}$ mice between the two congenic background strains, spinal cord extracts were collected at PND9 for immunoblot experiments. This time point was selected based on our observation that there was no MN loss in *Smn*$^{2B/-}$ mice on either background at this age. Initially, we assessed the activity of the Rho/ROCK pathway by measuring the ratio of phospho-cofilin (P-cofilin) to total cofilin protein levels. As expected, this pathway was more active in the *Smn*$^{2B/-}$ mice (Figure3.2.8 A and B). However, this pathway did not appear to be differentially regulated between the two genetic strains tested, although a small increase was noted in the FVB *Smn*$^{2B/-}$ mice. Next, we assessed profilin 1, which inhibits the polymerization of actin. Although there was no difference in the level of profilin between wild type and *Smn*$^{2B/-}$ mice, there was an increase in FVB mice compared to BL6 (Figure 3.2.8C and D). Finally, we assessed expression of *Plastin 3*, which has previously been identified a putative SMA modifier gene in humans (Oprea, Krober et al. 2008). At baseline, the levels of Pls3 were higher in FVB wild type mice than in BL6 wild type mice (Figure3.2.8E and F). Of interest, however, the level of Pls3 is significantly increased in BL6 *Smn*$^{2B/-}$ mice (+63.5±15.7%, $p<0.05$) but was slightly decreased in FVB *Smn*$^{2B/-}$ mice (-19.58 ± 7.910%, p=0.06) compared to their respective wild type controls (Figure 3.2.8E and F). A statistical comparison was also performed between BL6 *Smn*$^{2B/-}$ mice and FVB *Smn*$^{2B/-}$ mice, and we found lower levels of Pls3 in the latter strain background (Figure3.2.8E and F). Thus, there is a differential induction of Pls3 in BL6 *Smn*$^{2B/-}$ mice.

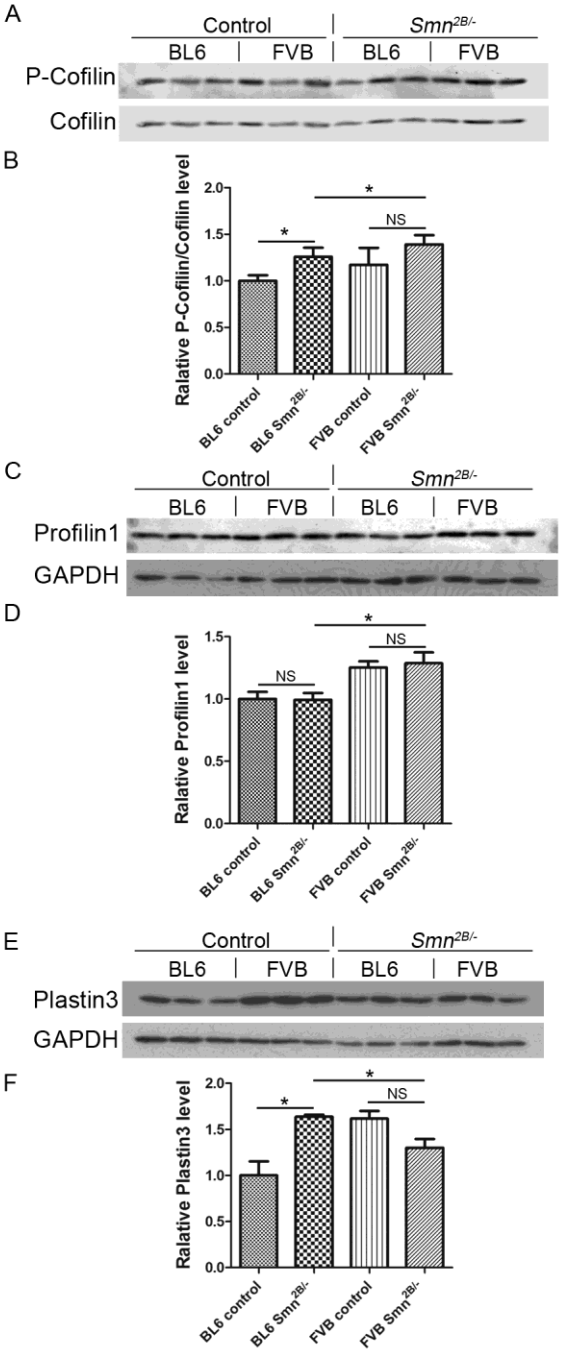
A
Control
Smn2B/-
BL6
FVB
BL6
FVB
P-Cofilin
Cofilin
B
Ralative P-Cofilin/Cofilin level
2.0
1.5
1.0
0.5
0.0
*
*
NS
BL6 control
BL6 Smn2B/-
FVB control
FVB Smn2B/-
C
Control
Smn2B/-
BL6
FVB
BL6
FVB
Profilin1
GAPDH
D
Ralative Profilin1 level
1.5
1.0
0.5
0.0
*
NS
NS
BL6 control
BL6 Smn2B/-
FVB control
FVB Smn2B/-
E
Control
Smn2B/-
BL6
FVB
BL6
FVB
Plastin3
GAPDH
F
Ralative Plastin3 level
2.0
1.5
1.0
0.5
0.0
*
*
NS
BL6 control
BL6 Smn2B/-
FVB control
FVB Smn2B/-

Figure 3.2.8. Differential expression of some actin regulating proteins in BL6 *vs.* FVB *Smn$^{2B/-}$ mice*.

Immunoblot analysis of lumbar spinal cord extracts of PND9 mice. A and B) The ratio of phospho-cofilin (P-cofilin) to cofilin protein levels is increased in BL6 *Smn$^{2B/-}$* mice compared to control mice (n=3, unpaired t test, $p<0.05$). However, there was no obvious differential regulation between the two genetic strains tested. C and D) There is no difference in the level of profilin 1 between wild type and *Smn$^{2B/-}$* mice. However, there is an increase in their levels in FVB mice compared to BL6 (n=3, unpaired t test, $p<0.05$). E and F) Differential induction of plastin 3 in spinal cords of BL6 *Smn$^{2B/-}$* mice. Plastin 3 levels are significantly higher in BL6 *Smn$^{2B/-}$* mice comparing to their control wild types (n=3, unpaired t test, $p<0.05$). In FVB *Smn$^{2B/-}$* mice however, the level of plastin 3 was not altered (n=3, unpaired t test, $p=0.06$). * indicates significant difference. NS = not significant.

Chapter 4 – Discussion

4.1- Characterization of proteomic alterations in the central synapses of *Smn*$^{2B/-}$ mouse model

The main goal of this study was to find out how depletion of Smn affects the proteome of central synapses of *Smn*$^{2B/-}$ mice before the onset of any obvious pathology in their motor units. We used several staining techniques on the brains and spinal cords of these mice and did not find any evidence that central synapses undergo degeneration until PND16 (a post-symptomatic stage). To characterize primary proteomic alterations within central synapses of *Smn*$^{2B/-}$ mice, we used a label free quantitative LC-MS technique which is a highly reproducible and efficient approach. This approach enabled us to identify more than 2,300 unique proteins in synaptosomes isolated from mouse spinal cords of *Smn*$^{2B/-}$ mice and their control littermates. Comparative analysis of MS results revealed that the levels of 362 proteins were significantly altered more than 30% in *Smn*$^{2B/-}$ mice. Functional cluster analysis on the altered proteins suggested that several molecular pathways are affected in synapses isolated from spinal cords of *Smn*$^{2B/-}$ mice at a presymptomatic stage (Table 3.1.1). Most of the affected molecular pathways are involved in basic cellular functions like energy metabolism, protein synthesis, cytoskeletal dynamics and intracellular trafficking. These results further confirm the pivotal roles of *Smn* (as a housekeeping gene) for proper function of synapses.

One advantage of studying synaptosomes is that they represent an almost pure neuronal sample. This is especially important because, in SMA (like other neurodegenerative disorders) astrocytes and microglia are activated and the alterations of their proteome may not parallel that of neurons (Tarabal, Caraballo-Miralles et al. 2014). However, molecular alterations in synapses may not include all the molecular changes happening within the soma (Saal, Briese et al. 2014).

We opted to perform proteomic analysis on central synapses of *Smn*$^{2B/-}$ mice at a presymptomatic stage because the pathologic changes of motor units at the post-symptomatic stages of SMA (i.e. myofiber atrophy and motor neuron loss) may result in non-specific

secondary changes in central synapses. *Smn*$^{2B/-}$ mice show a substantially long pre-symptomatic period (12-14 days) comparing to more severe mouse models of SMA (e.g. 'severe SMA' and 'delta 7 SMA' mice). The long presymptomatic period of *Smn*$^{2B/-}$ mice provides a valuable opportunity to decipher pathologic molecular events preceding the SMA phenotype in more detail (Eshraghi, McFall et al. 2016). Indeed, central nervous tissues in more severe mouse models of SMA show neuro-developmental abnormalities before and after birth (Liu, Shafey et al. 2010, Wishart, Huang et al. 2010). The density of synaptic inputs on motor neurons of spinal cords of *Smn*$^{2B/-}$ mice was not reduced at PND11. This contrasts with the studies which reported reduction of synaptic inputs on motor neurons in 'delta 7 SMA' mice during embryonic life and early after birth (Mentis, Blivis et al. 2011, Tarabal, Caraballo-Miralles et al. 2014). This is an advantage of *Smn*$^{2B/-}$ mice for the discovery of primary molecular events in SMA.

Synapses are among the most vulnerable cellular compartments to Smn depletion

The generation of animal models of SMA has provided unprecedented opportunities to look at early events in SMA and unveil which cellular compartments are more vulnerable to the depletion of Smn. It is quite sensible to consider that impairments of the more vulnerable cell compartments will contribute to more cellular defects and ultimately death and degenerative phenotypes.

Studies on different animal models of SMA have confirmed that NMJs, the synaptic compartments of motor units, are among the most vulnerable compartments to Smn depletion (Kariya, Park et al. 2008, Murray, Comley et al. 2008). As a matter of fact, NMJs show pathologic alterations before the onset of any clinical manifestations of SMA. We also observed

that NMJs in *Smn*$^{2B/-}$ mice with FVB background show pathologic changes at PND9, a time prior to any detectable muscle weakness or motor neuron loss.

The vulnerability of synapses has been reported in several neurodegenerative disorders and is believed to contribute to neurodegenerative process in these conditions. Synaptic impairments precede neuronal death in conditions like Alzheimer's, Parkinson's, Huntington's, ALS, SMA and prion diseases (Clinton, Forsyth et al. 1993, Sasaki and Maruyama 1994, Li, Plomann et al. 2003, Coleman, Federoff et al. 2004, Kariya, Park et al. 2008, Schirinzi, Madeo et al. 2016). Although, we did not observe any change in the synaptic density on lower motor neurons, we found that central synapses of *Smn*$^{2B/-}$ mice show molecular alterations which are similar to other neurodegenerative disorders.

Functional and structural deficits of NMJs have been characterized following depletion of Smn. These include disorganization of synaptic vesicles, reduced numbers of docked vesicles, decreased neurotransmitter release, accumulation of neurofilaments within presynaptic areas and delayed maturation of postsynaptic areas (Kong, Wang et al. 2009, Murray, Lee et al. 2010, Torres-Benito, Neher et al. 2011, Martinez-Hernandez, Bernal et al. 2013). Most of these findings have been made using severe mouse models of SMA. We showed that in a less severe mouse model of SMA (*Smn*$^{2B/-}$ mice), NMJs are affected at a presymptomatic stage and the severity of NMJ pathology increases with the progress of the disease in these animals. Even in very mild mouse models of SMA, the function of NMJs is affected. SMNA2G mice (i.e. *Smn*$^{-/-}$*;SMN2*$^{+/+}$*;SMNA2G*$^{+/+}$*)* recapitulate a very mild SMA phenotype with minimum reductions in weight and life span (Monani, Pastore et al. 2003). At 1 year of age, these mice do not show any SMA specific pathology within their NMJ (e.g. smaller size, defective maturation or neurofilament accumulation). However, functional analysis showed that the NMJs of

SMNA2G mice show a significant reduction in neurotransmitter release upon stimulation (Ruiz and Tabares 2014).

It seems that in addition to NMJs, central synapses are also affected in SMA. Both excitatory and inhibitory synaptic inputs on motor neuron soma and proximal dendrites are reduced in 'delta 7 SMA' mice at a presymptomatic stage (Mentis, Blivis et al. 2011, Tarabal, Caraballo-Miralles et al. 2014).

Some researchers have argued that the observed decrease in synaptic inputs to motor neurons in 'delta 7 SMA' mice might be secondary to motor neuron pathology (Thirumalai, Behrend et al. 2013). However, the results of several studies which used conditional models of SMA supported a role for depletion/restoration of Smn in other cells within the CNS in induction/rescue of SMA phenotype. Selective deletion of *Smn* in motor neurons of mice who carry two copies of *SMN2* and *SMNΔ7* did not decrease their life span. On the other hand, deletion of *Smn* in all neuronal and glial cells of the same mice reduced their survival significantly (McGovern, Iyer et al. 2015). Reciprocal experiments (using a conditional rescue model of 'delta 7 SMA' mouse model) also confirmed the role of other neuronal cells and glia in SMA; restoration of SMN levels specifically in motor neurons of 'delta 7 SMA' mice did not increase their life span significantly, however, restoration of SMN within all neuronal and glial cells increased the survival of 'delta 7 SMA' mice dramatically. So, the restoration/depletion of SMN within all neuronal and glial cells (and not only motor neurons) is critical for rescue/induction of the SMA phenotype in mouse (McGovern, Iyer et al. 2015). These results suggest that impairment of central synapses might contribute to the severity of SMA. To study this hypothesis, it would be necessary to investigate and compare the function and morphology of central synapses in the above mentioned conditional mouse models of SMA.

Several molecular pathways are affected in central synapses of *Smn*$^{2B/-}$ mice

Synapses consume huge amounts of energy for vesicle trafficking and ion homeostasis (especially calcium ions). And, the proper functions of cellular pathways involved in energy production are crucial for reliable synaptic transmission. Our analysis suggested that several molecular pathways involved in energy metabolism are probably affected within central synapses of *Smn*$^{2B/-}$ mice, including; oxidative phosphorylation, pyruvate metabolism, fatty acid metabolism, and glycolysis/gluconeogenesis.

A competent vesicle trafficking machinery is a necessity for sustainable synaptic transmission. Transport of synaptic vesicles within synapses is a cycle consisting of several stages including: 1) transport of the vesicles from inner vesicle pools to the active zone, 2) docking of the vesicles to presynaptic membrane, 3) exocytosis of the contents of the vesicle (i.e. neurotransmitters) into the synaptic cleft, 4) endocytosis and recycling of the vesicles and reloading them with neurotransmitters (Rust and Maritzen 2015). Our analysis also suggested that several molecular pathways involved in vesicle trafficking are affected in central synapses of *Smn*$^{2B/-}$ mice, including; 'SNARE in vesicular transport', 'regulation of actin cytoskeleton' and 'endocytosis'.

Local protein synthesis is crucial for synaptic function; our results also showed that the levels of several ribosomal proteins are altered in central synapses of *Smn*$^{2B/-}$ mice.

Oxidative phosphorylation

We found that the oxidative phosphorylation pathway is affected in synapses from spinal cords of *Smn*$^{2B/-}$ mice with the highest score in our analysis. Previously, our group also showed that

dysregulation of genes involved in the oxidative phosphorylation pathway are associated with vulnerability of motor neurons in SMA (Murray, Beauvais et al. 2015). Interestingly, alterations within the oxidative phosphorylation pathway were also the top hits on a proteomic analysis of synapses of hippocampus of 'severe SMA' mice at a presymptomatic stage (PND1) (Wishart, Mutsaers et al. 2014).

It is believed that most of the required energy for synaptic transmission is produced through the oxidative phosphorylation processes in mitochondria which reside within synapses and adjacent axonal areas. (Harris, Jolivet et al. 2012). Pharmacological suppression of oxidative phosphorylation resulted in inhibition of synaptic vesicle trafficking, especially vesicle endocytosis (Pathak, Shields et al. 2015). Indeed, energy failure of synapses is a common feature of several neurodegenerative disorders and contributes to the degeneration of synaptic terminals early in the course of these diseases (Rapoport 2003, Pathak, Berthet et al. 2013).

Interestingly the level of NADH dehydrogenase (ubiquinone) iron-sulfur protein 4 (Ndufs4) protein was decreased in synaptosomes we isolated from spinal cords of *Smn*$^{2B/-}$ mice. Ndufs4 is an important subunit of mitochondrial complex I. Mutations of *NDUFS4* gene are known to cause Leigh disease, a devastating neurological disorder in human (Leshinsky-Silver, Lebre et al. 2009). Depletion of Ndufs4 within synapses results in remarkable reduction of ATP production and synaptic vesicle trafficking (Pathak, Shields et al. 2015).

Fatty acid metabolism

The MS analysis on our synaptosome samples showed that the levels of several mitochondrial enzymes involved in β-oxidation of fatty acids are dysregulated in central

synapses of *Smn*$^{2B/-}$ mice. Functional cluster analysis of the MS results also proposed 'fatty acid metabolism' as an affected pathway in our samples.

Abnormal fatty acid metabolism has been reported in SMA patients before (Kelley and Sladky 1986, Tein, Sloane et al. 1995, Crawford, Sladky et al. 1999). SMA patients have higher fat mass even though they receive lower calorie intake and have lower body mass indexes (BMI) (Sproule, Montes et al. 2009). Dicarboxylic acids (DAs) are products of fatty acids oxidation/peroxidation and the urinary levels of DAs are increased when fatty acid oxidation is increased (e.g. ketosis) or inhibited (e.g. defects in beta-oxidation) (Mortensen 1992). Levels of dicarboxylic acids are unusually high in the urine of SMA patients (Kelley and Sladky 1986, Tein, Sloane et al. 1995). For energy production, fatty acids are transported into mitochondria through binding to L-carnitine (i.e. FA-Carn) to undergo β-oxidation (Marcovina, Sirtori et al. 2013). Levels of FA-Carn are unusually high in the serum of type I and II SMA patients (Tein, Sloane et al. 1995). Also, the activity of mitochondrial enzymes involved in fatty acid oxidation is significantly decreased in muscle samples of SMA patients. Crawford et al. investigated the abnormalities in fatty acid metabolism in muscle samples from SMA patients in comparing to patients with non-SMA muscle-denervating disorders. The authors concluded that the abnormalities of fatty acid metabolism in SMA are not a consequence of muscle denervation, and SMN probably has a specific function in the metabolism of fatty acids (Crawford, Sladky et al. 1999).

Alterations of the proteome of central synapses of *Smn*$^{2B/-}$ mice are overlapping with molecular changes observed in other neurodegenerative disorders

The functional cluster analysis on synaptosomes isolated from mouse spinal cords suggested that some molecular pathways related to neurodegenerative disorders (e.g. Parkinson's disease, Huntington's disease and Alzheimer's disease) are affected in central synapses of *Smn*$^{2B/-}$ mice. We found that several mitochondrial proteins involved in oxidative phosphorylation and some plasma membrane associated proteins involved in synaptic formation and plasticity are among the altered proteins belonging to these neurodegenerative pathways.

It seems that neurodegenerative disorders share some underlying pathogenic pathways. Using 2D gel electrophoresis followed by MALDI-TOF MS, Massignan et al. performed proteomic analysis on whole spinal cords isolated from a mouse model of ALS. Similar to our findings, they also showed that signalling pathways involved in oxidative phosphorylation, glycolysis, pyruvate metabolism, and actin cytoskeleton regulation are dysregulated within spinal cords of these mice at a presymptomatic stage (Massignan, Casoni et al. 2007).

'Synaptopathy' is a term being used more commonly in neurodegenerative disorders to explain how primary synaptic pathologies mediate neuronal pathology and degeneration (Brose, O'Connor et al. 2010). It is believed that during early stages of neurodegenerative disorders, synaptic pathological changes and even degeneration (i.e. synapoptosis) occur due to distinct mechanisms from degeneration of soma and axons (Mattson, Keller et al. 1998, Gillingwater and Ribchester 2001). Indeed, SMA is a very good example of a synaptopathy disease. As our work on *Smn*$^{2B/-}$ mice has shown, the accumulation of neurofilaments within NMJs starts at a time prior to any detectable pathologic change in motor neurons or muscles of the animal. As the disease progresses, the degree of neurofilament accumulation increases and they form huge

spheroid shape bodies within the NMJ. At this point, the axonal terminals degenerate and regress from the motor endplates (Bowerman, Murray et al. 2012). Whether the same pathologic changes happen in central synapses of *Smn*$^{2B/-}$ mice remains to be examined. However, degeneration of synaptic inputs to motor neurons has been reported in more severe mouse models of SMA at the late stages of the disease (Ling, Lin et al. 2010).

Regulation of actin cytoskeleton is affected in central synapses of *Smn*$^{2B/-}$ mice

The MS analysis on synaptosome fractions showed that the levels of several proteins involved in the regulation of actin cytoskeleton are altered in central synapses of *Smn*$^{2B/-}$ mice. We validated the results of the MS analysis and found that the levels of α-actinin and Kras are decreased but the levels of Moesin are increased in the synaptosomes isolated from the spinal cords of *Smn*$^{2B/-}$ mice.

Several studies have reported that the regulation of actin is impaired in SMA (Giesemann, Rathke-Hartlieb et al. 1999, Bowerman, Shafey et al. 2007, Oprea, Krober et al. 2008, Bowerman, Beauvais et al. 2010, Stratigopoulos, Lanzano et al. 2010, Bernal, Also-Rallo et al. 2011, Nolle, Zeug et al. 2011, Caraballo-Miralles, Cardona-Rossinyol et al. 2012, Hao le, Wolman et al. 2012). It is believed that SMN has a role in trafficking of *β-actin* mRNA to the axonal terminals of motor neurons (Rossoll, Jablonka et al. 2003). It is also known that SMN interacts with some actin binding proteins including plastin 3, α-actinin and profilin 2 (Giesemann, Rathke-Hartlieb et al. 1999, Rajendra, Gonsalvez et al. 2007, Oprea, Krober et al. 2008).

There is no doubt that a highly organized and dynamic actin cytoskeleton is necessary for the proper function of synapses. Actin is the most abundant protein in synapses (about 2% of

synaptosomal total protein) and has important roles within pre- and post-synaptic areas. (Wilhelm, Mandad et al. 2014). Actin in synapses is organized mainly as networks of branched filaments. Also, the clusters of synaptic vesicles are encircled by actin filaments, and individual vesicles bind to actin filaments through synapsin molecules (Greengard, Benfenati et al. 1994, Korobova and Svitkina 2010, Li, Bai et al. 2010).

Actin dynamics (i.e. assembly/disassembly of actin filaments) play important roles in synaptic function by mediating active transport of synaptic vesicles inside synapses. During synaptic activation, actin networks show a distinct pattern of activity; there is an initial increase in the assembly of actin filaments (mainly around synaptic vesicles), followed by an increase in the disassembly of actin filaments (Dillon and Goda 2005).

SMN depletion impairs actin dynamics in different cell types. In one study by our group, depletion of SMN in PC12 cells resulted in the increase of actin filaments at sub-membrane areas of these cells (Bowerman, Shafey et al. 2007). Others showed that knocking down of *SMN1* in human fibroblasts results in aberrant and unorganized actin networks (Gabanella, Pisani et al. 2016). In addition, the amount of actin filaments was reduced within the growing tips of filopodia in SMN depleted fibroblasts.

Studies on several animal models lacking different actin binding proteins showed that an intact dynamic actin network, rather than a net increase in the assembly or disassembly of actin filaments, is necessary for exocytosis and endocytosis of synaptic vesicles (Shupliakov, Bloom et al. 2002, Dason, Smith et al. 2014, Rust and Maritzen 2015). ADF and cofilin are actin binding proteins which promote disassembly of actin filaments. ADF/cofilin double knockout mice show an increase in actin filaments within synapses; however, the transport of synaptic vesicles to the active zone and vesicle exocytosis are reduced (Wolf, Zimmermann et al. 2015). Previously, our

group showed that the RhoA/ROCK pathway (an upstream negative regulator of cofilin activity) is upregulated within spinal cords of *Smn*$^{2B/-}$ mice. Interestingly, pharmaceutical inhibition of ROCK improved survival and muscle phenotypes in these mice (Bowerman, Beauvais et al. 2010, Bowerman, Murray et al. 2012).

Endocytosis

Endocytosis is of special importance for synaptic transmission; it mediates the recycling of released vesicles and contributes to replenishing of the vesicle pools. Our results showed that several proteins involved in endocytosis are affected in central synapses of *Smn*$^{2B/-}$ mice. Recently, the impairment of endocytosis has been reported in different models of SMA. Hosseinibarkooie et al. showed that endocytosis is impaired in different 'in vitro' and 'ex vivo models' of SMA. They further showed that overexpression of *Plastin 3* or *CORO1C* (two actin binding proteins) can restore normal levels of endocytosis in SMN depleted cells. The authors concluded that disruption of endocytosis in SMA is probably due to the impaired actin dynamics (Hosseinibarkooie, Peters et al. 2016). Dimitriadi et al. also performed a detailed examination of impairment of endocytic pathway in SMA. They conducted a series of genetic studies on a *C. elegans* model of SMA and found that in worm, *Smn* interacts with some genes involved in the endocytic pathway. The authors also observed structural and functional abnormalities in endocytic compartments within NMJs of the SMA worm. Finally, they showed that depletion of SMN in a human glial cell line impairs endocytosis-dependent viral infection (Dimitriadi, Derdowski et al. 2016).

Impaired endocytosis is also reported in other neurodegenerative disorders like Alzheimer's, Huntington's, Parkinson's and ALS. Indeed, the disruption of endocytic pathways

happen at very early stages and contributes to the pathogenesis of the disease (Trushina, Singh et al. 2006, Shin, Jeong et al. 2008, Yu, Shibata et al. 2014, Xu, Weissmiller et al. 2016).

We also found that the level of Amphiphysin is altered in the central synapses of *Smn*$^{2B/-}$ mice at both presymptomatic and post-symptomatic stages. Amphiphysin is an SH3 domain-containing protein which plays a critical role in clathrin-mediated endocytosis (CME) of synaptic vesicles. Within synapses, amphiphysin interacts with dynamin (the motor protein of the endocytosis process) and recruits it to the necks of budding endocytic vesicles (Wigge, Kohler et al. 1997, Takei, Slepnev et al. 1999). Recycling of synaptic vesicles is impaired in mice lacking amphiphysin. Accordingly, these mice show defective memory and learning, and die prematurely due to irreversible seizures (Di Paolo, Sankaranarayanan et al. 2002).

It is suggested that dysregulation of amphiphysin may play a role in the pathogenesis of other neurodegenerative disorders. The levels of amphiphysin are reduced in patients with Alzheimer's disease. Animal studies also showed that the reduction of amphiphysin is associated with accumulation of hyperphosphorylated tau aggregates (De Jesus-Cortes, Nogueras-Ortiz et al. 2012).

Ribosome

Local synaptic translation of specific proteins is an important component of synaptic plasticity (Kang and Schuman 1996, Huber, Gallagher et al. 2002). Defective synaptic translation is attributed to the pathogenesis of some neurological disorders including fragile X syndrome, ALS, spinocerebellar ataxia and autism (Liu-Yesucevitz, Bassell et al. 2011).

SMN might play important roles in local translation inside synapses. Several mRNAs are transported to synapses within macromolecules called RNA granules. SMN is associated with

RNA granules and probably has a role in the assembly and transport of these structures (Donlin-Asp, Bassell et al. 2016). SMN also binds to ribosomes and represses their translational activity (Sanchez, Dury et al. 2013).

The levels of several ribosomal proteins (including Rpl10a, Rpl36, Rpl7, RplP0, Rpl12) were altered in the synaptosome fractions which we isolated from spinal cords of *Smn*$^{2B/-}$ mice at a presymptomatic stage. Recently our group also showed that the expression of several ribosomal proteins is dysregulated in motor neurons isolated from spinal cords of *Smn*$^{2B/-}$ mice. Since most of the dysregulated proteins were ribosomal RNA (rRNA) binding proteins, it was concluded that SMN might have a role in the regulation of biogenesis and assembly of ribosomal ribonucleoproteins (rRNPS) (Murray, Beauvais et al. 2015). This is in accordance with several studies which reported a role for SMN in the assembly of other ribonucleoproteins (RNPs), besides its well known function in the assembly of snRNPs (Mourelatos, Abel et al. 2001, Battle, Kasim et al. 2006). In another study, Bernabò et al. reported widespread translational impairments in several tissues (including brain, spinal cord and kidney) of 'Taiwanese SMA' mice. The authors showed that translational defects happen at an early stage of the disease and the severity of these defects increases with the disease progression. They also observed that the number of ribosomes is decreased within axons of lower motor neurons of these mice (Bernabò, Tebaldi et al. 2017).

Ribosomal dysfunction and translational defects are also reported at early stages of other neurodegenerative disorders like ALS, Alzheimer's disease, Huntington's disease and Parkinson's disease (Ding, Markesbery et al. 2005, Lee, Hwang et al. 2011, Verheijen, Peviani et al. 2014, Taymans, Nkiliza et al. 2015, Hernandez-Ortega, Garcia-Esparcia et al. 2016)

It seems that motor neurons are susceptible to translational defects since mutations of genes involved in RNA metabolism (e.g. *TARDBP*, *FUS* and *SMN*) mediate motor neuron disorders (Baloh 2012).

Branched chain amino acids

We found that the catabolism pathway of branched chain amino acids (BCAAs) is dysregulated in synapses isolated from spinal cords of $Smn^{2B/-}$ mice. BCCAs are essential amino acids including valine, isoleucine and leucine. BCCAs are important for proper function of neurons especially for the synthesis of the neurotransmitter glutamate (Hutson, Berkich et al. 1998). The impaired catabolism of BCCAs (and their intracellular accumulation) is linked to maple syrup urine disease (MSUD; OMIM#248600), an autosomal recessive metabolic disorder with severe neurological deficits (Hutson, Berkich et al. 1998). On the other hand, lower levels of BCCAs have been attributed to the neurodevelopmental disorders like autism (Novarino, El-Fishawy et al. 2012). It is also proposed that inhibition of branched-chain aminotransferase (BCATc) (an enzyme responsible for catabolism of BCCAs) is beneficial for the treatment of the neurodegenerative disorders (Hu, Boxer et al. 2006). In ALS, it was suggested that dietary supplementation with BCCAs is beneficial for the patients. However, several clinical trials failed to confirm this hypothesis (Testa, Caraceni et al. 1989, Group 1993). Some studies also showed that excessive amounts of BCCAs might have harmful effects on neurons (Carunchio, Curcio et al. 2010).

Pyruvate metabolism

We found that the levels of several enzymes involved in pyruvate metabolism are altered in synapses of spinal cords of *Smn*$^{2B/-}$ mice. Pyruvate is one of the main products of the glycolysis pathway. Within cells, pyruvate molecules are important substrates for several pathways which contribute to the generation of energy, and synthesis of carbohydrates, amino acids and lipids. Aberrant pyruvate metabolism has been reported in several neurodegenerative disorders including Parkinson's disease, Alzheimer's disease and Leigh's syndrome (Gray, Tompkins et al. 2014). Increased levels of pyruvate in cerebrospinal fluid (CSF) have been reported in neurodegenerative disorders like ALS and Alzheimer's disease (Parnetti, Gaiti et al. 1995, Blasco, Corcia et al. 2010). Indeed it is proposed that CSF level of pyruvate is a biomarker for the diagnosis of Alzheimer's disease (Parnetti, Gaiti et al. 1995).

Glycolysis/ gluconeogenesis

In our study, 'Glycolysis/gluconeogenesis' was one of the affected pathways in synaptosomes isolated from spinal cords of *Smn*$^{2B/-}$ mice. Dysregulation of the 'glycolysis pathway' has been reported at early stages of several neurodegenerative disorders. It is believed that impairment of the glycolysis process contributes to energy failure and consequent neuronal loss in these diseases (Gouarne, Tardif et al. 2013, Knight, Yan et al. 2014, Vlassenko and Raichle 2015).

Glycolysis protects synapses against deleterious effects of hypoxia (Tian and Baker 2000). During hypoxia cytoplasmic glycolytic enzymes are localized to regions adjacent to synapses to provide high levels of ATP required for synaptic function. Disruption of this process results in impairment of synaptic vesicle trafficking (Jang, Nelson et al. 2016).

Dysregulation of ‘glycolysis/gluconeogenesis’ pathway in SMA has been reported in several studies. Interestingly, Wishart et al. reported that the glycolysis/gluconeogenesis pathway is among dysregulated pathways in synaptosome samples isolated from hippocampus of ‘severe SMA’ mice at PND1 (Wishart, Mutsaers et al. 2014). Wu et al. differentiated motor neurons from embryonic stem (ES) cells isolated from ‘severe SMA’ mice. The authors observed that lactate dehydrogenase, a key enzyme in the glycolysis pathway, is upregulated aberrantly in these cells (Wu, Whye et al. 2011). Impaired glycolysis is also reported in muscle biopsy samples from patients with SMA (Millino, Fanin et al. 2009).

Summary

Here, we showed widespread alterations in the proteome of synapses in spinal cords of *Smn*$^{2B/-}$ mice at a presymptomatic stage. The number of synapses was not decreased within spinal cords of these mice at this age. Functional clustering analysis on the altered proteins suggested that several molecular signalling pathways are affected in *Smn*$^{2B/-}$ mice (Figure 4.1). Interestingly, several molecular pathways involved in energy production, cell metabolism, protein synthesis, actin cytoskeleton and endocytosis were affected. We showed that the levels of some proteins involved in actin cytoskeleton regulation are changed in synapses isolated from spinal cords of *Smn*$^{2B/-}$ mice suggesting that actin dynamics is dysregulated in central synapses. However, more studies are required to determine the exact functional consequences of the affected pathways.

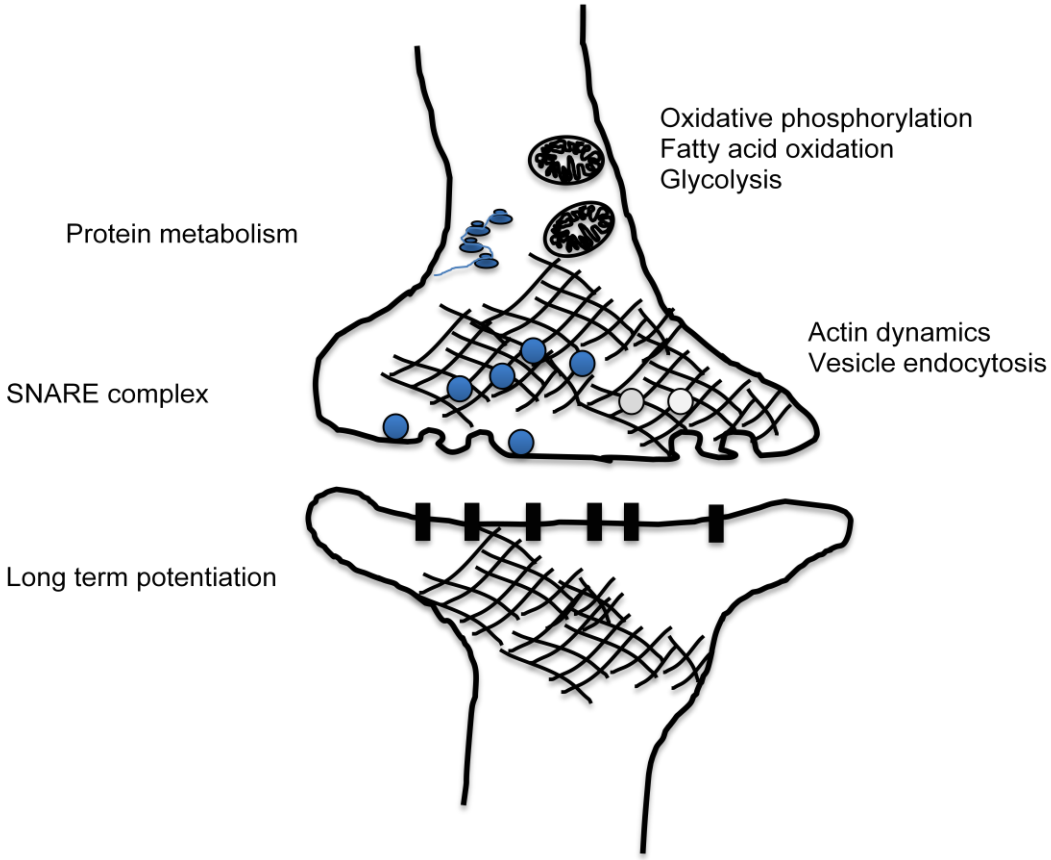

Figure 4.2.1. A schematic of dysregulated pathways within synapses of *Smn*$^{2B/-}$ mice. MS analysis on synaptosome samples isolated from *Smn*$^{2B/-}$ mice at PND11 revealed that the several molecular pathways involved in energy production, protein metabolism, synaptic transmission and actin cytoskeleton are dysregulated within central synapses of these mice.

4.2- Effect of genetic background on the phenotype of the *Smn*$^{2B/-}$ mouse model of spinal muscular atrophy

This part is adapted from:

Eshraghi M, McFall E, Gibeault S, Kothary R. Effect of genetic background on the phenotype of the Smn2B/- mouse model of spinal muscular atrophy. Hum Mol Genet. 2016 Oct 15; 25(20):4494-4506. doi: 10.1093/hmg/ddw278. PubMed PMID: 28172892.

The notion that genetic background can impact the phenotype of a mouse mutant is not new. Indeed, early observations made in spontaneous mutant mice have been supported by work in engineered and induced mutant mice (Nadeau 2001). In the recent past, gene targeting studies in mice have identified phenotypic differences between strain backgrounds. Collectively, this effect of genetic background on phenotype has been explained by the differential expression of so-called modifier genes. Such genes do not have any obvious phenotype on their own, but can impact the functional consequence of specific genetic mutations. As such, having congenic mouse strains for the study of gene mutations provides us with several advantages. It affords us more reliable models with consistent phenotypes and has the potential to identify modifier loci.

In this context, we have generated congenic mice on two separate backgrounds (BL6 and FVB) carrying the Smn^{2B} allele. We have characterized congenic mice at the 6th generation and report that $Smn^{2B/-}$ mice on the FVB background had an earlier onset and a more severe phenotype compared to the BL6 background. The generation of congenic $Smn^{2B/-}$ mice also resulted in a much tighter range of survival than observed in the original mixed background $Smn^{2B/-}$ mice (Bowerman, Murray et al. 2012, Bowerman, Murray et al. 2012). One confounding variable that we wanted to examine was the impact of litter size on survival. It is possible that the mutant pups in larger litters were not able to compete effectively with their normal littermates for breastfeeding, affecting their survival. Of the two congenic strains, the FVB mice consistently had larger litters. However, this did not correlate negatively with survival of $Smn^{2B/-}$ mice in these litters. Interestingly, survival of $Smn^{2B/-}$ mice in BL6 cages correlated positively with larger litter size. It appears that this feature is also strain dependent.

Degenerative changes involving motor units account for the major clinical presentations of SMA (i.e. progressive weakness and paralysis) (Crawford and Pardo 1996, Murray, Lee et al.

2010). These changes include atrophy of myofibers, lack of maturation of MEPs, swelling and disorganization of axonal terminals of MNs, and finally death of MNs. We investigated these changes in congenic *Smn*$^{2B/-}$ mice at different ages and observed that all of these pathologic changes occur at an earlier age in FVB *Smn*$^{2B/-}$ mice than they do in BL6 mice. At PND11, FVB *Smn*$^{2B/-}$ mice present with reduced muscle fibre cross-sectional area, smaller MEPs, neurofilament accumulation at NMJs and loss of MNs within the lumbar spinal cord. Of note, none of these pathological changes were observed in BL6 *Smn*$^{2B/-}$ mice at PND11. Moreover, we found that at PND16 these changes were more severe in FVB *Smn*$^{2B/-}$ mice than in BL6 *Smn*$^{2B/-}$ mice (summarized in Figure 4.2.2). Our results show that *Smn*$^{2B/-}$ mice on the FVB background present a more severe phenotype than on the BL6 background.

The effect of genetic background on the severity of the phenotype has also been observed in other mouse models of SMA. Congenic "severe SMA" mice on the BL6 background die before birth, but on the FVB background they have a median survival of 5 days (Monani, Sendtner et al. 2000, Le, Pham et al. 2005). Also, congenic "delta 7 SMA" mice on the BL6 background show a remarkable reduced life span compared to that on the FVB background (median survival of 1 and 10 days, respectively) (Le, Pham et al. 2005). On the other hand, the "Taiwanese SMA" mice when backcrossed on the BL6 background showed an increase in survival compared to the original congenic FVB mice (median survival of 15 and 10 days, respectively) (Ackermann, Krober et al. 2013). Based on survival, it appears that the "severe SMA" mice and the "delta 7 SMA" mice show a more severe phenotype on the BL6 background (Monani, Sendtner et al. 2000, Le, Pham et al. 2005), a trend that is opposite to that shown by the "Taiwanese model" and the *Smn*$^{2B/-}$ mice in the present study. An important consideration amongst all the different mouse models of SMA is the type of mutation introduced. In all cases,

the endogenous mouse *Smn* gene has been either completely silenced or only partially disrupted. Whether, this plays a role in the severity of the phenotype in different congenic backgrounds remains to be seen.

In search for an explanation for the difference in the onset and severity of disease phenotype between FVB and BL6 $Smn^{2B/-}$ mice, we measured Smn protein levels in extracts of lumbar spinal cords of PND9 mice. No significant difference was detectable between FVB and BL6 $Smn^{2B/-}$ mice at two different time points, excluding changes in Smn levels as a reason behind the differential severity. A more likely explanation is that there is an influence of one or more modifier genes on the overall disease pathogenesis in these mice. We have assessed levels of three different proteins that are involved in the regulation of the actin cytoskeleton. Although, the Rho kinase pathway was more active in the $Smn^{2B/-}$ mice, there did not appear to be any differential regulation of the pathway between the two genetic strains tested, as determined by assessing phospho-cofilin to total cofilin protein levels. Profilin1, which inhibits the polymerization of actin, had increased levels in FVB mice compared to BL6. Finally, the levels of Plastin 3 are significantly increased in spinal cords of BL6 $Smn^{2B/-}$ mice compared to their wild type littermates. A similar increase in FVB $Smn^{2B/-}$ mice was not observed. *PLS3* has been proposed to be a genetic modifier of SMA in both human and animal studies (Oprea, Krober et al. 2008, Bernal, Also-Rallo et al. 2011, Heesen, Peitz et al. 2016). In SMA patients, higher levels of Plastin 3 correlated with less severe SMA types (Stratigopoulos, Lanzano et al. 2010). Furthermore, Plastin 3 levels are decreased in *Smn* mutant zebra fish and overexpression of human *PLS3* rescues the SMA phenotype in these animals (Hao le, Wolman et al. 2012). Overexpression of *Pls3* in the "Taiwanese model" mice on the BL6, but not the FVB, background also resulted in a less severe phenotype (Ackermann, Krober et al. 2013). Although

Pls3 improves the NMJ pathology in the "Taiwanese model", it should be noted that the NMJ pathology in these mice is already less severe than most of the other SMA mouse models to begin with. Other studies have shown that overexpression of *Pls3* in the "delta 7 model" mice on the FVB background did not provide any benefit (McGovern, Massoni-Laporte et al. 2015). The differential induction of *Pls3* in BL6 $Smn^{2B/-}$ mice may contribute to the less severe phenotype compared to the FVB $Smn^{2B/-}$ mice, but this requires more investigation.

In summary, our studies have shown that the congenic strains of $Smn^{2B/-}$ mice on the FVB background have a more severe phenotype than on the BL6 background. Although this difference in severity correlates with a differential induction of $Smn^{2B/-}$ in the BL6 background, we cannot exclude the possibility that other genetic modifiers likely influence the overall disease picture in the congenic $Smn^{2B/-}$ mice. Future studies will be directed towards a systematic search for modifier genes influencing the phenotype in these mice. Identification of such genes could potentially reveal pathways involved in motor neuron survival and skeletal muscle amelioration, and contribute to new therapeutic approaches to treat SMA.

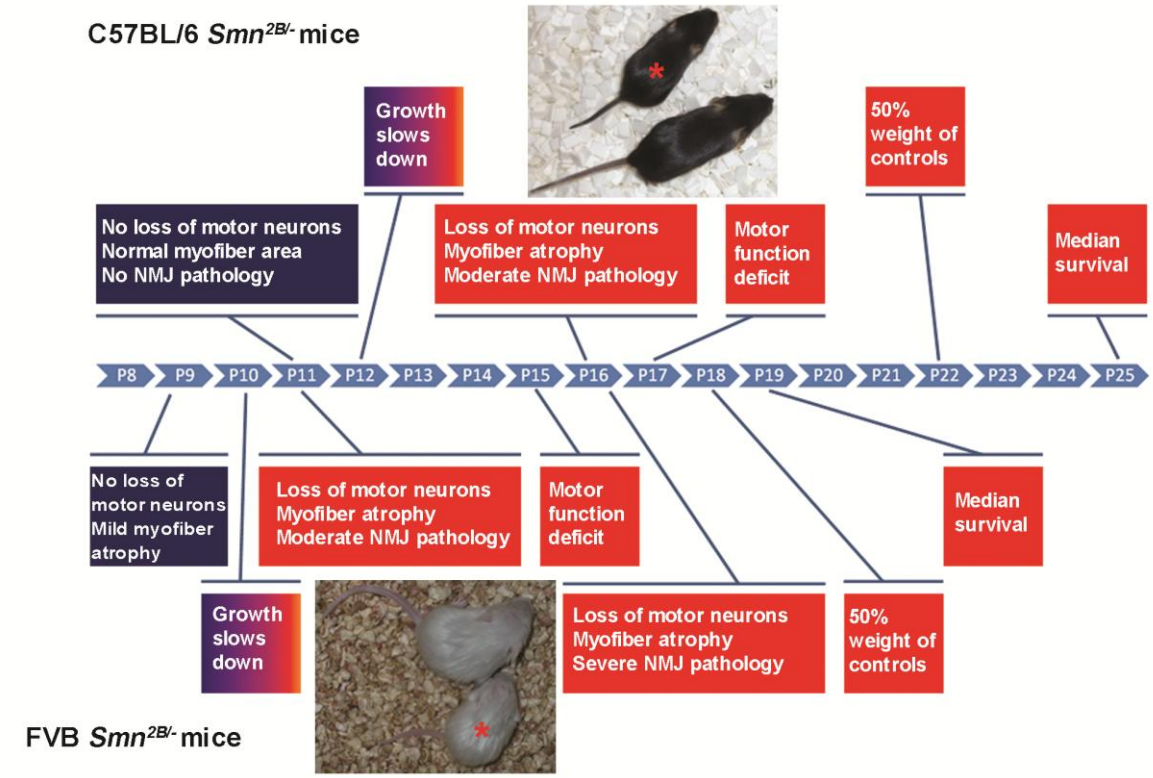

Figure 4.2.2. A schematic temporal comparison of various phenotypes in FVB *Smn*$^{2B/-}$ and BL6 *Smn*$^{2B/-}$ mice. P indicates postnatal day (PND). * indicates *Smn*$^{2B/-}$ mice beside their control littermates.

4.3- General Discussion

Spinal muscular atrophy as a multi organ disorder

Despite the traditional definition of SMA as a motor neuron disease, increasing evidence has revealed that other cell types are also affected in the course of this disease. This is in accordance with the fact that *SMN* is ubiquitously expressed in all cell types. And, considering the housekeeping functions of SMN, it could be postulated that depletion of SMN might cause molecular perturbations within all tissues. Comprehensive studies on SMA patients and SMA animal models have also confirmed that SMA is a multi-organ disorder. In addition to motor neurons, several organs including brain, heart, lung, intestine, pancreas, bones, liver and skeletal muscles undergo pathologic changes in SMA (for a review see (Shababi, Lorson et al. 2014)).

Here we showed widespread molecular alterations in central synapses isolated from spinal cords of $Smn^{2B/-}$ mice at a presymptomatic stage. In mouse, *Smn* is broadly expressed in the CNS during embryonic life, however its expression decreases after birth except for some regions of CNS including the anterior horns of spinal cord. Accordingly, pathologic alterations of CNS have been reported within CNS of severe mouse models of SMA (Liu, Shafey et al. 2010, Wishart, Huang et al. 2010, Mentis, Blivis et al. 2011). Alterations of the proteome of central synapses have also been reported in 'severe SMA' mice at a presymptomatic stage (i.e. PND1) (Wishart et al., 2014).

SMN has a pivotal role in the biogenesis of snRNPs in all cell types. However, depletion of SMN does not alter the levels of all individual snRNPs to the same extent and often results in a new profile of snRNPs in the cells (Gabanella, Butchbach et al. 2007, Zhang, Lotti et al. 2008). The alterations in snRNPs' profile are widespread and happen in different tissues; this supports that pathologic features of SMA are not restricted to motor neurons. Zhang et al. found that SMN

depletion affects the level of snRNAs in different tissues including brain, spinal cord, kidney, heart and skeletal muscles. Interestingly the alterations in the levels of individual snRNAs were not uniform among different tissues; the authors concluded that the depletion of SMN affects the snRNP profile in a tissue specific manner (Zhang, Lotti et al. 2008).

Mitochondria as primary affected organelles in SMA

Mitochondrial defects are reported in several 'in vitro' and 'in vivo' models of SMA. Knock down of *Smn* in cultured NSC-34 cells (a motor neuron like cell line) results in dysfunction of mitochondria and increased production of reactive oxygen species (ROS) (Acsadi, Lee et al. 2009). Using a systematic approach, Miller et al. investigated mitochondrial pathologic changes in motor neurons of 'delta 7 SMA' mice. The authors discovered that basal and maximal mitochondrial respiration is significantly reduced in cultured motor neurons isolated from 'delta 7 SMA' mice. They also observed increased levels of ROS and decreased mitochondrial membrane potential in these cells. In addition, the axonal transport of mitochondria was significantly slowed in motor neurons isolated from 'delta 7 SMA' mice. Electron microscopy on spinal cords of these mice also revealed ultrastructural abnormalities of mitochondria (e.g. fragmentation and edema) within motor neurons at a presymptomatic stage. Altogether, the authors concluded that mitochondrial defects may have a critical role in SMA pathogenesis (Miller, Shi et al. 2016).

Synaptic mitochondrial abnormalities are also reported in SMA. The total mitochondrial mass is reduced remarkably in NMJs of 'delta 7 SMA' mice (Kariya, Park et al. 2008, Kong, Wang et al. 2009, Torres-Benito, Neher et al. 2011). Swelling and degeneration of synaptic

mitochondria is also reported within presynaptic and postsynaptic areas of NMJs of animal models of SMA (Voigt, Meyer et al. 2010).

Besides providing the required energy for synaptic function, mitochondria also have an important role in calcium homeostasis within synapses (Zenisek and Matthews 2000, Billups and Forsythe 2002). Interestingly, calcium homeostasis is altered in motor nerve terminals of 'severe SMA' mice which might be due to the mitochondrial dysfunction in these mice (Ruiz, Casanas et al. 2010). Mitochondria also contribute to several other functions in synapses including management of reactive oxygen species, and biosynthesis of neurotransmitters, amino acids and lipids (Vos, Lauwers et al. 2010).

Our analysis revealed that the levels of several mitochondrial proteins are altered in synapses isolated from spinal cords of $Smn^{2B/-}$ mice at a presymptomatic stage. Especially, the levels of some subunits of mitochondrial complex I (i.e. NADH-ubiquinone oxidoreductase) were remarkably changed in our samples. Complex I is a gigantic protein complex consisting of 41 proteins encoded by both nuclear and mitochondrial genes (Hatefi 1985). Deficiencies of mitochondrial complex I result in inefficient mitochondrial respiration and an increase in the production of reactive oxygen species. Complex I deficiencies in human present with versatile clinical manifestations including macrocephaly, Leigh disease, Leber hereditary optic neuropathy, cardiomyopathy, myopathy, cataract, liver disease and Parkinsonism (Robinson 1998). The expression levels of several subunits of mitochondrial complex I are altered in neurodegenerative disorders (e.g. Parkinson's disease, Huntington disease, Alzheimer's disease). Indeed, it is believed that dysfunction of complex I (primary or secondary) playa an important role in pathogenesis of these disorders through production of excessive amounts of reactive oxygen species (ROS) (Kweon, Marks et al. 2004, Lenaz, Baracca et al. 2006, Rizzardini, Lupi

et al. 2006, Schapira 2010, Zhang, Guo et al. 2015). Interestingly, Miller et al. reported concentric lamellar inclusions within mitochondria of SMA motor neurons, which is a characteristic finding in Leigh disease (Miller, Shi et al. 2016).

Clinical studies also showed mitochondrial defects in SMA patients. Ripolone et al. studied muscle samples from patients with different types of SMA. The authors found that the overall mitochondrial mass is reduced within muscles of SMA patients (indicated by reduction of mitochondrial DNA and several mitochondrial proteins). They also observed that the expression levels of several genes involved in mitochondrial biogenesis were reduced within muscles of SMA patients while several myogenic factors were upregulated (Ripolone, Ronchi et al. 2015).

There is also some clinical evidence that defects of mitochondria contribute directly to the pathogenesis of SMA. There are reports of several *SMN*-independent SMA cases due to mutations in the *thymidine kinase 2* gene (*TK2*, MIM# 188250) (Mancuso, Salviati et al. 2002). *TK2* controls mtDNA replication and mutations of this gene result in depletion of mtDNA in neurons, and hence mitochondrial mass. A less frequent case of *SMN*-independent SMA is reported because of mutations in the *cytochrome-c oxidase assembly* gene (*SCO2*, MIM# 604377).

Clinical significance of altered molecular signalling pathways in SMA

So far, most of medical interventions for SMA patients have been based on providing general supportive care to facilitate the mobility and improve the quality of life of these patients. These interventions include respiratory support, dietary assistance, orthopedic adjustments, physical rehabilitation and psychological consultation (Farrar, Park et al. 2016). Recently, two novel therapeutic strategies have been introduced for treatment of SMA, antisense

oligonucleotide (ASO) therapy and gene therapy. These strategies are based on the restoration of full length SMN within cells, and show promise. However, the real effectiveness of these treatments will be known only after their long term and widespread administration. One major concern here is that the interventional approaches based on restoration of full length SMN have a narrow therapeutic window. Indeed, restoration of full length Smn in 'delta 7 SMA' mice after 8 days of age (using a genetic rescue model or viral gene therapy approaches) failed to extend the life span of these animals significantly (Lutz, Kariya et al. 2011, Robbins, Glascock et al. 2014). The exact nature of the 'SMA therapeutic window' and its contributing factors have not been defined yet. In addition, more reliable biological response markers are necessary for a precise assessment of the efficacy of any therapeutic approach in SMA.

Nusinersen is an approved ASO by the US FDA for administration in patients with different types of SMA. Nusinersen increases the level of FL-SMN by increasing the inclusion of exon 7 within the *SMN2* mRNA (Hoy 2017). So far, several clinical trials reported that the administration of nusinersen has resulted in significant but still modest and slow improvement of motor functions in SMA patients. Indeed, nusinersen was not able to restore the normal age-matched motor functions in the treated individuals (Finkel, Chiriboga et al. 2016). In addition, the overall costs of nusinersen therapy are estimated to be more than 1 million dollars for each patient (Morrow 2017).

It seems that more therapeutics options are required for treatment of SMA. In that case, physicians will be able to design and use personalized medicine approaches (using combination or adjunct therapy protocols). One logical strategy is to find defective molecular mechanisms underlying the pathogenesis of SMA. In this regard, high-throughput comparative molecular analyses (comparing diseased and normal populations, or vulnerable and resistant cells/tissues,

or different genetic backgrounds) are useful. Using high-throughput comparative analysis approaches, our group and others have found the regulation of the actin cytoskeleton pathway and some metabolic molecular pathways are affected in SMA. These pathways have the potential to be considered as viable therapeutic targets in SMA. Our group showed before that pharmaceutical inhibition of the Rho/ROCK pathway improves the SMA phenotype in *Smn*$^{2B/-}$ mice and others showed that overexpression of *Plastin3* in combination with suboptimal doses of ASO rescues the phenotype in 'Taiwanese SMA' mice (Bowerman, Beauvais et al. 2010, Bowerman, Murray et al. 2012, Hosseinibarkooie, Peters et al. 2016, Kaifer, Villalon et al. 2017). Inhibition of the Rho/ROCK pathway is also proposed to have beneficial effects in other neurodegenerative disorders (Mueller, Mack et al. 2005, Raad, El Tal et al. 2012).

Metabolic dysregulation is also reported in SMA. Previously our group reported impaired glucose metabolism in *Smn*$^{2B/-}$ mice at a presymptomatic stage. And, histological examinations of pancreas samples from SMA patients were suggestive of impaired glucose metabolism (Bowerman, Swoboda et al. 2012, Bowerman, Michalski et al. 2014). In addition, impaired lipid metabolism has been observed in SMA patients (Tein, Sloane et al. 1995). And, here we showed that several metabolic pathways involved in energy production and protein synthesis are affected in central synapses of *Smn*$^{2B/-}$ mice at a presymptomatic stage.

In addition to improving the quality of life of SMA patients, appropriate metabolic intervention may slow down the progress of the disease and extend the therapeutic window of SMA. Indeed, interventional metabolic approaches have been proposed to be beneficial in neurodegenerative diseases (Gray, Tompkins et al. 2014). Applying these approaches, several therapeutic protocols have been studied in ALS, including high calorie diets, ketogenic diets, alternative energy sources (e.g. triheptanoin, pyruvate, lactate, creatine) and several potent

antioxidants (Tefera and Borges 2016). Although there have been some benefits of these approaches in ALS, the value of such approaches remain to be determined in SMA.

Some components of metabolic pathways might also serve as valid and reliable biomarkers for assessment of prognosis of patients and their response to treatment. It is suggested that the level of pyruvate in CSF is a biomarker for several neurodegenerative disorders like Alzheimer's disease (Parnetti, Gaiti et al. 1995). The transport of pyruvate into mitochondria is mediated by a protein complex called mitochondrial pyruvate carrier (MPC). A recent study also reported that pharmacological inhibition of MPC has an anti-inflammatory effect and protects dopaminergic neurons from death in several models of Parkinson's disease (Ghosh, Tyson et al. 2016).

As mentioned before, mitochondria show several abnormalities in SMA including reduced biogenesis. It is suggested that enhancement of mitochondrial biogenesis within neurons might be beneficial in neuromuscular disorders. PGC-1α is the master regulator of mitochondrial biogenesis. So far, several pharmaceutical compounds which increase PGC-1α expression or its activity have been used in different models of neuromuscular disorders and showed promising results (for a comprehensive review please refer to Uittenbogaard and Chiaramello 2014, Valero 2014). Some clinical trials have showed beneficial effects of olesoxime in patients with type II and type III SMA (Bordet, Berna et al. 2010). Olesoxime (TRO-19622) is a cholesterol-like molecule which showed neuroprotective effects in primary cultures of motor neurons and some animal models of motor neuron disorders. It is believed that olesoxime targets mitochondria probably by occluding the mitochondrial permeability pore (mPTP) and thus inhibiting the release of proapoptotic factors from mitochondria (Martin 2010).

Closing remarks

SMN gene was discovered more than two decades ago (Lefebvre, Burglen et al. 1995). However, it is not very well understood how mutations of this gene result in SMA, a degenerative disorder with prominent neuromuscular manifestations (Pearn 1980). *SMN* is a ubiquitously expressed gene and strong evidence suggests that it has multiple housekeeping functions within cells. However, only the *SMN* role in the assembly of spliceosomal machinery is characterized in detail (Kolb, Battle et al. 2007). In addition, a comprehensive description of the molecular pathways affected by SMN depletion is not available yet. Recent studies also support that multiple systems are involved in the course of SMA which is against the traditional belief that SMA is a specific disorder of motor neurons (Shababi, Lorson et al. 2014).

Here, we studied molecular events prior to the onset of any SMA phenotype within central synapses of $Smn^{2B/-}$ mice, a less severe SMA mouse model with a relatively long presymptomatic period. We found that the levels of some proteins involved in the regulation of actin cytoskeleton, energy metabolism and protein synthesis are altered in central synapses of $Smn^{2B/-}$ mice, proposing that the dysregulation of these pathways may contribute to the pathogenesis of the disease. Our findings are in accordance with previous studies which also showed these molecular pathways are dysregulated in several '*in vitro*' and '*in vivo*' SMA models (Oprea, Krober et al. 2008, Acsadi, Lee et al. 2009, Bowerman, Anderson et al. 2009, Murray, Beauvais et al. 2015, Miller, Shi et al. 2016). Also, we found that the genetic background of the mouse modulates the phenotype of $Smn^{2B/-}$ mice. Interestingly, *Plastin 3*, a proposed SMA modifier gene, was differentially induced between $Smn^{2B/-}$ mice with different genetic backgrounds. This further suggests that dysregulation of the actin cytoskeleton contributes to the pathogenesis of SMA.

We hope that our findings have helped to have a better understanding of the molecular events mediating SMA phenotype in human. However, further studies are required to determine the exact nature of impairment of each of the proposed signalling pathway and also their therapeutic value in SMA.

Chapter 5 - Appendix

Supplementary Table 4.1. Proteins with more than 30% reduction in synaptosome fractions prepared from spinal cords of *Smn*$^{2B/-}$ mice (FC stands for fold change). Note that the lower $\log_2$(FC) correlates with more decrease in the levels of proteins.

	Gene Symbol	Protein Name	Log_2(FC)	*p* value
1	S100a1	S100-A1	-1.77	2.90E-02
2	Mtatp6	ATP synthase subunit a	-1.47	3.23E-06
3	Cplx2	Complexin-2	-1.22	1.16E-06
4	Mocs2	Molybdopterin synthase catalytic subunit 2	-1.19	4.75E-06
5	Rap2c	Ras-related protein Rap-2c	-1.14	8.82E-03
6	Plekhb1	Pleckstrin homology domain-containing family B member 1	-1.09	5.53E-04
7	L7rn6	Lethal gene on chromosome 7 Rinchik 6	-0.99	4.59E-05
8	Tmem126b	Transmembrane mitochondrial protein 126B	-0.95	1.27E-03
9	Fundc1	FUN14 domain-containing protein 1	-0.95	3.93E-02
10	Chchd4	Mitochondrial intermembrane space import and assembly protein 40	-0.89	7.71E-04
11	Rbbp9	Putative hydrolase RBBP9	-0.89	2.89E-04
12	Gtf3c4	General transcription factor 3C polypeptide 4	-0.81	8.65E-03
13	Arf1	ADP-ribosylation factor 1	-0.80	1.62E-03
14	Arf2	ADP-ribosylation factor 2	-0.80	1.39E-03
15	Cfl1	Cofilin-1	-0.75	2.42E-02
16	Grp	Gastrin-releasing peptide	-0.71	7.79E-03
17	Dctn5	Dynactin subunit 5	-0.68	6.92E-03
18	Ube2v2	Ubiquitin-conjugating enzyme E2 variant 2	-0.67	3.54E-02
19	Fgf1	Fibroblast growth factor 1	-0.66	1.33E-02
20	Ube2v1	Ubiquitin-conjugating enzyme E2 variant 1	-0.62	1.99E-02
21	Nudt10	Diphosphoinositol polyphosphate phosphohydrolase 3-alpha	-0.56	3.97E-08
22	Cd81	CD81 antigen	-0.54	4.33E-04
23	Tomm34	Mitochondrial import receptor subunit TOM34	-0.54	3.12E-04
24	Atp6ap2	Renin receptor	-0.53	4.08E-03
25	Sep8	Septin-8	-0.52	4.28E-05
26	Mcur1	Mitochondrial calcium uniporter regulator 1	-0.50	1.27E-02
27	Arpp19	cAMP-regulated phosphoprotein 19	-0.49	7.79E-05
28	Acaa1b	3-ketoacyl-CoA thiolase B, peroxisomal	-0.49	2.23E-02
29	Vamp3	Vesicle-associated membrane protein 3	-0.48	1.13E-02
30	Chgb	Secretogranin-1	-0.48	5.98E-04
31	Ptp4a2	Protein tyrosine phosphatase type IVA 2	-0.48	8.84E-04
32	Tomm7	Mitochondrial import receptor subunit TOM7 homolog	-0.48	2.46E-04
33	Ube2h	Ubiquitin-conjugating enzyme E2 H	-0.47	1.57E-02
34	Git1	ARF GTPase-activating protein GIT1	-0.46	1.34E-02
35	Ndufs4	NADH dehydrogenase [ubiquinone] iron-sulfur protein 4	-0.46	4.39E-04
36	Rap2b	Ras-related protein Rap-2b	-0.46	1.13E-02
37	Rpl36	60S ribosomal protein L36	-0.45	1.77E-02

Supplementary Table 4.1 (cont'd)

	Gene Symbol	Protein Name	Log_2(FC)	*p* value
38	Rbm3	RNA-binding protein 3	-0.45	2.00E-02
39	Rpl12	60S ribosomal protein L12	-0.45	6.16E-04
40	Penk	Proenkephalin-A	-0.44	1.33E-03
41	Ubl4a	Ubiquitin-like protein 4A	-0.43	5.95E-03
42	Cfl2	Cofilin-2	-0.42	6.61E-03
43	Rap1b	Ras-related protein Rap-1b	-0.42	1.28E-04
44	Cox7a2l	Cytochrome c oxidase subunit 7A-related protein, mitochondrial	-0.41	1.78E-04
45	Actn3	Alpha-actinin-3	-0.39	6.21E-04
46	Kras	GTPase Kras	-0.39	1.48E-03
47	Grcc10	Protein C10	-0.39	1.14E-03
48	Fabp7	Fatty acid-binding protein, brain	-0.38	1.85E-03
49	Arl6ip5	PRA1 family protein 3	-0.38	8.86E-03

Supplementary Table 4.2. Proteins with more than 30% increase in synaptosome fractions prepared from spinal cords of PND 11 *Smn*$^{2B/-}$ mice (FC stands for fold change). Note that the more $\log_2$(FC) correlates with more increase in the levels of proteins.

	Gene Symbol	Protein Name	Log_2(FC)	*p* value
1	Actbl2	Beta-actin-like protein 2	1.66	1.55E-04
2	Atp6ap1	V-type proton ATPase subunit S1	1.50	8.42E-03
3	Tmem186	Transmembrane protein 186	1.37	2.96E-02
4	Syt5	Synaptotagmin-5	1.35	2.01E-03
5	Fam49a	Protein FAM49A	1.30	1.24E-02
6	Slc25a19	Mitochondrial thiamine pyrophosphate carrier	1.29	1.15E-04
7	Eif2s1	Eukaryotic translation initiation factor 2 subunit 1	1.21	1.51E-04
8	Csnk1d	Casein kinase I isoform delta	1.17	8.59E-04
9	Kctd5	BTB/POZ domain-containing protein KCTD5	1.08	2.74E-03
10	Ccdc53	WASH complex subunit CCDC53	1.08	4.14E-03
11	Psma8	Proteasome subunit alpha type-7-like	1.05	4.33E-02
12	UPF0568	UPF0568 protein C14orf166 homolog	1.00	1.52E-02
13	Slc25a31	ADP/ATP translocase 4	0.92	1.34E-05
14	Cbr3	Carbonyl reductase [NADPH] 3	0.92	1.41E-05
15	Agpat1	1-acyl-sn-glycerol-3-phosphate acyltransferase alpha	0.91	1.34E-02
16	Dhrs7b	Dehydrogenase/reductase SDR family member 7B	0.91	7.90E-05
17	Memo1	Protein MEMO1	0.90	1.47E-02
18	Fahd1	Acylpyruvase FAHD1, mitochondrial	0.89	5.89E-05
19	Comtd1	Catechol O-methyltransferase domain-containing protein 1	0.88	2.47E-02
20	Add3	Gamma-adducin	0.87	1.18E-03
21	Scrn1	Secernin-1	0.86	3.03E-04
22	Mrps31	28S ribosomal protein S31, mitochondrial	0.85	4.23E-07
23	Hmgn5	High mobility group nucleosome-binding domain-containing protein 5	0.84	1.03E-03
24	Iglon5	IgLON family member 5	0.81	2.40E-04
25	Nudt7	Peroxisomal coenzyme A diphosphatase NUDT7	0.81	1.14E-03
26	Abhd10	Mycophenolic acid acyl-glucuronide esterase, mitochondrial	0.80	2.21E-03
27	Atp6v1e2	V-type proton ATPase subunit E 2	0.76	4.82E-02
28	Arhgdib	Rho GDP-dissociation inhibitor 2	0.75	1.11E-03
29	Rab3c	Ras-related protein Rab-3C	0.74	1.47E-05
30	Hspa2	Heat shock-related 70 kDa protein 2	0.73	3.86E-03
31	Slc25a14	Brain mitochondrial carrier protein 1	0.72	2.94E-02
32	Atp5sl	ATP synthase subunit s-like protein	0.72	2.81E-05
33	Cap1	Adenylyl cyclase-associated protein 1	0.72	3.33E-05
34	Atad3	ATPase family AAA domain-containing protein 3	0.71	1.96E-04
35	Akap5	A-kinase anchor protein 5	0.71	1.37E-02
36	Lyrm9	LYR motif-containing protein 9	0.71	1.55E-03
37	Ppp3cb	Serine/threonine-protein phosphatase 2B catalytic subunit beta iso	0.70	2.64E-04

Supplementary Table 4.2 (cont'd)

	Gene Symbol	Protein Name	Log_2(FC)	*p* value
38	Haghl	Hydroxyacylglutathione hydrolase-like protein	0.70	1.99E-02
39	Hmgb1	High mobility group protein B1	0.70	1.38E-02
40	Atg3	Ubiquitin-like-conjugating enzyme ATG3	0.69	1.60E-04
41	Ppp1r1a	Protein phosphatase 1 regulatory subunit 1A	0.69	1.51E-03
42	Blmh	Bleomycin hydrolase; Short=BH	0.68	1.45E-05
43	Cops3	COP9 signalosome complex subunit 3	0.67	8.45E-05
44	Armc1	Armadillo repeat-containing protein 1	0.67	1.03E-05
45	Mrpl1	39S ribosomal protein L1, mitochondrial	0.66	7.17E-06
46	Capza1	F-actin-capping protein subunit alpha-1	0.66	3.96E-04
47	Ddx3y	ATP-dependent RNA helicase DDX3Y	0.66	3.67E-06
48	Gmps	GMP synthase [glutamine-hydrolyzing]	0.66	1.92E-06
49	Gnaq	Guanine nucleotide-binding protein G(q) subunit alpha	0.65	1.35E-03
50	Agap3	Arf-GAP with GTPase, ANK repeat and PH domain-containing protein 3	0.65	1.26E-03
51	Atxn10	Ataxin-10	0.65	9.11E-04
52	Psmc4	26S protease regulatory subunit 6B	0.64	1.00E-03
53	Tpd52l2	Tumor protein D54	0.63	1.17E-03
54	Tspan7	Tetraspanin-7	0.63	9.85E-03
55	Anxa2	Annexin A2	0.63	3.96E-04
56	Psmb7	Proteasome subunit beta type-7	0.63	2.81E-02
57	Purb	Transcriptional activator protein Pur-beta	0.63	1.10E-05
58		Quinone oxidoreductase-like protein 2	0.62	2.08E-03
59	Crip2	Cysteine-rich protein 2	0.61	7.26E-03
60	Gad1	Glutamate decarboxylase 1	0.61	6.74E-06
61	Tstd3	Thiosulfate sulfurtransferase/rhodanese-like domain-containing protein 3	0.61	2.84E-02
62	Lss	Lanosterol synthase	0.61	1.20E-05
63	Plbd2	Putative phospholipase B-like 2	0.61	2.32E-02
64	Cyp51a1	Lanosterol 14-alpha demethylase; Short=LDM	0.61	1.33E-04
65	Mmab	Cob(I)yrinic acid a,c-diamide adenosyltransferase, mitochondrial	0.60	2.37E-02
66	Cxadr	Coxsackievirus and adenovirus receptor homolog	0.60	8.49E-04
67	Hadh	Hydroxyacyl-coenzyme A dehydrogenase, mitochondrial	0.60	1.54E-03
68	Pygl	Glycogen phosphorylase, liver form	0.60	5.38E-04
69	Ostf1	Osteoclast-stimulating factor 1	0.60	1.48E-02
70	Ptcd3	Pentatricopeptide repeat domain-containing protein 3, mitochondrial	0.59	2.15E-06
71	Hddc2	HD domain-containing protein 2	0.59	5.59E-03
72	Tmem14c	Transmembrane protein 14C	0.59	7.96E-04
73	Eno3	Beta-enolase	0.59	8.69E-03
74	Avil	Advillin	0.58	1.07E-02
75	Mrpl15	39S ribosomal protein L15, mitochondrial	0.58	1.17E-02
76	Mrpl44	39S ribosomal protein L44, mitochondrial	0.58	1.29E-03

Supplementary Table 4.2 (cont'd)

	Gene Symbol	Protein Name	Log_2(FC)	*p* value
77	Vps25	Vacuolar protein-sorting-associated protein 25	0.58	3.13E-03
78	Dguok	Deoxyguanosine kinase, mitochondrial	0.58	2.60E-03
79	Ntmt1	N-terminal Xaa-Pro-Lys N-methyltransferase 1	0.57	3.37E-03
80	Pdap1	28 kDa heat- and acid-stable phosphoprotein	0.57	3.77E-04
81	Grhpr	Glyoxylate reductase/hydroxypyruvate reductase	0.56	1.40E-02
82	Tpp2	Tripeptidyl-peptidase 2	0.56	7.85E-04
83	Tk2	Thymidine kinase 2, mitochondrial	0.56	1.98E-07
84	Asap2	Arf-GAP with SH3 domain	0.56	9.92E-03
85	App	Amyloid beta A4 protein	0.56	1.94E-03
86	Oxr1	Oxidation resistance protein 1	0.56	2.86E-04
87	Mgea5	Protein O-GlcNAcase	0.55	1.18E-03
88	Tmem106b	Transmembrane protein 106B	0.55	3.68E-09
89	Ethe1	Persulfide dioxygenase ETHE1, mitochondrial	0.55	4.27E-03
90	Gbas	Protein NipSnap homolog 2; Short=NipSnap2	0.55	1.37E-04
91	Cox20	Cytochrome c oxidase protein 20 homolog	0.55	4.62E-02
92	Dcun1d1	DCN1-like protein 1	0.55	4.12E-02
93	Pgk2	Phosphoglycerate kinase 2	0.55	4.72E-04
94	Hbs1l	HBS1-like protein	0.55	2.01E-04
95	Aldh4a1	Delta-1-pyrroline-5-carboxylate dehydrogenase, mitochondrial	0.55	4.15E-04
96	Gars	Glycine--tRNA ligase	0.55	6.69E-05
97	Lcp1	Plastin-2	0.55	2.26E-03
98	Yars2	Tyrosine--tRNA ligase, mitochondrial	0.55	4.47E-06
99	Ddah2	N(G),N(G)-dimethylarginine dimethylaminohydrolase 2	0.54	2.15E-03
100	Sep9	Septin-9; AltName	0.54	6.34E-03
101	Pgrmc2	Membrane-associated progesterone receptor component 2	0.54	1.24E-05
102	Mthfd1	C-1-tetrahydrofolate synthase, cytoplasmic	0.54	5.84E-03
103	Tuba1a	Tubulin alpha-1A chain	0.54	4.22E-04
104	Dnpep	Aspartyl aminopeptidase	0.54	1.83E-06
105	Pgls	6-phosphogluconolactonase	0.54	1.50E-03
106	Basp1	Brain acid soluble protein 1	0.53	7.19E-03
107	Eif3a	Eukaryotic translation initiation factor 3 subunit A	0.53	7.94E-07
108	Aip	AH receptor-interacting protein; Short=AIP	0.53	2.12E-03
109	Actr1b	Beta-centractin	0.53	1.10E-03
110	Srgap2	SLIT-ROBO Rho GTPase-activating protein 2	0.52	7.26E-04
111	Eif3b	Eukaryotic translation initiation factor 3 subunit B	0.52	2.51E-04
112	Ech1	Delta(3,5)-Delta(2,4)-dienoyl-CoA isomerase, mitochondrial	0.52	4.03E-04
113	Dync1i2	Cytoplasmic dynein 1 intermediate chain 2	0.52	1.69E-05
114	Msn	Moesin	0.52	1.67E-04
115	Ralb	Ras-related protein Ral-B	0.52	5.12E-03
116	Pgp	Phosphoglycolate phosphatase	0.52	1.28E-05

Supplementary Table 4.2 (cont'd)

	Gene Symbol	Protein Name	Log_2(FC)	*p* value
117	Tmem163	Transmembrane protein 163	0.52	1.47E-05
118	Ppid	Peptidyl-prolyl cis-trans isomerase D	0.52	1.61E-04
119	Rab3b	Ras-related protein Rab-3B	0.51	4.04E-05
120	Cct5	T-complex protein 1 subunit epsilon	0.51	1.35E-03
121	Hars2	Probable histidine--tRNA ligase, mitochondrial	0.51	1.90E-07
122	Uros	Uroporphyrinogen-III synthase	0.51	5.16E-05
123	Gamt	Guanidinoacetate N-methyltransferase	0.51	4.42E-03
124	Acly	ATP-citrate synthase	0.51	3.47E-03
125	Akr1a1	Alcohol dehydrogenase [NADP(+)]	0.51	1.39E-03
126	Idh1	Isocitrate dehydrogenase [NADP] cytoplasmic	0.50	1.86E-06
127	Gpsm1	G-protein-signaling modulator 1	0.50	2.17E-03
128	Nsfl1c	NSFL1 cofactor p47	0.50	4.04E-03
129	Fam73a	Protein FAM73A	0.50	6.37E-03
130	Rims1	Regulating synaptic membrane exocytosis protein 1	0.50	1.61E-03
131	Dpp3	Dipeptidyl peptidase 3	0.50	1.68E-06
132	Fscn1	Fascin	0.50	1.41E-03
133	Hmgcs1	Hydroxymethylglutaryl-CoA synthase, cytoplasmic	0.50	1.40E-06
134	Kctd8	BTB/POZ domain-containing protein KCTD8	0.50	3.54E-05
135	Phf24	PHD finger protein 24	0.50	2.46E-03
136	Eps15l1	Epidermal growth factor receptor substrate 15-like 1	0.50	2.29E-03
137	Cul3	Cullin-3; Short=CUL-3	0.50	2.34E-04
138	Gprin1	G protein-regulated inducer of neurite outgrowth 1	0.49	4.47E-03
139	Rab11fip5	Rab11 family-interacting protein 5	0.49	1.24E-03
140	Rpl7	60S ribosomal protein L7	0.49	2.60E-04
141	Alpl	Alkaline phosphatase, tissue-nonspecific isozyme	0.49	5.64E-05
142	Aco1	Cytoplasmic aconitate hydratase	0.49	6.75E-05
143	Echs1	Enoyl-CoA hydratase, mitochondrial	0.49	1.21E-05
144	Tigar	Fructose-2,6-bisphosphatase TIGAR	0.49	4.82E-03
145	Prep	Prolyl endopeptidase	0.49	4.16E-07
146	Mea1	Male-enhanced antigen 1	0.49	1.91E-02
147	Pcbp2	Poly(rC)-binding protein 2	0.48	3.08E-04
148	Dbn1	Drebrin	0.48	2.33E-02
149	Pdpr	Pyruvate dehydrogenase phosphatase regulatory subunit, mitochondrial	0.48	8.50E-04
150	Hnrnpk	Heterogeneous nuclear ribonucleoprotein K	0.48	4.91E-02
151	Aldh5a1	Succinate-semialdehyde dehydrogenase, mitochondrial	0.48	7.76E-05
152	Nceh1	Neutral cholesterol ester hydrolase 1	0.48	2.33E-03
153	Slc6a5	Sodium- and chloride-dependent glycine transporter 2	0.48	6.14E-04
154	Sugt1	Protein SGT1 homolog	0.48	3.59E-04
155	Srgap3	SLIT-ROBO Rho GTPase-activating protein 3	0.48	1.02E-02
156	Eci2	Enoyl-CoA delta isomerase 2, mitochondrial	0.48	1.04E-04

Supplementary Table 4.2 (cont'd)

	Gene Symbol	Protein Name	Log_2(FC)	*p* value
157	Pygb	Glycogen phosphorylase, brain form	0.48	6.04E-03
158	Immt	MICOS complex subunit Mic60	0.48	6.07E-10
159	Picalm	Phosphatidylinositol-binding clathrin assembly protein	0.48	4.55E-02
160	Gpd2	Glycerol-3-phosphate dehydrogenase, mitochondrial	0.48	4.48E-06
161	Pdxk	Pyridoxal kinase	0.48	6.56E-04
162	Atpaf2	ATP synthase mitochondrial F1 complex assembly factor 2	0.48	5.00E-05
163	Fkbp4	Peptidyl-prolyl cis-trans isomerase FKBP4	0.48	1.80E-02
164	Sv2b	Synaptic vesicle glycoprotein 2B	0.47	6.73E-04
165	Pafah1b3	Platelet-activating factor acetylhydrolase IB subunit gamma	0.47	2.25E-03
166	Eef1a2	Elongation factor 1-alpha 2	0.47	2.70E-09
167	Aldh1l1	Cytosolic 10-formyltetrahydrofolate dehydrogenase	0.47	4.81E-06
168	Sarm1	Sterile alpha and TIR motif-containing protein 1	0.47	5.07E-05
169	Nudt8	Nucleoside diphosphate-linked moiety X motif 8, mitochondrial	0.47	2.45E-02
170	Acsl6	Long-chain-fatty-acid--CoA ligase 6	0.47	1.65E-07
171	Lonp1	Lon protease homolog, mitochondrial	0.47	8.17E-10
172	Hk1	Hexokinase-1	0.47	9.42E-05
173	Synj1	Synaptojanin-1	0.47	1.27E-03
174	Clpp	ATP-dependent Clp protease proteolytic subunit, mitochondrial	0.47	1.52E-04
175	Soga3	Protein SOGA3	0.47	1.84E-02
176	Ivd	Isovaleryl-CoA dehydrogenase, mitochondrial	0.47	1.61E-03
177	Arvcf	Armadillo repeat protein deleted in velo-cardio-facial syndrome homolog	0.46	4.21E-05
178	Gtpbp8	GTP-binding protein 8	0.46	7.97E-06
179	Pacs1	Phosphofurin acidic cluster sorting protein 1	0.46	1.23E-04
180	Ppt1	Palmitoyl-protein thioesterase 1	0.46	2.35E-05
181	Rab5b	Ras-related protein Rab-5B	0.46	3.20E-03
182	Hip1	Huntingtin-interacting protein 1	0.46	1.92E-03
183	Fermt2	Fermitin family homolog 2	0.46	8.02E-03
184	Rpl3	60S ribosomal protein L3	0.46	2.73E-03
185	Pck2	Phosphoenolpyruvate carboxykinase [GTP], mitochondrial	0.45	1.01E-08
186	Ak3	GTP:AMP phosphotransferase AK3, mitochondrial	0.45	5.39E-06
187	Acat1	Acetyl-CoA acetyltransferase, mitochondrial	0.45	1.08E-07
188	Tmsb4x	Thymosin beta-4; Short=T beta 4	0.45	1.38E-02
189	Hspa4l	Heat shock 70 kDa protein 4L	0.45	1.76E-03
190	Pgrmc1	Membrane-associated progesterone receptor component 1	0.45	7.07E-04
191	Dbt	Branched-chain alpha-keto acid dehydrogenase complex component E2	0.45	1.57E-11
192	Acsl1	Long-chain-fatty-acid--CoA ligase 1	0.45	5.50E-05
193	Vars	Valine--tRNA ligase	0.45	2.77E-04
194	Kif5a	Kinesin heavy chain isoform 5A	0.45	2.73E-03
195	Hspa4	Heat shock 70 kDa protein 4	0.45	6.36E-04

Supplementary Table 4.2 (cont'd)

	Gene Symbol	Protein Name	Log_2(FC)	*p* value
196	Ccdc90b	Coiled-coil domain-containing protein 90B, mitochondrial	0.45	7.58E-04
197	Sars	Serine--tRNA ligase, cytoplasmic	0.45	4.03E-04
198	Pex11b	Peroxisomal membrane protein 11B	0.45	2.80E-04
199	Mtif2	Translation initiation factor IF-2, mitochondrial	0.44	3.27E-06
200	Caskin1	Caskin-1	0.44	4.94E-04
201	Rit2	GTP-binding protein Rit2	0.44	8.73E-03
202	Rqcd1	Cell differentiation protein RCD1 homolog	0.44	2.01E-03
203	Tsn	Translin	0.44	2.85E-04
204	Gdap1l1	Ganglioside-induced differentiation-associated protein 1-like 1	0.44	8.73E-09
205	Gid8	Glucose-induced degradation protein 8 homolog	0.44	2.21E-02
206	Clasp1	CLIP-associating protein 1	0.44	2.09E-05
207	Syn3	Synapsin-3	0.44	1.18E-07
208	Sep2	Septin-2	0.44	2.10E-05
209	Plxna1	Plexin-A1; Short=Plex 1; Short=Plexin-1	0.44	6.48E-03
210	Hspa1l	Heat shock 70 kDa protein 1-like	0.44	1.24E-05
211	Sec23a	Protein transport protein Sec23A	0.44	1.44E-05
212	Nap1l5	Nucleosome assembly protein 1-like 5	0.44	1.36E-02
213	D10Jhu81e	ES1 protein homolog, mitochondrial	0.44	3.59E-04
214	Bcs1l	Mitochondrial chaperone BCS1	0.44	1.24E-07
215	Ppp3ca	Serine/threonine-protein phosphatase 2B catalytic subunit alpha isoform	0.43	1.98E-04
216	Mthfd1l	Monofunctional C1-tetrahydrofolate synthase, mitochondrial	0.43	7.06E-04
217	Arhgdia	Rho GDP-dissociation inhibitor 1	0.43	2.10E-03
218	Hip1r	Huntingtin-interacting protein 1-related protein	0.43	9.60E-04
219	Acsf2	Acyl-CoA synthetase family member 2, mitochondrial	0.43	2.63E-11
220	Gnai1	Guanine nucleotide-binding protein G(i) subunit alpha-1	0.43	2.65E-03
221	Uchl3	Ubiquitin carboxyl-terminal hydrolase isozyme L3	0.43	4.64E-04
222	Aldh2	Aldehyde dehydrogenase, mitochondrial	0.43	2.14E-06
223	Rab3a	Ras-related protein Rab-3A	0.43	1.78E-05
224	Clic4	Chloride intracellular channel protein 4	0.43	2.06E-02
225	Myo5a	Unconventional myosin-Va	0.43	5.74E-04
226	Ncdn	Neurochondrin	0.43	1.23E-06
227	Sco2	Protein SCO2 homolog, mitochondrial	0.43	3.50E-03
228	Cttn	Src substrate cortactin	0.43	4.35E-03
229	Letm1	LETM1 and EF-hand domain-containing protein 1, mitochondrial	0.42	3.49E-08
230	Wdr37	WD repeat-containing protein 37	0.42	1.90E-04
231	Olfm1	Noelin	0.42	2.87E-03
232	Marcksl1	MARCKS-related protein	0.42	7.43E-03
233	Cltc	Clathrin heavy chain 1	0.42	1.18E-04
234	Cul2	Cullin-2	0.42	4.80E-07
235	Rufy3	Protein RUFY3	0.42	3.97E-04

Supplementary Table 4.2 (cont'd)

	Gene Symbol	Protein Name	Log_2(FC)	*p* value
236	Cops4	COP9 signalosome complex subunit 4	0.42	5.33E-04
237	Ran	GTP-binding nuclear protein Ran	0.42	1.70E-05
238	Pbdc1	Protein PBDC1	0.42	5.94E-04
239	Tsnax	Translin-associated protein X	0.42	1.01E-02
240	Acsl3	Long-chain-fatty-acid--CoA ligase 3	0.42	9.45E-03
241	Vti1b	Vesicle transport through interaction with t-SNAREs homolog 1B	0.42	2.71E-02
242	Pfkp	ATP-dependent 6-phosphofructokinase, platelet type	0.42	1.23E-06
243	Ola1	Obg-like ATPase 1	0.42	2.33E-05
244	Sparcl1	SPARC-like protein 1	0.42	1.26E-03
245	Calb1	Calbindin	0.42	5.89E-03
246	Vps52	Vacuolar protein sorting-associated protein 52 homolog	0.42	8.20E-03
247	Abcd3	ATP-binding cassette sub-family D member 3	0.42	5.72E-06
248	Mfn2	Mitofusin-2	0.42	8.71E-07
249	Hspa9	Stress-70 protein, mitochondrial	0.41	1.13E-06
250	Stx8	Syntaxin-8	0.41	3.29E-02
251	Ppp1cc	Serine/threonine-protein phosphatase PP1-gamma catalytic subunit	0.41	3.76E-02
252	Nadk2	NAD kinase 2, mitochondrial	0.41	2.22E-03
253	Cs	Citrate synthase, mitochondrial	0.41	6.38E-05
254	Rab35	Ras-related protein Rab-35	0.41	2.25E-06
255	Cnn3	Calponin-3	0.41	1.22E-02
256	Sars2	Serine--tRNA ligase, mitochondrial	0.41	1.14E-05
257	Cab39	Calcium-binding protein 39	0.41	3.40E-02
258	Rnh1	Ribonuclease inhibitor	0.41	1.27E-03
259	Rph3a	Rabphilin-3A	0.41	1.87E-03
260	Cntn1	Contactin-1	0.41	7.26E-04
261	Itpa	Inosine triphosphate pyrophosphatase	0.40	1.25E-03
262	Mrpl10	39S ribosomal protein L10, mitochondrial	0.40	4.50E-04
263	Aars2	Alanine--tRNA ligase, mitochondrial	0.40	1.10E-04
264	Isoc2a	Isochorismatase domain-containing protein 2A, mitochondrial	0.40	3.06E-02
265	Taco1	Translational activator of cytochrome c oxidase 1	0.40	4.02E-03
266	Prkacb	cAMP-dependent protein kinase catalytic subunit beta	0.40	8.01E-03
267	Hsdl2	Hydroxysteroid dehydrogenase-like protein 2	0.40	3.78E-05
268	P4hb	Protein disulfide-isomerase	0.40	6.49E-05
269	Vac14	Protein VAC14 homolog	0.40	1.83E-03
270	Aqp1	Aquaporin-1	0.40	1.88E-02
271	Rpl10a	60S ribosomal protein L10a	0.40	1.71E-03
272	Fam173a	Protein FAM173A	0.40	1.67E-03
273	Dctn1	Dynactin subunit 1	0.40	3.22E-04
274	Add2	Beta-adducin	0.40	4.32E-02
275	Ppp2r4	Serine/threonine-protein phosphatase 2A activator	0.40	6.27E-04

Supplementary Table 4.2 (cont'd)

	Gene Symbol	Protein Name	Log_2(FC)	*p* value
276	Rplp0	60S acidic ribosomal protein P0	0.40	7.21E-05
277	Micu1	Calcium uptake protein 1, mitochondrial	0.39	1.07E-04
278	Hsp90ab1	Heat shock protein HSP 90-beta	0.39	1.56E-03
279	Opa1	Dynamin-like 120 kDa protein, mitochondrial	0.39	4.13E-06
280	Gstm7	Glutathione S-transferase Mu 7	0.39	2.71E-03
281	Acss1	Acetyl-coenzyme A synthetase 2-like, mitochondrial	0.39	3.74E-02
282	Hdhd2	Haloacid dehalogenase-like hydrolase domain-containing protein 2	0.39	1.36E-02
283	Prps1	Ribose-phosphate pyrophosphokinase 1	0.39	3.45E-04
284	Etfa	Electron transfer flavoprotein subunit alpha, mitochondrial	0.39	3.53E-04
285	Gfer	FAD-linked sulfhydryl oxidase ALR	0.39	1.02E-04
286	Eif5	Eukaryotic translation initiation factor 5	0.39	1.88E-04
287	Slc6a11	Sodium- and chloride-dependent GABA transporter 3	0.39	2.33E-04
288	Ndufs1	NADH-ubiquinone oxidoreductase 75 kDa subunit, mitochondrial	0.39	2.07E-09
289	Naca	Nascent polypeptide-associated complex subunit alpha, muscle-specific form	0.39	2.45E-04
290	Idh3a	Isocitrate dehydrogenase [NAD] subunit alpha, mitochondrial	0.39	8.07E-05
291	Exog	Nuclease EXOG, mitochondrial	0.39	1.02E-07
292	Pafah1b2	Platelet-activating factor acetylhydrolase IB subunit beta	0.39	1.63E-02
293	Nsf	Vesicle-fusing ATPase	0.39	3.22E-04
294	Vps35	Vacuolar protein sorting-associated protein 35	0.39	2.37E-04
295	Pgm2l1	Glucose 1,6-bisphosphate synthase	0.39	5.76E-04
296	Syt1	Synaptotagmin-1	0.38	1.52E-05
297	Abat	4-aminobutyrate aminotransferase, mitochondrial	0.38	5.06E-07
298	Lamp1	Lysosome-associated membrane glycoprotein 1	0.38	1.05E-02
299	Atp8a1	Phospholipid-transporting ATPase IA	0.38	3.16E-03
300	Gmppa	Mannose-1-phosphate guanyltransferase alpha	0.38	2.52E-04
301	Nedd4	E3 ubiquitin-protein ligase NEDD4	0.38	2.24E-04
302	Stxbp1	Syntaxin-binding protein 1	0.38	6.35E-07
303	Aldh1b1	Aldehyde dehydrogenase X, mitochondrial	0.38	1.30E-04
304	Pcca	Propionyl-CoA carboxylase alpha chain, mitochondrial	0.38	3.68E-05
305	Dpm1	Dolichol-phosphate mannosyltransferase subunit 1	0.38	1.88E-05
306	Map6	Microtubule-associated protein 6; Short=MAP-6	0.38	3.56E-03
307	Uba1	Ubiquitin-like modifier-activating enzyme 1	0.38	8.56E-03
308	Ndufa9	NADH dehydrogenase [ubiquinone] 1 alpha subcomplex subunit 9, mitochondrial	0.38	8.88E-07
309	Gabbr2	Gamma-aminobutyric acid type B receptor subunit 2	0.38	4.84E-03
310	Ap3d1	AP-3 complex subunit delta-1	0.38	7.96E-05
311	Napg	Gamma-soluble NSF attachment protein	0.38	1.07E-04
312	Aldh18a1	Delta-1-pyrroline-5-carboxylate synthase	0.38	1.03E-05

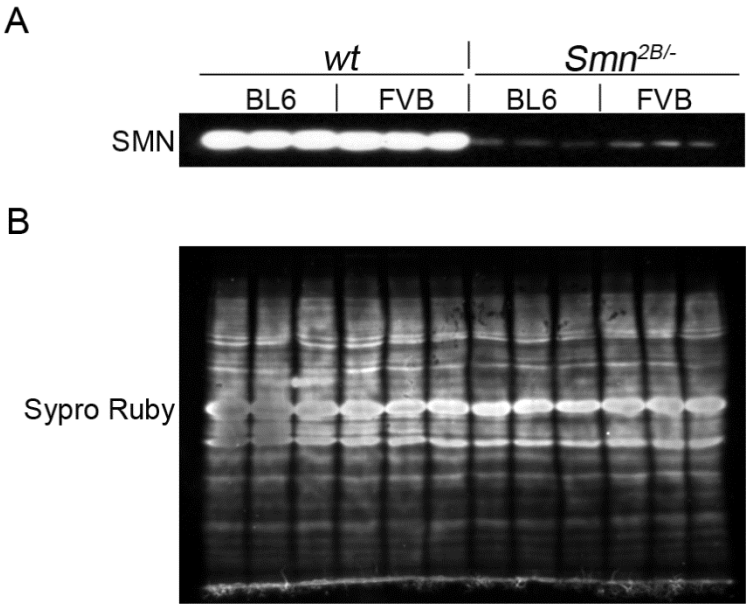

Supplementary Figure 4.1. The signals of immunoblotting experiments were normalized to the signals of total proteins. A) A representative image of immunoblotting experiments B) A representative image of Sypro Ruby staining. The immunoblotting signal of each sample was normalized to the signal of total protein of the corresponding lane.

A

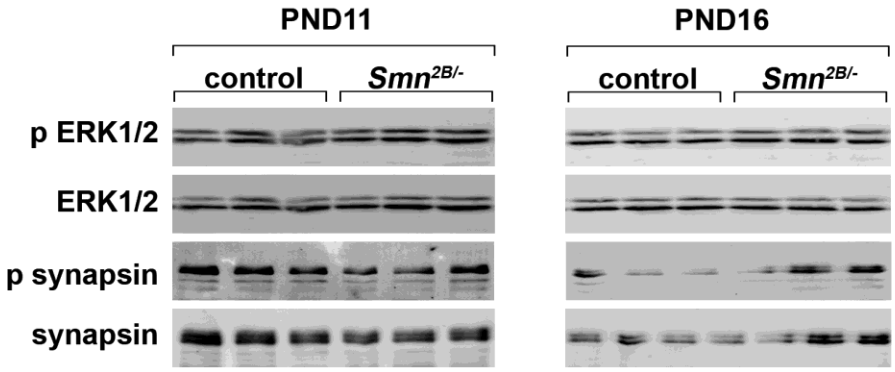
PND11
PND16
control
Smn2B/-
control
Smn2B/-
p ERK1/2
ERK1/2
p synapsin
synapsin

B

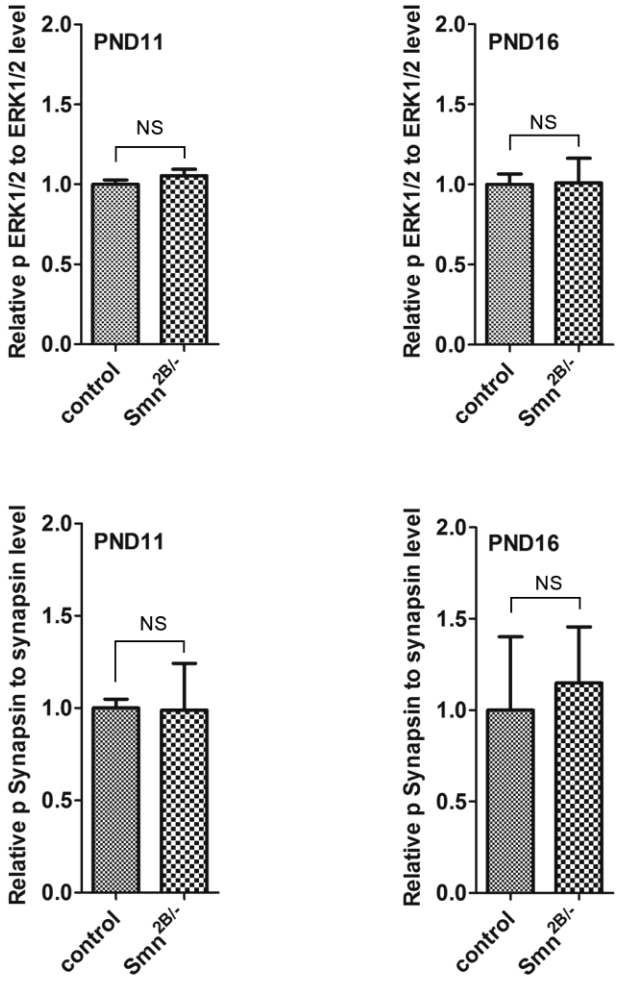
Relative p ERK1/2 to ERK1/2 level
PND11
NS
2.0
1.5
1.0
0.5
0.0
control
Smn2B/-
Relative p ERK1/2 to ERK1/2 level
PND16
NS
Relative p Synapsin to synapsin level
PND11
NS
Relative p Synapsin to synapsin level
PND16
NS

Supplementary Figure 4.2. The activity of ERK1/2-synapsin pathway is not altered within synapses of spinal cords of *Smn*$^{2B/-}$ mice. A) Representative images of immunoblotting experiments on synaptosome fractions prepared from spinal cords of *Smn*$^{2B/-}$ mice and their control littermates at PND11 and PND16. B) Quantification of immunoblotting images did not show any alteration in the relative levels of phosphorylated ERK1/2 or phosphorylated synapsin (unpaired t test, n=3, $p > 0.05$).

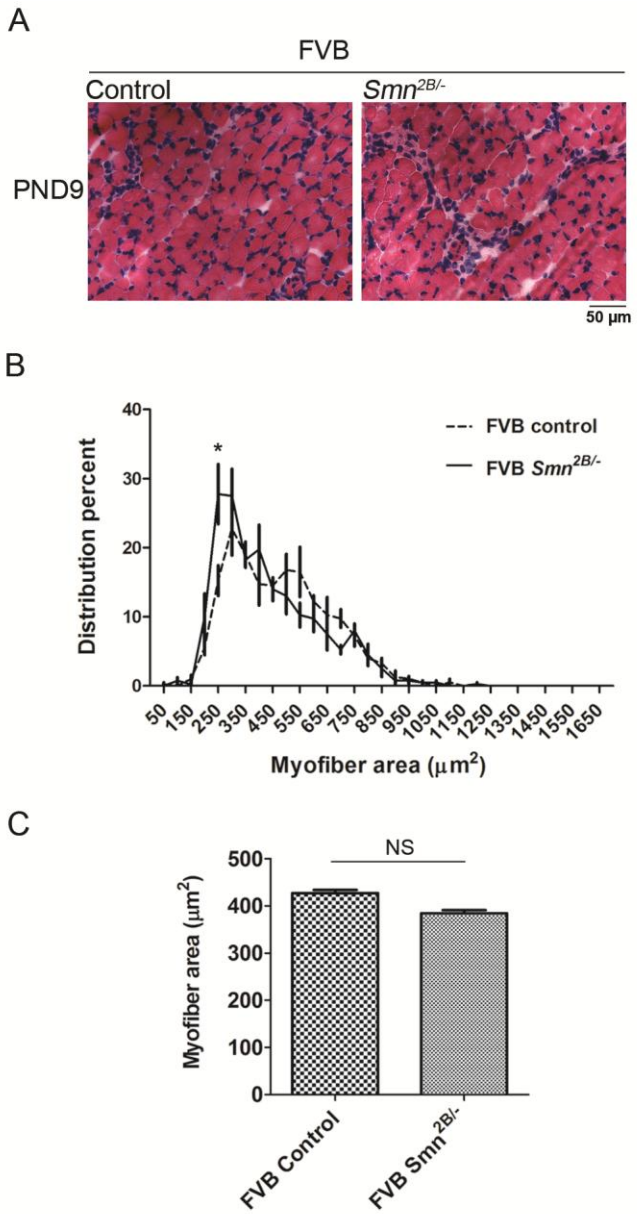

Supplement Figure 4.3. Mild myofiber atrophy was observed at PND9 in FVB *Smn*$^{2B/-}$ mice. A) Representative images of H&E stained TA muscle sections from PND9 FVB mice. B and C) Quantification and analysis of myofiber cross-sectional areas showed that at PND11 there is a higher percentage of small caliber myofibers in FVB *Smn*$^{2B/-}$ mice compared to their control littermates, however there was no difference in the average myofiber area between FVB *Smn*$^{2B/-}$ mice and their control littermates (Mann Whitney test, $p>0.05$). * indicates significant difference between *Smn*$^{2B/-}$ mice and their control littermates.

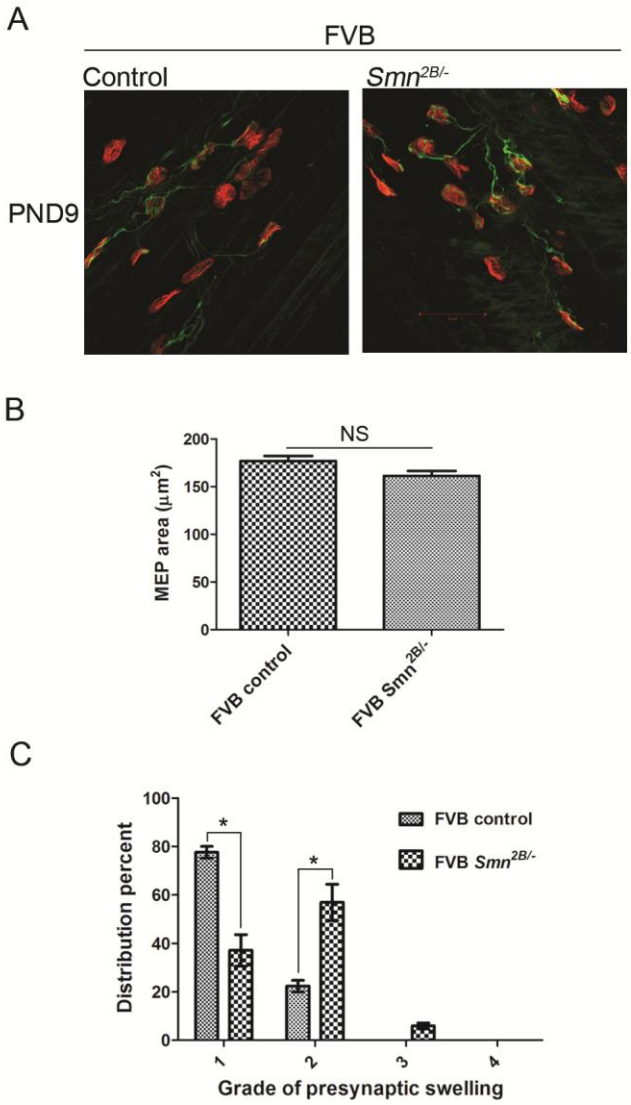

Supplement Figure 4.4. NMJ pathology was observed at PND9 in FVB *Smn*$^{2B/-}$ mice. A) Representative images of TVA muscle sections from PND9 FVB mice stained for neurofilament-M (red) and motor endplates (α-BTX, green). B) There is no significant difference in the MEP size between FVB *Smn*$^{2B/-}$ mice and controls at this age (n=3, unpaired t test, $p>0.05$). C) However, FVB *Smn*$^{2B/-}$ mice show higher grades of presynaptic swelling (n=3, two way ANOVA, $p<0.05$). * indicates significant difference.

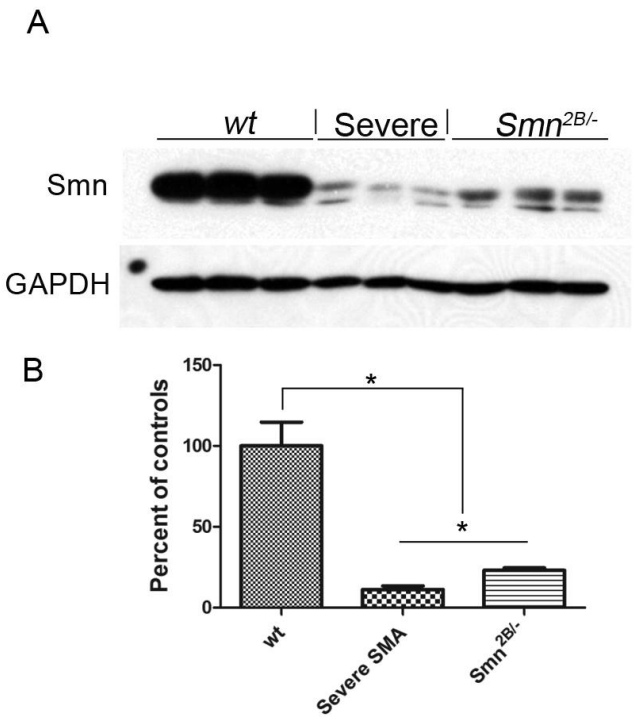

Supplement Figure 4.5. Higher expression of Smn in FVB *Smn*$^{2B/-}$ mice than FVB severe SMA (FVB.Cg-Tg(SMN2)89Ahmb *Smn1*$^{<tm1Msd>}$/J) mice. A) A representative immunoblot using PND1 mouse lumbar spinal cords (probed by an anti-SMN antibody which detects both human and mouse protein). B) Quantification of the signals showed that there is a higher level of Smn within spinal cords of FVB *Smn*$^{2B/-}$ mice than FVB severe SMA mice at PND1 (n=3, one way ANOVA, $p<0.05$). * indicates significant difference.

References

Abbadi, N., C. Philippe, M. Chery, H. Gilgenkrantz, F. Tome, H. Collin, D. Theau, D. Recan, O. Broux, M. Fardeau and et al. (1994). "Additional case of female monozygotic twins discordant for the clinical manifestations of Duchenne muscular dystrophy due to opposite X-chromosome inactivation." Am J Med Genet 52(2): 198-206.

Ackermann, B., S. Krober, L. Torres-Benito, A. Borgmann, M. Peters, S. M. Hosseini Barkooie, R. Tejero, M. Jakubik, J. Schreml, J. Milbradt, T. F. Wunderlich, M. Riessland, L. Tabares and B. Wirth (2013). "Plastin 3 ameliorates spinal muscular atrophy via delayed axon pruning and improves neuromuscular junction functionality." Hum Mol Genet 22(7): 1328-1347.

Acsadi, G., I. Lee, X. Li, M. Khaidakov, A. Pecinova, G. C. Parker and M. Huttemann (2009). "Mitochondrial dysfunction in a neural cell model of spinal muscular atrophy." J Neurosci Res 87(12): 2748-2756.

Aghamaleky Sarvestany, A., G. Hunter, A. Tavendale, D. J. Lamont, M. Llavero Hurtado, L. C. Graham, T. M. Wishart and T. H. Gillingwater (2014). "Label-free quantitative proteomic profiling identifies disruption of ubiquitin homeostasis as a key driver of Schwann cell defects in spinal muscular atrophy." J Proteome Res 13(11): 4546-4557.

Akten, B., M. J. Kye, T. Hao le, M. H. Wertz, S. Singh, D. Nie, J. Huang, T. T. Merianda, J. L. Twiss, C. E. Beattie, J. A. Steen and M. Sahin (2011). "Interaction of survival of motor neuron (SMN) and HuD proteins with mRNA cpg15 rescues motor neuron axonal deficits." Proc Natl Acad Sci U S A 108(25): 10337-10342.

Al-Chalabi, A., P. M. Andersen, B. Chioza, C. Shaw, P. C. Sham, W. Robberecht, G. Matthijs, W. Camu, S. L. Marklund, L. Forsgren, G. Rouleau, N. G. Laing, P. V. Hurse, T. Siddique, P. N. Leigh and J. F. Powell (1998). "Recessive amyotrophic lateral sclerosis families with the D90A SOD1 mutation share a common founder: evidence for a linked protective factor." Hum Mol Genet 7(13): 2045-2050.

Arnold, A. S., M. Gueye, S. Guettier-Sigrist, I. Courdier-Fruh, G. Coupin, P. Poindron and J. P. Gies (2004). "Reduced expression of nicotinic AChRs in myotubes from spinal muscular atrophy I patients." Lab Invest 84(10): 1271-1278.

Baloh, R. H. (2012). "How do the RNA-binding proteins TDP-43 and FUS relate to amyotrophic lateral sclerosis and frontotemporal degeneration, and to each other?" Curr Opin Neurol 25(6): 701-707.

Battaglia, G., A. Princivalle, F. Forti, C. Lizier and M. Zeviani (1997). "Expression of the SMN gene, the spinal muscular atrophy determining gene, in the mammalian central nervous system." Hum Mol Genet 6(11): 1961-1971.

Battle, D. J., M. Kasim, J. Yong, F. Lotti, C. K. Lau, J. Mouaikel, Z. Zhang, K. Han, L. Wan and G. Dreyfuss (2006). "The SMN complex: an assembly machine for RNPs." Cold Spring Harb Symp Quant Biol 71: 313-320.

Bebee, T. W., C. E. Dominguez and D. S. Chandler (2012). "Mouse models of SMA: tools for disease characterization and therapeutic development." Hum Genet 131(8): 1277-1293.

Bechade, C., P. Rostaing, C. Cisterni, R. Kalisch, V. La Bella, B. Pettmann and A. Triller (1999). "Subcellular distribution of survival motor neuron (SMN) protein: possible involvement in nucleocytoplasmic and dendritic transport." Eur J Neurosci 11(1): 293-304.

Bernabò, P., T. Tebaldi, E. J. Groen, F. M. Lane, E. Perenthaler, F. Mattedi, H. J. Newbery, H. Zhou, P. Zuccotti, V. Potrich, F. Muntoni, A. Quattrone, T. H. Gillingwater and G. Viero (2017). "In vivo translatome profiling reveals early defects in ribosome biology underlying SMA pathogenesis." bioRxiv.

Bernal, S., E. Also-Rallo, R. Martinez-Hernandez, L. Alias, F. J. Rodriguez-Alvarez, J. M. Millan, C. Hernandez-Chico, M. Baiget and E. F. Tizzano (2011). "Plastin 3 expression in discordant spinal muscular atrophy (SMA) siblings." Neuromuscul Disord 21(6): 413-419.

Billups, B. and I. D. Forsythe (2002). "Presynaptic mitochondrial calcium sequestration influences transmission at mammalian central synapses." J Neurosci 22(14): 5840-5847.

Blasco, H., P. Corcia, C. Moreau, S. Veau, C. Fournier, P. Vourc'h, P. Emond, P. Gordon, P. F. Pradat, J. Praline, D. Devos, L. Nadal-Desbarats and C. R. Andres (2010). "1H-NMR-based metabolomic profiling of CSF in early amyotrophic lateral sclerosis." PLoS One 5(10): e13223.

Bordet, T., P. Berna, J. L. Abitbol and R. M. Pruss (2010). "Olesoxime (TRO19622): A Novel Mitochondrial-Targeted Neuroprotective Compound." Pharmaceuticals (Basel) 3(2): 345-368.

Bowerman, M., C. L. Anderson, A. Beauvais, P. P. Boyl, W. Witke and R. Kothary (2009). "SMN, profilin IIa and plastin 3: a link between the deregulation of actin dynamics and SMA pathogenesis." Mol Cell Neurosci 42(1): 66-74.

Bowerman, M., A. Beauvais, C. L. Anderson and R. Kothary (2010). "Rho-kinase inactivation prolongs survival of an intermediate SMA mouse model." Hum Mol Genet 19(8): 1468-1478.

Bowerman, M., J. P. Michalski, A. Beauvais, L. M. Murray, Y. DeRepentigny and R. Kothary (2014). "Defects in pancreatic development and glucose metabolism in SMN-depleted mice independent of canonical spinal muscular atrophy neuromuscular pathology." Hum Mol Genet 23(13): 3432-3444.

Bowerman, M., L. M. Murray, A. Beauvais, B. Pinheiro and R. Kothary (2012). "A critical smn threshold in mice dictates onset of an intermediate spinal muscular atrophy phenotype associated with a distinct neuromuscular junction pathology." Neuromuscul Disord 22(3): 263-276.

Bowerman, M., L. M. Murray, J. G. Boyer, C. L. Anderson and R. Kothary (2012). "Fasudil improves survival and promotes skeletal muscle development in a mouse model of spinal muscular atrophy." BMC Med 10: 24.

Bowerman, M., D. Shafey and R. Kothary (2007). "Smn depletion alters profilin II expression and leads to upregulation of the RhoA/ROCK pathway and defects in neuronal integrity." J Mol Neurosci 32(2): 120-131.

Bowerman, M., K. J. Swoboda, J. P. Michalski, G. S. Wang, C. Reeks, A. Beauvais, K. Murphy, J. Woulfe, R. A. Screaton, F. W. Scott and R. Kothary (2012). "Glucose metabolism and pancreatic defects in spinal muscular atrophy." Ann Neurol 72(2): 256-268.

Boyer, J. G., M. O. Deguise, L. M. Murray, A. Yazdani, Y. De Repentigny, C. Boudreau-Lariviere and R. Kothary (2014). "Myogenic program dysregulation is contributory to disease pathogenesis in spinal muscular atrophy." Hum Mol Genet 23(16): 4249-4259.

Boyer, J. G., L. M. Murray, K. Scott, Y. De Repentigny, J. M. Renaud and R. Kothary (2013). "Early onset muscle weakness and disruption of muscle proteins in mouse models of spinal muscular atrophy." Skelet Muscle 3(1): 24.

Brahe, C., S. Servidei, S. Zappata, E. Ricci, P. Tonali and G. Neri (1995). "Genetic homogeneity between childhood-onset and adult-onset autosomal recessive spinal muscular atrophy." Lancet 346(8977): 741-742.

Briese, M., B. Esmaeili and D. B. Sattelle (2005). "Is spinal muscular atrophy the result of defects in motor neuron processes?" Bioessays 27(9): 946-957.

Bromberg, M. B. and K. J. Swoboda (2002). "Motor unit number estimation in infants and children with spinal muscular atrophy." Muscle Nerve 25(3): 445-447.

Brose, N., V. O'Connor and P. Skehel (2010). "Synaptopathy: dysfunction of synaptic function?" Biochem Soc Trans 38(2): 443-444.

Brzustowicz, L. M., T. Lehner, L. H. Castilla, G. K. Penchaszadeh, K. C. Wilhelmsen, R. Daniels, K. E. Davies, M. Leppert, F. Ziter, D. Wood and et al. (1990). "Genetic mapping of chronic childhood-onset spinal muscular atrophy to chromosome 5q11.2-13.3." Nature 344(6266): 540-541.

Buhler, D., V. Raker, R. Luhrmann and U. Fischer (1999). "Essential role for the tudor domain of SMN in spliceosomal U snRNP assembly: implications for spinal muscular atrophy." Hum Mol Genet 8(13): 2351-2357.

Burghes, A. H. and C. E. Beattie (2009). "Spinal muscular atrophy: why do low levels of survival motor neuron protein make motor neurons sick?" Nat Rev Neurosci 10(8): 597-609.

Burglen, L., S. Lefebvre, O. Clermont, P. Burlet, L. Viollet, C. Cruaud, A. Munnich and J. Melki (1996). "Structure and organization of the human survival motor neurone (SMN) gene." Genomics 32(3): 479-482.

Cannizzaro, L. A., P. Madaule, F. Hecht, R. Axel, C. M. Croce and K. Huebner (1990). "Chromosome localization of human ARH genes, a ras-related gene family." Genomics 6(2): 197-203.

Caraballo-Miralles, V., A. Cardona-Rossinyol, A. Garcera, P. Villalonga, R. M. Soler, G. Olmos and J. Llado (2012). "SMN deficiency attenuates migration of U87MG astroglioma cells through the activation of RhoA." Mol Cell Neurosci 49(3): 282-289.

Carlsson, L., L. E. Nystrom, I. Sundkvist, F. Markey and U. Lindberg (1977). "Actin polymerizability is influenced by profilin, a low molecular weight protein in non-muscle cells." J Mol Biol 115(3): 465-483.

Carrel, T. L., M. L. McWhorter, E. Workman, H. Zhang, E. C. Wolstencroft, C. Lorson, G. J. Bassell, A. H. Burghes and C. E. Beattie (2006). "Survival motor neuron function in motor axons is independent of functions required for small nuclear ribonucleoprotein biogenesis." J Neurosci 26(43): 11014-11022.

Cartegni, L. and A. R. Krainer (2002). "Disruption of an SF2/ASF-dependent exonic splicing enhancer in SMN2 causes spinal muscular atrophy in the absence of SMN1." Nat Genet 30(4): 377-384.

Cartegni, L. and A. R. Krainer (2003). "Correction of disease-associated exon skipping by synthetic exon-specific activators." Nat Struct Biol 10(2): 120-125.

Carunchio, I., L. Curcio, M. Pieri, F. Pica, S. Caioli, M. T. Viscomi, M. Molinari, N. Canu, G. Bernardi and C. Zona (2010). "Increased levels of p70S6 phosphorylation in the G93A mouse model of Amyotrophic Lateral Sclerosis and in valine-exposed cortical neurons in culture." Exp Neurol 226(1): 218-230.

Chan, Y. B., I. Miguel-Aliaga, C. Franks, N. Thomas, B. Trulzsch, D. B. Sattelle, K. E. Davies and M. van den Heuvel (2003). "Neuromuscular defects in a Drosophila survival motor neuron gene mutant." Hum Mol Genet 12(12): 1367-1376.

Chen, Q., S. D. Baird, M. Mahadevan, A. Besner-Johnston, R. Farahani, J. Xuan, X. Kang, C. Lefebvre, J. E. Ikeda, R. G. Korneluk and A. E. MacKenzie (1998). "Sequence of a 131-kb region of 5q13.1 containing the spinal muscular atrophy candidate genes SMN and NAIP." Genomics 48(1): 121-127.

Cifuentes-Diaz, C., T. Frugier, F. D. Tiziano, E. Lacene, N. Roblot, V. Joshi, M. H. Moreau and J. Melki (2001). "Deletion of murine SMN exon 7 directed to skeletal muscle leads to severe muscular dystrophy." J Cell Biol 152(5): 1107-1114.

Clelland, A. K., N. P. Kinnear, L. Oram, J. Burza and J. E. Sleeman (2009). "The SMN protein is a key regulator of nuclear architecture in differentiating neuroblastoma cells." Traffic 10(11): 1585-1598.

Clermont, O., P. Burlet, S. Lefebvre, L. Burglen, A. Munnich and J. Melki (1995). "SMN gene deletions in adult-onset spinal muscular atrophy." Lancet 346(8991-8992): 1712-1713.

Clinton, J., C. Forsyth, M. C. Royston and G. W. Roberts (1993). "Synaptic degeneration is the primary neuropathological feature in prion disease: a preliminary study." Neuroreport 4(1): 65-68.

Coleman, P., H. Federoff and R. Kurlan (2004). "A focus on the synapse for neuroprotection in Alzheimer disease and other dementias." Neurology 63(7): 1155-1162.

Coley, W. D., L. Bogdanik, M. C. Vila, Q. Yu, J. H. Van Der Meulen, S. Rayavarapu, J. S. Novak, M. Nearing, J. L. Quinn, A. Saunders, C. Dolan, W. Andrews, C. Lammert, A. Austin, T. A. Partridge, G. A. Cox, C. Lutz and K. Nagaraju (2016). "Effect of genetic background on the dystrophic phenotype in mdx mice." Hum Mol Genet 25(1): 130-145.

Coovert, D. D., T. T. Le, P. E. McAndrew, J. Strasswimmer, T. O. Crawford, J. R. Mendell, S. E. Coulson, E. J. Androphy, T. W. Prior and A. H. Burghes (1997). "The survival motor neuron protein in spinal muscular atrophy." Hum Mol Genet 6(8): 1205-1214.

Cote, J. and S. Richard (2005). "Tudor domains bind symmetrical dimethylated arginines." J Biol Chem 280(31): 28476-28483.

Crawford, T. O. and C. A. Pardo (1996). "The neurobiology of childhood spinal muscular atrophy." Neurobiol Dis 3(2): 97-110.

Crawford, T. O., J. T. Sladky, O. Hurko, A. Besner-Johnston and R. I. Kelley (1999). "Abnormal fatty acid metabolism in childhood spinal muscular atrophy." Ann Neurol 45(3): 337-343.

Cudkowicz, M. E., D. McKenna-Yasek, P. E. Sapp, W. Chin, B. Geller, D. L. Hayden, D. A. Schoenfeld, B. A. Hosler, H. R. Horvitz and R. H. Brown (1997). "Epidemiology of mutations in superoxide dismutase in amyotrophic lateral sclerosis." Ann Neurol 41(2): 210-221.

Dachs, E., M. Hereu, L. Piedrafita, A. Casanovas, J. Caldero and J. E. Esquerda (2011). "Defective neuromuscular junction organization and postnatal myogenesis in mice with severe spinal muscular atrophy." J Neuropathol Exp Neurol 70(6): 444-461.

Dason, J. S., A. J. Smith, L. Marin and M. P. Charlton (2014). "Cholesterol and F-actin are required for clustering of recycling synaptic vesicle proteins in the presynaptic plasma membrane." J Physiol 592(4): 621-633.

De Jesus-Cortes, H. J., C. J. Nogueras-Ortiz, M. Gearing, S. E. Arnold and I. E. Vega (2012). "Amphiphysin-1 protein level changes associated with tau-mediated neurodegeneration." Neuroreport 23(16): 942-946.

Deguise, M. O., Y. De Repentigny, E. McFall, N. Auclair, S. Sad and R. Kothary (2017). "Immune dysregulation may contribute to disease pathogenesis in spinal muscular atrophy mice." Hum Mol Genet.

Di Paolo, G., S. Sankaranarayanan, M. R. Wenk, L. Daniell, E. Perucco, B. J. Caldarone, R. Flavell, M. R. Picciotto, T. A. Ryan, O. Cremona and P. De Camilli (2002). "Decreased synaptic vesicle recycling efficiency and cognitive deficits in amphiphysin 1 knockout mice." Neuron 33(5): 789-804.

DiDonato, C. J., C. L. Lorson, Y. De Repentigny, L. Simard, C. Chartrand, E. J. Androphy and R. Kothary (2001). "Regulation of murine survival motor neuron (Smn) protein levels by modifying Smn exon 7 splicing." Hum Mol Genet 10(23): 2727-2736.

Dillon, C. and Y. Goda (2005). "The actin cytoskeleton: integrating form and function at the synapse." Annu Rev Neurosci 28: 25-55.

Dimitriadi, M., A. Derdowski, G. Kalloo, M. S. Maginnis, P. O'Hern, B. Bliska, A. Sorkac, K. C. Nguyen, S. J. Cook, G. Poulogiannis, W. J. Atwood, D. H. Hall and A. C. Hart (2016). "Decreased function of survival motor neuron protein impairs endocytic pathways." Proc Natl Acad Sci U S A 113(30): E4377-4386.

Ding, Q., W. R. Markesbery, Q. Chen, F. Li and J. N. Keller (2005). "Ribosome dysfunction is an early event in Alzheimer's disease." J Neurosci 25(40): 9171-9175.

Dombert, B., R. Sivadasan, C. M. Simon, S. Jablonka and M. Sendtner (2014). "Presynaptic localization of Smn and hnRNP R in axon terminals of embryonic and postnatal mouse motoneurons." PLoS One 9(10): e110846.

Donlin-Asp, P. G., G. J. Bassell and W. Rossoll (2016). "A role for the survival of motor neuron protein in mRNP assembly and transport." Curr Opin Neurobiol 39: 53-61.

Donnelly, C. J., M. Park, M. Spillane, S. Yoo, A. Pacheco, C. Gomes, D. Vuppalanchi, M. McDonald, H. H. Kim, T. T. Merianda, G. Gallo and J. L. Twiss (2013). "Axonally synthesized beta-actin and GAP-43 proteins support distinct modes of axonal growth." J Neurosci 33(8): 3311-3322.

Dunkley, P. R., P. E. Jarvie, J. W. Heath, G. J. Kidd and J. A. Rostas (1986). "A rapid method for isolation of synaptosomes on Percoll gradients." Brain Res 372(1): 115-129.

Dunkley, P. R., P. E. Jarvie and P. J. Robinson (2008). "A rapid Percoll gradient procedure for preparation of synaptosomes." Nat Protoc 3(11): 1718-1728.

Eschbach, J., B. Schwalenstocker, S. M. Soyal, H. Bayer, D. Wiesner, C. Akimoto, A. C. Nilsson, A. Birve, T. Meyer, L. Dupuis, K. M. Danzer, P. M. Andersen, A. Witting, A. C. Ludolph, W. Patsch and P. Weydt (2013). "PGC-1alpha is a male-specific disease modifier of human and experimental amyotrophic lateral sclerosis." Hum Mol Genet 22(17): 3477-3484.

Eshraghi, M., E. McFall, S. Gibeault and R. Kothary (2016). "Effect of genetic background on the phenotype of the Smn2B/- mouse model of spinal muscular atrophy." Hum Mol Genet 25(20): 4494-4506.

Fallini, C., H. Zhang, Y. Su, V. Silani, R. H. Singer, W. Rossoll and G. J. Bassell (2011). "The survival of motor neuron (SMN) protein interacts with the mRNA-binding protein HuD and regulates localization of poly(A) mRNA in primary motor neuron axons." J Neurosci 31(10): 3914-3925.

Fan, L. and L. R. Simard (2002). "Survival motor neuron (SMN) protein: role in neurite outgrowth and neuromuscular maturation during neuronal differentiation and development." Hum Mol Genet 11(14): 1605-1614.

Farrar, M. A., S. B. Park, S. Vucic, K. A. Carey, B. J. Turner, T. H. Gillingwater, K. J. Swoboda and M. C. Kiernan (2016). "Emerging therapies and challenges in spinal muscular atrophy." Ann Neurol.

Felbecker, A., W. Camu, P. N. Valdmanis, A. D. Sperfeld, S. Waibel, P. Steinbach, G. A. Rouleau, A. C. Ludolph and P. M. Andersen (2010). "Four familial ALS pedigrees discordant for two SOD1 mutations: are all SOD1 mutations pathogenic?" J Neurol Neurosurg Psychiatry 81(5): 572-577.

Feldkotter, M., V. Schwarzer, R. Wirth, T. F. Wienker and B. Wirth (2002). "Quantitative analyses of SMN1 and SMN2 based on real-time lightCycler PCR: fast and highly reliable carrier testing and prediction of severity of spinal muscular atrophy." Am J Hum Genet 70(2): 358-368.

Finkel, R. S., C. A. Chiriboga, J. Vajsar, J. W. Day, J. Montes, D. C. De Vivo, M. Yamashita, F. Rigo, G. Hung, E. Schneider, D. A. Norris, S. Xia, C. F. Bennett and K. M. Bishop (2016). "Treatment of infantile-onset spinal muscular atrophy with nusinersen: a phase 2, open-label, dose-escalation study." Lancet 388(10063): 3017-3026.

Fischer, U., Q. Liu and G. Dreyfuss (1997). "The SMN-SIP1 complex has an essential role in spliceosomal snRNP biogenesis." Cell 90(6): 1023-1029.

for a comprehensive review please refer to Uittenbogaard, M. and A. Chiaramello (2014). "Mitochondrial biogenesis: a therapeutic target for neurodevelopmental disorders and neurodegenerative diseases." Curr Pharm Des 20(35): 5574-5593.

Friesen, W. J., S. Massenet, S. Paushkin, A. Wyce and G. Dreyfuss (2001). "SMN, the product of the spinal muscular atrophy gene, binds preferentially to dimethylarginine-containing protein targets." Mol Cell 7(5): 1111-1117.

Frugier, T., F. D. Tiziano, C. Cifuentes-Diaz, P. Miniou, N. Roblot, A. Dierich, M. Le Meur and J. Melki (2000). "Nuclear targeting defect of SMN lacking the C-terminus in a mouse model of spinal muscular atrophy." Hum Mol Genet 9(5): 849-858.

Gabanella, F., M. E. Butchbach, L. Saieva, C. Carissimi, A. H. Burghes and L. Pellizzoni (2007). "Ribonucleoprotein assembly defects correlate with spinal muscular atrophy severity and preferentially affect a subset of spliceosomal snRNPs." PLoS One 2(9): e921.

Gabanella, F., C. Pisani, A. Borreca, S. Farioli-Vecchioli, M. T. Ciotti, T. Ingegnere, A. Onori, M. Ammassari-Teule, N. Corbi, N. Canu, L. Monaco, C. Passananti and M. G. Di Certo (2016). "SMN affects membrane remodelling and anchoring of the protein synthesis machinery." J Cell Sci 129(4): 804-816.

Genin, E., J. Feingold and F. Clerget-Darpoux (2008). "Identifying modifier genes of monogenic disease: strategies and difficulties." Hum Genet 124(4): 357-368.

Gennarelli, M., M. Lucarelli, F. Capon, A. Pizzuti, L. Merlini, C. Angelini, G. Novelli and B. Dallapiccola (1995). "Survival motor neuron gene transcript analysis in muscles from spinal muscular atrophy patients." Biochem Biophys Res Commun 213(1): 342-348.

Ghosh, A., T. Tyson, S. George, E. N. Hildebrandt, J. A. Steiner, Z. Madaj, E. Schulz, E. Machiela, W. G. McDonald, M. L. Escobar Galvis, J. H. Kordower, J. M. Van Raamsdonk, J. R. Colca and P. Brundin (2016). "Mitochondrial pyruvate carrier regulates autophagy, inflammation, and neurodegeneration in experimental models of Parkinson's disease." Sci Transl Med 8(368): 368ra174.

Giachello, C. N., F. Fiumara, C. Giacomini, A. Corradi, C. Milanese, M. Ghirardi, F. Benfenati and P. G. Montarolo (2010). "MAPK/Erk-dependent phosphorylation of synapsin mediates formation of functional synapses and short-term homosynaptic plasticity." J Cell Sci 123(Pt 6): 881-893.

Giavazzi, A., V. Setola, A. Simonati and G. Battaglia (2006). "Neuronal-specific roles of the survival motor neuron protein: evidence from survival motor neuron expression patterns in the developing human central nervous system." J Neuropathol Exp Neurol 65(3): 267-277.

Giesemann, T., S. Rathke-Hartlieb, M. Rothkegel, J. W. Bartsch, S. Buchmeier, B. M. Jockusch and H. Jockusch (1999). "A role for polyproline motifs in the spinal muscular atrophy protein SMN. Profilins bind to and colocalize with smn in nuclear gems." J Biol Chem 274(53): 37908-37914.

Gilliam, T. C., L. M. Brzustowicz, L. H. Castilla, T. Lehner, G. K. Penchaszadeh, R. J. Daniels, B. C. Byth, J. Knowles, J. E. Hislop, Y. Shapira and et al. (1990). "Genetic homogeneity between acute and chronic forms of spinal muscular atrophy." Nature 345(6278): 823-825.

Gillingwater, T. H. and R. R. Ribchester (2001). "Compartmental neurodegeneration and synaptic plasticity in the Wld(s) mutant mouse." J Physiol 534(Pt 3): 627-639.

Gladman, J. T., T. W. Bebee, C. Edwards, X. Wang, Z. Sahenk, M. M. Rich and D. S. Chandler (2010). "A humanized Smn gene containing the SMN2 nucleotide alteration in exon 7 mimics SMN2 splicing and the SMA disease phenotype." Hum Mol Genet 19(21): 4239-4252.

Gombash, S. E., C. J. Cowley, J. A. Fitzgerald, C. C. Iyer, D. Fried, V. L. McGovern, K. C. Williams, A. H. Burghes, F. L. Christofi, B. D. Gulbransen and K. D. Foust (2015). "SMN deficiency disrupts gastrointestinal and enteric nervous system function in mice." Hum Mol Genet 24(13): 3847-3860.

Gouarne, C., G. Tardif, J. Tracz, V. Latyszenok, M. Michaud, L. E. Clemens, L. Yu-Taeger, H. P. Nguyen, T. Bordet and R. M. Pruss (2013). "Early deficits in glycolysis are specific to striatal neurons from a rat model of huntington disease." PLoS One 8(11): e81528.

Gray, L. R., S. C. Tompkins and E. B. Taylor (2014). "Regulation of pyruvate metabolism and human disease." Cell Mol Life Sci 71(14): 2577-2604.

Greengard, P., F. Benfenati and F. Valtorta (1994). "Synapsin I, an actin-binding protein regulating synaptic vesicle traffic in the nerve terminal." Adv Second Messenger Phosphoprotein Res 29: 31-45.

Group, I. A. S. (1993). "Branched-chain amino acids and amyotrophic lateral sclerosis: a treatment failure? The Italian ALS Study Group." Neurology 43(12): 2466-2470.

Gupta, K., R. Martin, R. Sharp, K. L. Sarachan, N. S. Ninan and G. D. Van Duyne (2015). "Oligomeric Properties of Survival Motor Neuron.Gemin2 Complexes." J Biol Chem 290(33): 20185-20199.

Hahnen, E., J. Schonling, S. Rudnik-Schoneborn, H. Raschke, K. Zerres and B. Wirth (1997). "Missense mutations in exon 6 of the survival motor neuron gene in patients with spinal muscular atrophy (SMA)." Hum Mol Genet 6(5): 821-825.

Hanein, D., N. Volkmann, S. Goldsmith, A. M. Michon, W. Lehman, R. Craig, D. DeRosier, S. Almo and P. Matsudaira (1998). "An atomic model of fimbrin binding to F-actin and its implications for filament crosslinking and regulation." Nat Struct Biol 5(9): 787-792.

Hao le, T., M. Wolman, M. Granato and C. E. Beattie (2012). "Survival motor neuron affects plastin 3 protein levels leading to motor defects." J Neurosci 32(15): 5074-5084.

Harris, J. J., R. Jolivet and D. Attwell (2012). "Synaptic energy use and supply." Neuron 75(5): 762-777.

Hatefi, Y. (1985). "The mitochondrial electron transport and oxidative phosphorylation system." Annu Rev Biochem 54: 1015-1069.

Hatzipetros, T., L. P. Bogdanik, V. R. Tassinari, J. D. Kidd, A. J. Moreno, C. Davis, M. Osborne, A. Austin, F. G. Vieira, C. Lutz and S. Perrin (2014). "C57BL/6J congenic Prp-TDP43A315T mice develop progressive neurodegeneration in the myenteric plexus of the colon without exhibiting key features of ALS." Brain Res 1584: 59-72.

Hebert, M. D., K. B. Shpargel, J. K. Ospina, K. E. Tucker and A. G. Matera (2002). "Coilin methylation regulates nuclear body formation." Dev Cell 3(3): 329-337.

Heesen, L., M. Peitz, L. Torres-Benito, I. Holker, K. Hupperich, K. Dobrindt, J. Jungverdorben, S. Ritzenhofen, B. Weykopf, D. Eckert, S. M. Hosseini-Barkooie, M. Storbeck, N. Fusaki, R. Lonigro, R. Heller, M. J. Kye, O. Brustle and B. Wirth (2016). "Plastin 3 is upregulated in iPSC-derived motoneurons from asymptomatic SMN1-deleted individuals." Cell Mol Life Sci 73(10): 2089-2104.

Heiman-Patterson, T. D., J. S. Deitch, E. P. Blankenhorn, K. L. Erwin, M. J. Perreault, B. K. Alexander, N. Byers, I. Toman and G. M. Alexander (2005). "Background and gender effects on survival in the TgN(SOD1-G93A)1Gur mouse model of ALS." J Neurol Sci 236(1-2): 1-7.

Heiman-Patterson, T. D., R. B. Sher, E. A. Blankenhorn, G. Alexander, J. S. Deitch, C. B. Kunst, N. Maragakis and G. Cox (2011). "Effect of genetic background on phenotype variability in transgenic mouse models of amyotrophic lateral sclerosis: a window of opportunity in the search for genetic modifiers." Amyotroph Lateral Scler 12(2): 79-86.

Hernandez-Ortega, K., P. Garcia-Esparcia, L. Gil, J. J. Lucas and I. Ferrer (2016). "Altered Machinery of Protein Synthesis in Alzheimer's: From the Nucleolus to the Ribosome." Brain Pathol 26(5): 593-605.

Hoffmann, J. (1893). "Ueber chronische spinale Muskelatrophie im Kindesalter, auf familia¨rer Basis." Dtsch Z Nervenheilk 3: 427-470.

Hoffmann, J. (1897). "Weiterer Beitrag zur Lehre von der heredita¨ren progressiven spinalen Muskelatrophie im Kindesalter nebst Bemerkungen u¨ber den fortschreitenden Muskelschwund im Allgemeinen." Dtsch Z Nervenheilk 10: 292-320.

Hosseinibarkooie, S., M. Peters, L. Torres-Benito, R. H. Rastetter, K. Hupperich, A. Hoffmann, N. Mendoza-Ferreira, A. Kaczmarek, E. Janzen, J. Milbradt, T. Lamkemeyer, F. Rigo, C. F. Bennett, C. Guschlbauer, A. Buschges, M. Hammerschmidt, M. Riessland, M. J. Kye, C. S. Clemen and B. Wirth (2016). "The Power of Human Protective Modifiers: PLS3 and CORO1C Unravel Impaired Endocytosis in Spinal Muscular Atrophy and Rescue SMA Phenotype." Am J Hum Genet 99(3): 647-665.

Hoy, S. M. (2017). "Nusinersen: First Global Approval." Drugs.

Hsieh-Li, H. M., J. G. Chang, Y. J. Jong, M. H. Wu, N. M. Wang, C. H. Tsai and H. Li (2000). "A mouse model for spinal muscular atrophy." Nat Genet 24(1): 66-70.

Hu, L. Y., P. A. Boxer, S. R. Kesten, H. J. Lei, D. J. Wustrow, D. W. Moreland, L. Zhang, K. Ahn, T. R. Ryder, X. Liu, J. R. Rubin, K. Fahnoe, R. T. Carroll, S. Dutta, D. C. Fahnoe, A. W. Probert, R. L. Roof, M. F. Rafferty, C. R. Kostlan, J. D. Scholten, M. Hood, X. D. Ren, G. P. Schielke, T. Z. Su, C. P. Taylor, A. Mistry, P. McConnell, C. Hasemann and J. Ohren (2006). "The design and synthesis of human branched-chain amino acid aminotransferase inhibitors for treatment of neurodegenerative diseases." Bioorg Med Chem Lett 16(9): 2337-2340.

Hua, Y., K. Sahashi, F. Rigo, G. Hung, G. Horev, C. F. Bennett and A. R. Krainer (2011). "Peripheral SMN restoration is essential for long-term rescue of a severe spinal muscular atrophy mouse model." Nature 478(7367): 123-126.

Huber, K. M., S. M. Gallagher, S. T. Warren and M. F. Bear (2002). "Altered synaptic plasticity in a mouse model of fragile X mental retardation." Proc Natl Acad Sci U S A 99(11): 7746-7750.

Hubers, L., H. Valderrama-Carvajal, J. Laframboise, J. Timbers, G. Sanchez and J. Cote (2011). "HuD interacts with survival motor neuron protein and can rescue spinal muscular atrophy-like neuronal defects." Hum Mol Genet 20(3): 553-579.

Hutson, S. M., D. Berkich, P. Drown, B. Xu, M. Aschner and K. F. LaNoue (1998). "Role of branched-chain aminotransferase isoenzymes and gabapentin in neurotransmitter metabolism." J Neurochem 71(2): 863-874.

Ioannides, Z. A., S. T. Ngo, R. D. Henderson, P. A. McCombe and F. J. Steyn (2016). "Altered Metabolic Homeostasis in Amyotrophic Lateral Sclerosis: Mechanisms of Energy Imbalance and Contribution to Disease Progression." Neurodegener Dis 16(5-6): 382-397.

Ito, Y., S. Kumada, A. Uchiyama, K. Saito, M. Osawa, A. Yagishita, K. Kurata and M. Hayashi (2004). "Thalamic lesions in a long-surviving child with spinal muscular atrophy type I: MRI and EEG findings." Brain Dev 26(1): 53-56.

Iyer, C. C., V. L. McGovern, J. D. Murray, S. E. Gombash, P. G. Zaworski, K. D. Foust, P. M. Janssen and A. H. Burghes (2015). "Low levels of Survival Motor Neuron protein are sufficient for normal muscle function in the SMNDelta7 mouse model of SMA." Hum Mol Genet 24(21): 6160-6173.

Jablonka, S., M. Bandilla, S. Wiese, D. Buhler, B. Wirth, M. Sendtner and U. Fischer (2001). "Co-regulation of survival of motor neuron (SMN) protein and its interactor SIP1 during development and in spinal muscular atrophy." Hum Mol Genet 10(5): 497-505.

Jablonka, S., B. Schrank, M. Kralewski, W. Rossoll and M. Sendtner (2000). "Reduced survival motor neuron (Smn) gene dose in mice leads to motor neuron degeneration: an animal model for spinal muscular atrophy type III." Hum Mol Genet 9(3): 341-346.

Jang, S., J. C. Nelson, E. G. Bend, L. Rodriguez-Laureano, F. G. Tueros, L. Cartagenova, K. Underwood, E. M. Jorgensen and D. A. Colon-Ramos (2016). "Glycolytic Enzymes Localize to Synapses under Energy Stress to Support Synaptic Function." Neuron 90(2): 278-291.

Kaifer, K. A., E. Villalon, E. Y. Osman, J. J. Glascock, L. L. Arnold, D. D. Cornelison and C. L. Lorson (2017). "Plastin-3 extends survival and reduces severity in mouse models of spinal muscular atrophy." JCI Insight 2(5): e89970.

Kalman, L., J. Leonard, N. Gerry, J. Tarleton, C. Bridges, J. M. Gastier-Foster, R. E. Pyatt, E. Stonerock, M. A. Johnson, C. S. Richards, I. Schrijver, T. Ma, V. R. Miller, Y. Adadevoh, P. Furlong, C. Beiswanger and L. Toji (2011). "Quality assurance for Duchenne and Becker muscular dystrophy genetic testing: development of a genomic DNA reference material panel." J Mol Diagn 13(2): 167-174.

Kambach, C., S. Walke and K. Nagai (1999). "Structure and assembly of the spliceosomal small nuclear ribonucleoprotein particles." Curr Opin Struct Biol 9(2): 222-230.

Kambach, C., S. Walke, R. Young, J. M. Avis, E. de la Fortelle, V. A. Raker, R. Luhrmann, J. Li and K. Nagai (1999). "Crystal structures of two Sm protein complexes and their implications for the assembly of the spliceosomal snRNPs." Cell 96(3): 375-387.

Kang, H. and E. M. Schuman (1996). "A requirement for local protein synthesis in neurotrophin-induced hippocampal synaptic plasticity." Science 273(5280): 1402-1406.

Kariya, S., G. H. Park, Y. Maeno-Hikichi, O. Leykekhman, C. Lutz, M. S. Arkovitz, L. T. Landmesser and U. R. Monani (2008). "Reduced SMN protein impairs maturation of the neuromuscular junctions in mouse models of spinal muscular atrophy." Hum Mol Genet 17(16): 2552-2569.

Kashima, T. and J. L. Manley (2003). "A negative element in SMN2 exon 7 inhibits splicing in spinal muscular atrophy." Nat Genet 34(4): 460-463.

Kausch, K., C. R. Muller, T. Grimm, K. Ricker, M. Rietschel, S. Rudnik-Schoneborn and K. Zerres (1991). "No evidence for linkage of autosomal dominant proximal spinal muscular atrophies to chromosome 5q markers." Hum Genet 86(3): 317-318.

Kelley, R. I. and J. T. Sladky (1986). "Dicarboxylic aciduria in an infant with spinal muscular atrophy." Ann Neurol 20(6): 734-736.

Kerr, D. A., J. P. Nery, R. J. Traystman, B. N. Chau and J. M. Hardwick (2000). "Survival motor neuron protein modulates neuron-specific apoptosis." Proc Natl Acad Sci U S A 97(24): 13312-13317.

Knight, A. L., X. Yan, S. Hamamichi, R. R. Ajjuri, J. R. Mazzulli, M. W. Zhang, J. G. Daigle, S. Zhang, A. R. Borom, L. R. Roberts, S. K. Lee, S. M. DeLeon, C. Viollet-Djelassi, D. Krainc, J. M. O'Donnell, K. A. Caldwell and G. A. Caldwell (2014). "The glycolytic enzyme, GPI, is a functionally conserved modifier of dopaminergic neurodegeneration in Parkinson's models." Cell Metab 20(1): 145-157.

Kolb, S. J., D. J. Battle and G. Dreyfuss (2007). "Molecular functions of the SMN complex." J Child Neurol 22(8): 990-994.

Kong, L., X. Wang, D. W. Choe, M. Polley, B. G. Burnett, M. Bosch-Marce, J. W. Griffin, M. M. Rich and C. J. Sumner (2009). "Impaired synaptic vesicle release and immaturity of neuromuscular junctions in spinal muscular atrophy mice." J Neurosci 29(3): 842-851.

Konkel, D. A., S. M. Tilghman and P. Leder (1978). "The sequence of the chromosomal mouse beta-globin major gene: homologies in capping, splicing and poly(A) sites." Cell 15(4): 1125-1132.

Korobova, F. and T. Svitkina (2010). "Molecular architecture of synaptic actin cytoskeleton in hippocampal neurons reveals a mechanism of dendritic spine morphogenesis." Mol Biol Cell 21(1): 165-176.

Kugelberg, E. and L. Welander (1956). "Heredofamilial juvenile muscular atrophy simulating muscular dystrophy." AMA Arch Neurol Psychiatry 75(5): 500-509.

Kweon, G. R., J. D. Marks, R. Krencik, E. H. Leung, P. T. Schumacker, K. Hyland and U. J. Kang (2004). "Distinct mechanisms of neurodegeneration induced by chronic complex I inhibition in dopaminergic and non-dopaminergic cells." J Biol Chem 279(50): 51783-51792.

La Spada, A. R., E. M. Wilson, D. B. Lubahn, A. E. Harding and K. H. Fischbeck (1991). "Androgen receptor gene mutations in X-linked spinal and bulbar muscular atrophy." Nature 352(6330): 77-79.

Lamar, K. M. and E. M. McNally (2014). "Genetic Modifiers for Neuromuscular Diseases." J Neuromuscul Dis 1(1): 3-13.

Lauber, J., G. Plessel, S. Prehn, C. L. Will, P. Fabrizio, K. Groning, W. S. Lane and R. Luhrmann (1997). "The human U4/U6 snRNP contains 60 and 90kD proteins that are structurally homologous to the yeast splicing factors Prp4p and Prp3p." Rna 3(8): 926-941.

Le, T. T., D. D. Coovert, U. R. Monani, G. E. Morris and A. H. Burghes (2000). "The survival motor neuron (SMN) protein: effect of exon loss and mutation on protein localization." Neurogenetics 3(1): 7-16.

Le, T. T., L. T. Pham, M. E. Butchbach, H. L. Zhang, U. R. Monani, D. D. Coovert, T. O. Gavrilina, L. Xing, G. J. Bassell and A. H. Burghes (2005). "SMNDelta7, the major product of the centromeric survival motor neuron (SMN2) gene, extends survival in mice with spinal muscular atrophy and associates with full-length SMN." Hum Mol Genet 14(6): 845-857.

Lee, J., Y. J. Hwang, J. H. Boo, D. Han, O. K. Kwon, K. Todorova, N. W. Kowall, Y. Kim and H. Ryu (2011). "Dysregulation of upstream binding factor-1 acetylation at K352 is linked to impaired ribosomal DNA transcription in Huntington's disease." Cell Death Differ 18(11): 1726-1735.

Lee, Y. I., M. Mikesh, I. Smith, M. Rimer and W. Thompson (2011). "Muscles in a mouse model of spinal muscular atrophy show profound defects in neuromuscular development even in the absence of failure in neuromuscular transmission or loss of motor neurons." Dev Biol 356(2): 432-444.

Lefebvre, S., L. Burglen, J. Frezal, A. Munnich and J. Melki (1998). "The role of the SMN gene in proximal spinal muscular atrophy." Hum Mol Genet 7(10): 1531-1536.

Lefebvre, S., L. Burglen, S. Reboullet, O. Clermont, P. Burlet, L. Viollet, B. Benichou, C. Cruaud, P. Millasseau, M. Zeviani and et al. (1995). "Identification and characterization of a spinal muscular atrophy-determining gene." Cell 80(1): 155-165.

Lefebvre, S., P. Burlet, Q. Liu, S. Bertrandy, O. Clermont, A. Munnich, G. Dreyfuss and J. Melki (1997). "Correlation between severity and SMN protein level in spinal muscular atrophy." Nat Genet 16(3): 265-269.

Lenaz, G., A. Baracca, R. Fato, M. L. Genova and G. Solaini (2006). "Mitochondrial Complex I: structure, function, and implications in neurodegeneration." Ital J Biochem 55(3-4): 232-253.

Leshinsky-Silver, E., A. S. Lebre, L. Minai, A. Saada, J. Steffann, S. Cohen, A. Rotig, A. Munnich, D. Lev and T. Lerman-Sagie (2009). "NDUFS4 mutations cause Leigh syndrome with predominant brainstem involvement." Mol Genet Metab 97(3): 185-189.

Li, J. Y., M. Plomann and P. Brundin (2003). "Huntington's disease: a synaptopathy?" Trends Mol Med 9(10): 414-420.

Li, Y. C., W. Z. Bai, L. Zhou, L. K. Sun and T. Hashikawa (2010). "Nonhomogeneous distribution of filamentous actin in the presynaptic terminals on the spinal motoneurons." J Comp Neurol 518(16): 3184-3192.

Liautard, J. P., J. Sri Widada and C. Brunel (1981). "Particles containing small molecular weight nuclear RNAs (snRNPs). Structure and possible functions." Mol Biol Rep 7(1-3): 41-45.

Lim, S. R. and K. J. Hertel (2001). "Modulation of survival motor neuron pre-mRNA splicing by inhibition of alternative 3' splice site pairing." J Biol Chem 276(48): 45476-45483.

Lin, C. S., R. H. Aebersold, S. B. Kent, M. Varma and J. Leavitt (1988). "Molecular cloning and characterization of plastin, a human leukocyte protein expressed in transformed human fibroblasts." Mol Cell Biol 8(11): 4659-4668.

Ling, K. K., M. Y. Lin, B. Zingg, Z. Feng and C. P. Ko (2010). "Synaptic defects in the spinal and neuromuscular circuitry in a mouse model of spinal muscular atrophy." PLoS One 5(11): e15457.

Liu-Yesucevitz, L., G. J. Bassell, A. D. Gitler, A. C. Hart, E. Klann, J. D. Richter, S. T. Warren and B. Wolozin (2011). "Local RNA translation at the synapse and in disease." J Neurosci 31(45): 16086-16093.

Liu, H., A. Beauvais, A. N. Baker, C. Tsilfidis and R. Kothary (2011). "Smn deficiency causes neuritogenesis and neurogenesis defects in the retinal neurons of a mouse model of spinal muscular atrophy." Dev Neurobiol 71(2): 153-169.

Liu, H., D. Shafey, J. N. Moores and R. Kothary (2010). "Neurodevelopmental consequences of Smn depletion in a mouse model of spinal muscular atrophy." J Neurosci Res 88(1): 111-122.

Liu, Q. and G. Dreyfuss (1996). "A novel nuclear structure containing the survival of motor neurons protein." Embo j 15(14): 3555-3565.

Liu, Q., U. Fischer, F. Wang and G. Dreyfuss (1997). "The spinal muscular atrophy disease gene product, SMN, and its associated protein SIP1 are in a complex with spliceosomal snRNP proteins." Cell 90(6): 1013-1021.

Lorson, C. L., E. Hahnen, E. J. Androphy and B. Wirth (1999). "A single nucleotide in the SMN gene regulates splicing and is responsible for spinal muscular atrophy." Proc Natl Acad Sci U S A 96(11): 6307-6311.

Lorson, C. L., J. Strasswimmer, J. M. Yao, J. D. Baleja, E. Hahnen, B. Wirth, T. Le, A. H. Burghes and E. J. Androphy (1998). "SMN oligomerization defect correlates with spinal muscular atrophy severity." Nat Genet 19(1): 63-66.

Lupski, J. R., C. A. Garcia, H. Y. Zoghbi, E. P. Hoffman and R. G. Fenwick (1991). "Discordance of muscular dystrophy in monozygotic female twins: evidence supporting asymmetric splitting of the inner cell mass in a manifesting carrier of Duchenne dystrophy." Am J Med Genet 40(3): 354-364.

Lutz, C. M., S. Kariya, S. Patruni, M. A. Osborne, D. Liu, C. E. Henderson, D. K. Li, L. Pellizzoni, J. Rojas, D. M. Valenzuela, A. J. Murphy, M. L. Winberg and U. R. Monani (2011). "Postsymptomatic restoration of SMN rescues the disease phenotype in a mouse model of severe spinal muscular atrophy." J Clin Invest 121(8): 3029-3041.

Maekawa, M., T. Ishizaki, S. Boku, N. Watanabe, A. Fujita, A. Iwamatsu, T. Obinata, K. Ohashi, K. Mizuno and S. Narumiya (1999). "Signaling from Rho to the actin cytoskeleton through protein kinases ROCK and LIM-kinase." Science 285(5429): 895-898.

Mailman, M. D., J. W. Heinz, A. C. Papp, P. J. Snyder, M. S. Sedra, B. Wirth, A. H. Burghes and T. W. Prior (2002). "Molecular analysis of spinal muscular atrophy and modification of the phenotype by SMN2." Genet Med 4(1): 20-26.

Mancuso, M., L. Salviati, S. Sacconi, D. Otaegui, P. Camano, A. Marina, S. Bacman, C. T. Moraes, J. R. Carlo, M. Garcia, M. Garcia-Alvarez, L. Monzon, A. B. Naini, M. Hirano, E. Bonilla, A. L. Taratuto, S. DiMauro and T. H. Vu (2002). "Mitochondrial DNA depletion: mutations in thymidine kinase gene with myopathy and SMA." Neurology 59(8): 1197-1202.

Marcovina, S. M., C. Sirtori, A. Peracino, M. Gheorghiade, P. Borum, G. Remuzzi and H. Ardehali (2013). "Translating the basic knowledge of mitochondrial functions to metabolic therapy: role of L-carnitine." Transl Res 161(2): 73-84.

Martin, L. J. (2010). "Olesoxime, a cholesterol-like neuroprotectant for the potential treatment of amyotrophic lateral sclerosis." IDrugs 13(8): 568-580.

Martin, R., K. Gupta, N. S. Ninan, K. Perry and G. D. Van Duyne (2012). "The survival motor neuron protein forms soluble glycine zipper oligomers." Structure 20(11): 1929-1939.

Martinez-Hernandez, R., S. Bernal, E. Also-Rallo, L. Alias, M. J. Barcelo, M. Hereu, J. E. Esquerda and E. F. Tizzano (2013). "Synaptic defects in type I spinal muscular atrophy in human development." J Pathol 229(1): 49-61.

Martinez-Hernandez, R., C. Soler-Botija, E. Also, L. Alias, L. Caselles, I. Gich, S. Bernal and E. F. Tizzano (2009). "The developmental pattern of myotubes in spinal muscular atrophy indicates prenatal delay of muscle maturation." J Neuropathol Exp Neurol 68(5): 474-481.

Martinez, T. L., L. Kong, X. Wang, M. A. Osborne, M. E. Crowder, J. P. Van Meerbeke, X. Xu, C. Davis, J. Wooley, D. J. Goldhamer, C. M. Lutz, M. M. Rich and C. J. Sumner (2012). "Survival motor neuron protein in motor neurons determines synaptic integrity in spinal muscular atrophy." J Neurosci 32(25): 8703-8715.

Massignan, T., F. Casoni, M. Basso, P. Stefanazzi, E. Biasini, M. Tortarolo, M. Salmona, E. Gianazza, C. Bendotti and V. Bonetto (2007). "Proteomic analysis of spinal cord of presymptomatic amyotrophic lateral sclerosis G93A SOD1 mouse." Biochem Biophys Res Commun 353(3): 719-725.

Mattson, M. P., J. N. Keller and J. G. Begley (1998). "Evidence for synaptic apoptosis." Exp Neurol 153(1): 35-48.

McAndrew, P. E., D. W. Parsons, L. R. Simard, C. Rochette, P. N. Ray, J. R. Mendell, T. W. Prior and A. H. Burghes (1997). "Identification of proximal spinal muscular atrophy carriers and patients by analysis of SMNT and SMNC gene copy number." Am J Hum Genet 60(6): 1411-1422.

McGovern, V. L., T. O. Gavrilina, C. E. Beattie and A. H. Burghes (2008). "Embryonic motor axon development in the severe SMA mouse." Hum Mol Genet 17(18): 2900-2909.

McGovern, V. L., C. C. Iyer, W. D. Arnold, S. E. Gombash, P. G. Zaworski, A. J. Blatnik, 3rd, K. D. Foust and A. H. Burghes (2015). "SMN expression is required in motor neurons to rescue

electrophysiological deficits in the SMNDelta7 mouse model of SMA." Hum Mol Genet 24(19): 5524-5541.

McGovern, V. L., A. Massoni-Laporte, X. Wang, T. T. Le, H. T. Le, C. E. Beattie, M. M. Rich and A. H. Burghes (2015). "Plastin 3 Expression Does Not Modify Spinal Muscular Atrophy Severity in the 7 SMA Mouse." PLoS One 10(7): e0132364.

McWhorter, M. L., U. R. Monani, A. H. Burghes and C. E. Beattie (2003). "Knockdown of the survival motor neuron (Smn) protein in zebrafish causes defects in motor axon outgrowth and pathfinding." J Cell Biol 162(5): 919-931.

Melki, J., S. Abdelhak, P. Sheth, M. F. Bachelot, P. Burlet, A. Marcadet, J. Aicardi, A. Barois, J. P. Carriere, M. Fardeau and et al. (1990). "Gene for chronic proximal spinal muscular atrophies maps to chromosome 5q." Nature 344(6268): 767-768.

Melki, J., P. Sheth, S. Abdelhak, P. Burlet, M. F. Bachelot, M. G. Lathrop, J. Frezal and A. Munnich (1990). "Mapping of acute (type I) spinal muscular atrophy to chromosome 5q12-q14. The French Spinal Muscular Atrophy Investigators." Lancet 336(8710): 271-273.

Mentis, G. Z., D. Blivis, W. Liu, E. Drobac, M. E. Crowder, L. Kong, F. J. Alvarez, C. J. Sumner and M. J. O'Donovan (2011). "Early functional impairment of sensory-motor connectivity in a mouse model of spinal muscular atrophy." Neuron 69(3): 453-467.

Michaelides, M., L. L. Chen, M. A. Brantley, Jr., J. L. Andorf, E. M. Isaak, S. A. Jenkins, G. E. Holder, A. C. Bird, E. M. Stone and A. R. Webster (2007). "ABCA4 mutations and discordant ABCA4 alleles in patients and siblings with bull's-eye maculopathy." Br J Ophthalmol 91(12): 1650-1655.

Mier, P. and A. J. Perez-Pulido (2012). "Fungal Smn and Spf30 homologues are mainly present in filamentous fungi and genomes with many introns: implications for spinal muscular atrophy." Gene 491(2): 135-141.

Miller, N., H. Shi, A. S. Zelikovich and Y. C. Ma (2016). "Motor neuron mitochondrial dysfunction in spinal muscular atrophy." Hum Mol Genet 25(16): 3395-3406.

Millino, C., M. Fanin, A. Vettori, P. Laveder, M. L. Mostacciuolo, C. Angelini and G. Lanfranchi (2009). "Different atrophy-hypertrophy transcription pathways in muscles affected by severe and mild spinal muscular atrophy." BMC Med 7: 14.

Miyajima, H., H. Miyaso, M. Okumura, J. Kurisu and K. Imaizumi (2002). "Identification of a cis-acting element for the regulation of SMN exon 7 splicing." J Biol Chem 277(26): 23271-23277.

Monani, U. R. (2005). "Spinal muscular atrophy: a deficiency in a ubiquitous protein; a motor neuron-specific disease." Neuron 48(6): 885-896.

Monani, U. R., C. L. Lorson, D. W. Parsons, T. W. Prior, E. J. Androphy, A. H. Burghes and J. D. McPherson (1999). "A single nucleotide difference that alters splicing patterns distinguishes the SMA gene SMN1 from the copy gene SMN2." Hum Mol Genet 8(7): 1177-1183.

Monani, U. R., M. T. Pastore, T. O. Gavrilina, S. Jablonka, T. T. Le, C. Andreassi, J. M. DiCocco, C. Lorson, E. J. Androphy, M. Sendtner, M. Podell and A. H. Burghes (2003). "A transgene carrying an A2G missense mutation in the SMN gene modulates phenotypic severity in mice with severe (type I) spinal muscular atrophy." J Cell Biol 160(1): 41-52.

Monani, U. R., M. Sendtner, D. D. Coovert, D. W. Parsons, C. Andreassi, T. T. Le, S. Jablonka, B. Schrank, W. Rossoll, T. W. Prior, G. E. Morris and A. H. Burghes (2000). "The human centromeric survival motor neuron gene (SMN2) rescues embryonic lethality in Smn(-/-) mice and results in a mouse with spinal muscular atrophy." Hum Mol Genet 9(3): 333-339.

Morrow, T. (2017). "New Therapy for Spinal Muscular Atrophy Offers Modest Bang for Pharamaceutical Buck." Manag Care 26(2): 36-37.

Mortensen, P. B. (1992). "Formation and degradation of dicarboxylic acids in relation to alterations in fatty acid oxidation in rats." Biochim Biophys Acta 1124(1): 71-79.

Mourelatos, Z., L. Abel, J. Yong, N. Kataoka and G. Dreyfuss (2001). "SMN interacts with a novel family of hnRNP and spliceosomal proteins." Embo j 20(19): 5443-5452.

Mueller, B. K., H. Mack and N. Teusch (2005). "Rho kinase, a promising drug target for neurological disorders." Nat Rev Drug Discov 4(5): 387-398.

Munsat, T. L. and K. E. Davies (1992). "International SMA consortium meeting. (26-28 June 1992, Bonn, Germany)." Neuromuscul Disord 2(5-6): 423-428.

Murray, L., T. H. Gillingwater and R. Kothary (2014). "Dissection of the transversus abdominis muscle for whole-mount neuromuscular junction analysis." J Vis Exp(83): e51162.

Murray, L. M., A. Beauvais, S. Gibeault, N. L. Courtney and R. Kothary (2015). "Transcriptional profiling of differentially vulnerable motor neurons at pre-symptomatic stage in the Smn (2b/-) mouse model of spinal muscular atrophy." Acta Neuropathol Commun 3: 55.

Murray, L. M., L. H. Comley, D. Thomson, N. Parkinson, K. Talbot and T. H. Gillingwater (2008). "Selective vulnerability of motor neurons and dissociation of pre- and post-synaptic pathology at the neuromuscular junction in mouse models of spinal muscular atrophy." Hum Mol Genet 17(7): 949-962.

Murray, L. M., S. Lee, D. Baumer, S. H. Parson, K. Talbot and T. H. Gillingwater (2010). "Pre-symptomatic development of lower motor neuron connectivity in a mouse model of severe spinal muscular atrophy." Hum Mol Genet 19(3): 420-433.

Nadeau, J. H. (2001). "Modifier genes in mice and humans." Nat Rev Genet 2(3): 165-174.

Neveling, K., L. A. Martinez-Carrera, I. Holker, A. Heister, A. Verrips, S. M. Hosseini-Barkooie, C. Gilissen, S. Vermeer, M. Pennings, R. Meijer, M. te Riele, C. J. Frijns, O. Suchowersky, L. MacLaren, S. Rudnik-Schoneborn, R. J. Sinke, K. Zerres, R. B. Lowry, H. H. Lemmink, L. Garbes, J. A. Veltman, H. J. Schelhaas, H. Scheffer and B. Wirth (2013). "Mutations in BICD2, which encodes a golgin and important motor adaptor, cause congenital autosomal-dominant spinal muscular atrophy." Am J Hum Genet 92(6): 946-954.

Ngo, S. T. and F. J. Steyn (2015). "The interplay between metabolic homeostasis and neurodegeneration: insights into the neurometabolic nature of amyotrophic lateral sclerosis." Cell Regen (Lond) 4(1): 5.

Ning, K., C. Drepper, C. F. Valori, M. Ahsan, M. Wyles, A. Higginbottom, T. Herrmann, P. Shaw, M. Azzouz and M. Sendtner (2010). "PTEN depletion rescues axonal growth defect and improves survival in SMN-deficient motor neurons." Hum Mol Genet 19(16): 3159-3168.

Nolle, A., A. Zeug, J. van Bergeijk, L. Tonges, R. Gerhard, H. Brinkmann, S. Al Rayes, N. Hensel, Y. Schill, D. Apkhazava, S. Jablonka, J. O'Mer, R. K. Srivastav, A. Baasner, P. Lingor, B. Wirth, E. Ponimaskin, R. Niedenthal, C. Grothe and P. Claus (2011). "The spinal muscular atrophy disease protein SMN is linked to the Rho-kinase pathway via profilin." Hum Mol Genet 20(24): 4865-4878.

Novarino, G., P. El-Fishawy, H. Kayserili, N. A. Meguid, E. M. Scott, J. Schroth, J. L. Silhavy, M. Kara, R. O. Khalil, T. Ben-Omran, A. G. Ercan-Sencicek, A. F. Hashish, S. J. Sanders, A. R. Gupta, H. S. Hashem, D. Matern, S. Gabriel, L. Sweetman, Y. Rahimi, R. A. Harris, M. W. State and J. G. Gleeson (2012). "Mutations in BCKD-kinase lead to a potentially treatable form of autism with epilepsy." Science 338(6105): 394-397.

Novelli, G., M. Gennarelli, E. Menegazzo, C. Angelini and B. Dallapiccola (1995). "Discordant clinical outcome in myotonic dystrophy relatives showing (CTG)n > 700 repeats." Neuromuscul Disord 5(2): 157-159.

Nyman, U., H. Hallman, G. Hadlaczky, I. Pettersson, G. Sharp and N. R. Ringertz (1986). "Intranuclear localization of snRNP antigens." J Cell Biol 102(1): 137-144.

Ogino, S., D. G. Leonard, H. Rennert, W. J. Ewens and R. B. Wilson (2002). "Genetic risk assessment in carrier testing for spinal muscular atrophy." Am J Med Genet 110(4): 301-307.

Ohno, M., A. Segref, A. Bachi, M. Wilm and I. W. Mattaj (2000). "PHAX, a mediator of U snRNA nuclear export whose activity is regulated by phosphorylation." Cell 101(2): 187-198.

Oprea, G. E., S. Krober, M. L. McWhorter, W. Rossoll, S. Muller, M. Krawczak, G. J. Bassell, C. E. Beattie and B. Wirth (2008). "Plastin 3 is a protective modifier of autosomal recessive spinal muscular atrophy." Science 320(5875): 524-527.

Pagliardini, S., A. Giavazzi, V. Setola, C. Lizier, M. Di Luca, S. DeBiasi and G. Battaglia (2000). "Subcellular localization and axonal transport of the survival motor neuron (SMN) protein in the developing rat spinal cord." Hum Mol Genet 9(1): 47-56.

Park, G. H., Y. Maeno-Hikichi, T. Awano, L. T. Landmesser and U. R. Monani (2010). "Reduced survival of motor neuron (SMN) protein in motor neuronal progenitors functions cell autonomously to

cause spinal muscular atrophy in model mice expressing the human centromeric (SMN2) gene." J Neurosci 30(36): 12005-12019.

Parnetti, L., A. Gaiti, M. Brunetti, L. Avellini, C. Polidori, R. Cecchetti, B. Palumbo and U. Senin (1995). "Increased CSF pyruvate levels as a marker of impaired energy metabolism in Alzheimer's disease." J Am Geriatr Soc 43(3): 316-318.

Parnetti, L., A. Gaiti, M. C. Polidori, M. Brunetti, B. Palumbo, F. Chionne, D. Cadini, R. Cecchetti and U. Senin (1995). "Increased cerebrospinal fluid pyruvate levels in Alzheimer's disease." Neurosci Lett 199(3): 231-233.

Pathak, D., A. Berthet and K. Nakamura (2013). "Energy failure: does it contribute to neurodegeneration?" Ann Neurol 74(4): 506-516.

Pathak, D., L. Y. Shields, B. A. Mendelsohn, D. Haddad, W. Lin, A. A. Gerencser, H. Kim, M. D. Brand, R. H. Edwards and K. Nakamura (2015). "The role of mitochondrially derived ATP in synaptic vesicle recycling." J Biol Chem 290(37): 22325-22336.

Pearn, J. (1978). "Incidence, prevalence, and gene frequency studies of chronic childhood spinal muscular atrophy." J Med Genet 15(6): 409-413.

Pearn, J. (1980). "Classification of spinal muscular atrophies." Lancet 1(8174): 919-922.

Pearn, J. H. (1973). "The gene frequency of acute Werdnig-Hoffmann disease (SMA type 1). A total population survey in North-East England." J Med Genet 10(3): 260-265.

Pearn, J. H., P. Hudgson and J. N. Walton (1978). "A clinical and genetic study of spinal muscular atrophy of adult onset: the autosomal recessive form as a discrete disease entity." Brain 101(4): 591-606.

Pek, J. W., A. Anand and T. Kai (2012). "Tudor domain proteins in development." Development 139(13): 2255-2266.

Pellizzoni, L., B. Charroux and G. Dreyfuss (1999). "SMN mutants of spinal muscular atrophy patients are defective in binding to snRNP proteins." Proc Natl Acad Sci U S A 96(20): 11167-11172.

Pellizzoni, L., N. Kataoka, B. Charroux and G. Dreyfuss (1998). "A novel function for SMN, the spinal muscular atrophy disease gene product, in pre-mRNA splicing." Cell 95(5): 615-624.

Pellizzoni, L., J. Yong and G. Dreyfuss (2002). "Essential role for the SMN complex in the specificity of snRNP assembly." Science 298(5599): 1775-1779.

Plessel, G., U. Fischer and R. Luhrmann (1994). "m3G cap hypermethylation of U1 small nuclear ribonucleoprotein (snRNP) in vitro: evidence that the U1 small nuclear RNA-(guanosine-N2)-methyltransferase is a non-snRNP cytoplasmic protein that requires a binding site on the Sm core domain." Mol Cell Biol 14(6): 4160-4172.

Plessel, G., R. Luhrmann and B. Kastner (1997). "Electron microscopy of assembly intermediates of the snRNP core: morphological similarities between the RNA-free (E.F.G) protein heteromer and the intact snRNP core." J Mol Biol 265(2): 87-94.

Powis, R. A., C. A. Mutsaers, T. M. Wishart, G. Hunter, B. Wirth and T. H. Gillingwater (2014). "Increased levels of UCHL1 are a compensatory response to disrupted ubiquitin homeostasis in spinal muscular atrophy and do not represent a viable therapeutic target." Neuropathol Appl Neurobiol 40(7): 873-887.

Praveen, K., Y. Wen, K. M. Gray, J. J. Noto, A. R. Patlolla, G. D. Van Duyne and A. G. Matera (2014). "SMA-causing missense mutations in survival motor neuron (Smn) display a wide range of phenotypes when modeled in Drosophila." PLoS Genet 10(8): e1004489.

Raad, M., T. El Tal, R. Gul, S. Mondello, Z. Zhang, R. M. Boustany, J. Guingab, K. K. Wang and F. Kobeissy (2012). "Neuroproteomics approach and neurosystems biology analysis: ROCK inhibitors as promising therapeutic targets in neurodegeneration and neurotrauma." Electrophoresis 33(24): 3659-3668.

Rabbitts, T. H. (1978). "Evidence for splicing of interrupted immunoglobulin variable and constant region sequences in nuclear RNA." Nature 275(5678): 291-296.

Rajendra, T. K., G. B. Gonsalvez, M. P. Walker, K. B. Shpargel, H. K. Salz and A. G. Matera (2007). "A Drosophila melanogaster model of spinal muscular atrophy reveals a function for SMN in striated muscle." J Cell Biol 176(6): 831-841.

Raker, V. A., G. Plessel and R. Luhrmann (1996). "The snRNP core assembly pathway: identification of stable core protein heteromeric complexes and an snRNP subcore particle in vitro." Embo j 15(9): 2256-2269.

Ramser, J., M. E. Ahearn, C. Lenski, K. O. Yariz, H. Hellebrand, M. von Rhein, R. D. Clark, R. K. Schmutzler, P. Lichtner, E. P. Hoffman, A. Meindl and L. Baumbach-Reardon (2008). "Rare missense and synonymous variants in UBE1 are associated with X-linked infantile spinal muscular atrophy." Am J Hum Genet 82(1): 188-193.

Rapoport, S. I. (2003). "Coupled reductions in brain oxidative phosphorylation and synaptic function can be quantified and staged in the course of Alzheimer disease." Neurotox Res 5(6): 385-398.

Reinhard, M., K. Giehl, K. Abel, C. Haffner, T. Jarchau, V. Hoppe, B. M. Jockusch and U. Walter (1995). "The proline-rich focal adhesion and microfilament protein VASP is a ligand for profilins." Embo j 14(8): 1583-1589.

Richards, C. S., S. C. Watkins, E. P. Hoffman, N. R. Schneider, I. W. Milsark, K. S. Katz, J. D. Cook, L. M. Kunkel and J. M. Cortada (1990). "Skewed X inactivation in a female MZ twin results in Duchenne muscular dystrophy." Am J Hum Genet 46(4): 672-681.

Ripolone, M., D. Ronchi, R. Violano, D. Vallejo, G. Fagiolari, E. Barca, V. Lucchini, I. Colombo, L. Villa, A. Berardinelli, U. Balottin, L. Morandi, M. Mora, A. Bordoni, F. Fortunato, S. Corti, D. Parisi, A. Toscano, M. Sciacco, S. DiMauro, G. P. Comi and M. Moggio (2015). "Impaired Muscle Mitochondrial Biogenesis and Myogenesis in Spinal Muscular Atrophy." JAMA Neurol 72(6): 666-675.

Rizzardini, M., M. Lupi, A. Mangolini, E. Babetto, P. Ubezio and L. Cantoni (2006). "Neurodegeneration induced by complex I inhibition in a cellular model of familial amyotrophic lateral sclerosis." Brain Res Bull 69(4): 465-474.

Robbins, K. L., J. J. Glascock, E. Y. Osman, M. R. Miller and C. L. Lorson (2014). "Defining the therapeutic window in a severe animal model of spinal muscular atrophy." Hum Mol Genet 23(17): 4559-4568.

Robinson, B. H. (1998). "Human complex I deficiency: clinical spectrum and involvement of oxygen free radicals in the pathogenicity of the defect." Biochim Biophys Acta 1364(2): 271-286.

Rossoll, W., S. Jablonka, C. Andreassi, A. K. Kroning, K. Karle, U. R. Monani and M. Sendtner (2003). "Smn, the spinal muscular atrophy-determining gene product, modulates axon growth and localization of beta-actin mRNA in growth cones of motoneurons." J Cell Biol 163(4): 801-812.

Rossoll, W., A. K. Kroning, U. M. Ohndorf, C. Steegborn, S. Jablonka and M. Sendtner (2002). "Specific interaction of Smn, the spinal muscular atrophy determining gene product, with hnRNP-R and gry-rbp/hnRNP-Q: a role for Smn in RNA processing in motor axons?" Hum Mol Genet 11(1): 93-105.

Rudnik-Schoneborn, S., R. Forkert, E. Hahnen, B. Wirth and K. Zerres (1996). "Clinical spectrum and diagnostic criteria of infantile spinal muscular atrophy: further delineation on the basis of SMN gene deletion findings." Neuropediatrics 27(1): 8-15.

Rudnik-Schoneborn, S., H. H. Goebel, W. Schlote, S. Molaian, H. Omran, U. Ketelsen, R. Korinthenberg, D. Wenzel, H. Lauffer, M. Kreiss-Nachtsheim, B. Wirth and K. Zerres (2003). "Classical infantile spinal muscular atrophy with SMN deficiency causes sensory neuronopathy." Neurology 60(6): 983-987.

Ruiz, R., J. J. Casanas, L. Torres-Benito, R. Cano and L. Tabares (2010). "Altered intracellular Ca2+ homeostasis in nerve terminals of severe spinal muscular atrophy mice." J Neurosci 30(3): 849-857.

Ruiz, R. and L. Tabares (2014). "Neurotransmitter release in motor nerve terminals of a mouse model of mild spinal muscular atrophy." J Anat 224(1): 74-84.

Rust, M. B. and T. Maritzen (2015). "Relevance of presynaptic actin dynamics for synapse function and mouse behavior." Exp Cell Res 335(2): 165-171.

Saal, L., M. Briese, S. Kneitz, M. Glinka and M. Sendtner (2014). "Subcellular transcriptome alterations in a cell culture model of spinal muscular atrophy point to widespread defects in axonal growth and presynaptic differentiation." Rna 20(11): 1789-1802.

Sanchez, G., A. Y. Dury, L. M. Murray, O. Biondi, H. Tadesse, R. El Fatimy, R. Kothary, F. Charbonnier, E. W. Khandjian and J. Cote (2013). "A novel function for the survival motoneuron protein as a translational regulator." Hum Mol Genet 22(4): 668-684.

Sasaki, S. and S. Maruyama (1994). "Synapse loss in anterior horn neurons in amyotrophic lateral sclerosis." Acta Neuropathol 88(3): 222-227.

Schapira, A. H. (2010). "Complex I: inhibitors, inhibition and neurodegeneration." Exp Neurol 224(2): 331-335.

Schirinzi, T., G. Madeo, G. Martella, M. Maltese, B. Picconi, P. Calabresi and A. Pisani (2016). "Early synaptic dysfunction in Parkinson's disease: Insights from animal models." Mov Disord 31(6): 802-813.

Schrank, B., R. Gotz, J. M. Gunnersen, J. M. Ure, K. V. Toyka, A. G. Smith and M. Sendtner (1997). "Inactivation of the survival motor neuron gene, a candidate gene for human spinal muscular atrophy, leads to massive cell death in early mouse embryos." Proc Natl Acad Sci U S A 94(18): 9920-9925.

Schreml, J., M. Riessland, M. Paterno, L. Garbes, K. Rossbach, B. Ackermann, J. Kramer, E. Somers, S. H. Parson, R. Heller, A. Berkessel, A. Sterner-Kock and B. Wirth (2013). "Severe SMA mice show organ impairment that cannot be rescued by therapy with the HDACi JNJ-26481585." Eur J Hum Genet 21(6): 643-652.

Segref, A., I. W. Mattaj and M. Ohno (2001). "The evolutionarily conserved region of the U snRNA export mediator PHAX is a novel RNA-binding domain that is essential for U snRNA export." Rna 7(3): 351-360.

Selenko, P., R. Sprangers, G. Stier, D. Buhler, U. Fischer and M. Sattler (2001). "SMN tudor domain structure and its interaction with the Sm proteins." Nat Struct Biol 8(1): 27-31.

Seng, C. O., C. Magee, P. J. Young, C. L. Lorson and J. P. Allen (2015). "The SMN structure reveals its crucial role in snRNP assembly." Hum Mol Genet 24(8): 2138-2146.

Setola, V., M. Terao, D. Locatelli, S. Bassanini, E. Garattini and G. Battaglia (2007). "Axonal-SMN (a-SMN), a protein isoform of the survival motor neuron gene, is specifically involved in axonogenesis." Proc Natl Acad Sci U S A 104(6): 1959-1964.

Shababi, M., J. Habibi, L. Ma, J. J. Glascock, J. R. Sowers and C. L. Lorson (2012). "Partial restoration of cardio-vascular defects in a rescued severe model of spinal muscular atrophy." J Mol Cell Cardiol 52(5): 1074-1082.

Shababi, M., J. Habibi, H. T. Yang, S. M. Vale, W. A. Sewell and C. L. Lorson (2010). "Cardiac defects contribute to the pathology of spinal muscular atrophy models." Hum Mol Genet 19(20): 4059-4071.

Shababi, M., C. L. Lorson and S. S. Rudnik-Schoneborn (2014). "Spinal muscular atrophy: a motor neuron disorder or a multi-organ disease?" J Anat 224(1): 15-28.

Shafey, D., P. D. Cote and R. Kothary (2005). "Hypomorphic Smn knockdown C2C12 myoblasts reveal intrinsic defects in myoblast fusion and myotube morphology." Exp Cell Res 311(1): 49-61.

Sharma, A., A. Lambrechts, T. Hao le, T. T. Le, C. A. Sewry, C. Ampe, A. H. Burghes and G. E. Morris (2005). "A role for complexes of survival of motor neurons (SMN) protein with gemins and profilin in neurite-like cytoplasmic extensions of cultured nerve cells." Exp Cell Res 309(1): 185-197.

Shin, N., H. Jeong, J. Kwon, H. Y. Heo, J. J. Kwon, H. J. Yun, C. H. Kim, B. S. Han, Y. Tong, J. Shen, T. Hatano, N. Hattori, K. S. Kim, S. Chang and W. Seol (2008). "LRRK2 regulates synaptic vesicle endocytosis." Exp Cell Res 314(10): 2055-2065.

Shishikura, K., M. Hara, Y. Sasaki and K. Misugi (1983). "A neuropathologic study of Werdnig-Hoffmann disease with special reference to the thalamus and posterior roots." Acta Neuropathol 60(1-2): 99-106.

Shupliakov, O., O. Bloom, J. S. Gustafsson, O. Kjaerulff, P. Low, N. Tomilin, V. A. Pieribone, P. Greengard and L. Brodin (2002). "Impaired recycling of synaptic vesicles after acute perturbation of the presynaptic actin cytoskeleton." Proc Natl Acad Sci U S A 99(22): 14476-14481.

Simic, G. (2008). "Pathogenesis of proximal autosomal recessive spinal muscular atrophy." Acta Neuropathol 116(3): 223-234.

Simic, G., M. Mladinov, D. Seso Simic, N. Jovanov Milosevic, A. Islam, A. Pajtak, N. Barisic, J. Sertic, P. J. Lucassen, P. R. Hof and B. Kruslin (2008). "Abnormal motoneuron migration, differentiation, and axon outgrowth in spinal muscular atrophy." Acta Neuropathol 115(3): 313-326.

Skordis, L. A., M. G. Dunckley, B. Yue, I. C. Eperon and F. Muntoni (2003). "Bifunctional antisense oligonucleotides provide a trans-acting splicing enhancer that stimulates SMN2 gene expression in patient fibroblasts." Proc Natl Acad Sci U S A 100(7): 4114-4119.

Sleeman, J. E. and A. I. Lamond (1999). "Newly assembled snRNPs associate with coiled bodies before speckles, suggesting a nuclear snRNP maturation pathway." Curr Biol 9(19): 1065-1074.

Somers, E., Z. Stencel, T. M. Wishart, T. H. Gillingwater and S. H. Parson (2012). "Density, calibre and ramification of muscle capillaries are altered in a mouse model of severe spinal muscular atrophy." Neuromuscul Disord 22(5): 435-442.

Sproule, D. M., J. Montes, M. Montgomery, V. Battista, D. Koenigsberger, W. Shen, M. Punyanitya, D. C. De Vivo and P. Kaufmann (2009). "Increased fat mass and high incidence of overweight despite low body mass index in patients with spinal muscular atrophy." Neuromuscul Disord 19(6): 391-396.

Steitz, J. A., C. Berg, E. Gottlieb, J. A. Hardin, C. Hashimoto, J. P. Hendrick, M. Hinterberger, M. Krikeles, M. R. Lerner, S. M. Mount and et al. (1982). "Structure and function of small ribonucleoproteins from eukaryotic cells." Princess Takamatsu Symp 12: 101-107.

Strasswimmer, J., C. L. Lorson, D. E. Breiding, J. J. Chen, T. Le, A. H. Burghes and E. J. Androphy (1999). "Identification of survival motor neuron as a transcriptional activator-binding protein." Hum Mol Genet 8(7): 1219-1226.

Stratigopoulos, G., P. Lanzano, L. Deng, J. Guo, P. Kaufmann, B. Darras, R. Finkel, R. Tawil, M. P. McDermott, W. Martens, D. C. Devivo and W. K. Chung (2010). "Association of plastin 3 expression with disease severity in spinal muscular atrophy only in postpubertal females." Arch Neurol 67(10): 1252-1256.

Sumner, C. (2010). "Grip strength." TREAT-NMD Neuromuscular Network , Experimental protocols for SMA animal models SMA_M.2.1.002.

Sumner, C. (2011). "Behavioral Phenotyping for Neonates: Hind Limb Suspension Test (a.k.a. Tube Test)." TREAT-NMD Neuromuscular Network , Experimental protocols for SMA animal models SMA_M.2.1.002.

Tadesse, H., J. Deschenes-Furry, S. Boisvenue and J. Cote (2008). "KH-type splicing regulatory protein interacts with survival motor neuron protein and is misregulated in spinal muscular atrophy." Hum Mol Genet 17(4): 506-524.

Takei, K., V. I. Slepnev, V. Haucke and P. De Camilli (1999). "Functional partnership between amphiphysin and dynamin in clathrin-mediated endocytosis." Nat Cell Biol 1(1): 33-39.

Talbot, K., I. Miguel-Aliaga, P. Mohaghegh, C. P. Ponting and K. E. Davies (1998). "Characterization of a gene encoding survival motor neuron (SMN)-related protein, a constituent of the spliceosome complex." Hum Mol Genet 7(13): 2149-2156.

Talbot, K., C. P. Ponting, A. M. Theodosiou, N. R. Rodrigues, R. Surtees, R. Mountford and K. E. Davies (1997). "Missense mutation clustering in the survival motor neuron gene: a role for a conserved tyrosine and glycine rich region of the protein in RNA metabolism?" Hum Mol Genet 6(3): 497-500.

Tarabal, O., V. Caraballo-Miralles, A. Cardona-Rossinyol, F. J. Correa, G. Olmos, J. Llado, J. E. Esquerda and J. Caldero (2014). "Mechanisms involved in spinal cord central synapse loss in a mouse model of spinal muscular atrophy." J Neuropathol Exp Neurol 73(6): 519-535.

Tarnopolsky, M. A., J. M. Bourgeois, M. H. Fu, G. Kataeva, J. Shah, D. K. Simon, D. Mahoney, D. Johns, N. MacKay and B. H. Robinson (2004). "Novel SCO2 mutation (G1521A) presenting as a spinal muscular atrophy type I phenotype." Am J Med Genet A 125a(3): 310-314.

Tawil, R., D. Storvick, B. Weiffenbach, M. R. Altherr, T. E. Feasby and R. C. Griggs (1993). "Chromosome 4q DNA rearrangement in monozygotic twins discordant for facioscapulohumeral muscular dystrophy." Hum Mutat 2(6): 492-494.

Taymans, J. M., A. Nkiliza and M. C. Chartier-Harlin (2015). "Deregulation of protein translation control, a potential game-changing hypothesis for Parkinson's disease pathogenesis." Trends Mol Med 21(8): 466-472.

Tefera, T. W. and K. Borges (2016). "Metabolic Dysfunctions in Amyotrophic Lateral Sclerosis Pathogenesis and Potential Metabolic Treatments." Front Neurosci 10: 611.

Tein, I., A. E. Sloane, E. J. Donner, D. C. Lehotay, D. S. Millington and R. I. Kelley (1995). "Fatty acid oxidation abnormalities in childhood-onset spinal muscular atrophy: primary or secondary defect(s)?" Pediatr Neurol 12(1): 21-30.

Testa, D., T. Caraceni and V. Fetoni (1989). "Branched-chain amino acids in the treatment of amyotrophic lateral sclerosis." J Neurol 236(8): 445-447.

Thirumalai, V., R. M. Behrend, S. Birineni, W. Liu, D. Blivis and M. J. O'Donovan (2013). "Preservation of VGLUT1 synapses on ventral calbindin-immunoreactive interneurons and normal locomotor function in a mouse model of spinal muscular atrophy." J Neurophysiol 109(3): 702-710.

Tian, G. F. and A. J. Baker (2000). "Glycolysis prevents anoxia-induced synaptic transmission damage in rat hippocampal slices." J Neurophysiol 83(4): 1830-1839.

Timmerman, C. and S. Sanyal (2012). "Behavioral and electrophysiological outcomes of tissue-specific Smn knockdown in Drosophila melanogaster." Brain Res 1489: 66-80.

Tisdale, S. and L. Pellizzoni (2015). "Disease mechanisms and therapeutic approaches in spinal muscular atrophy." J Neurosci 35(23): 8691-8700.

Torres-Benito, L., M. F. Neher, R. Cano, R. Ruiz and L. Tabares (2011). "SMN requirement for synaptic vesicle, active zone and microtubule postnatal organization in motor nerve terminals." PLoS One 6(10): e26164.

Trushina, E., R. D. Singh, R. B. Dyer, S. Cao, V. H. Shah, R. G. Parton, R. E. Pagano and C. T. McMurray (2006). "Mutant huntingtin inhibits clathrin-independent endocytosis and causes accumulation of cholesterol in vitro and in vivo." Hum Mol Genet 15(24): 3578-3591.

Vainzof, M., L. Feitosa, M. Canovas, D. Ayub-Guerrieri, C. Pavanello Rde and M. Zatz (2016). "Concordant utrophin upregulation in phenotypically discordant DMD/BMD brothers." Neuromuscul Disord 26(3): 197-200.

Valero, T. (2014). "Mitochondrial biogenesis: pharmacological approaches." Curr Pharm Des 20(35): 5507-5509.

Verheijen, M. H., M. Peviani, R. Hendricusdottir, E. M. Bell, M. Lammens, A. B. Smit, C. Bendotti and J. van Minnen (2014). "Increased axonal ribosome numbers is an early event in the pathogenesis of amyotrophic lateral sclerosis." PLoS One 9(1): e87255.

Vitte, J. M., B. Davoult, N. Roblot, M. Mayer, V. Joshi, S. Courageot, F. Tronche, J. Vadrot, M. H. Moreau, F. Kemeny and J. Melki (2004). "Deletion of murine Smn exon 7 directed to liver leads to severe defect of liver development associated with iron overload." Am J Pathol 165(5): 1731-1741.

Vlassenko, A. G. and M. E. Raichle (2015). "Brain aerobic glycolysis functions and Alzheimer's disease." Clin Transl Imaging 3(1): 27-37.

Vogelaar, C. F., N. M. Gervasi, L. F. Gumy, D. J. Story, R. Raha-Chowdhury, K. M. Leung, C. E. Holt and J. W. Fawcett (2009). "Axonal mRNAs: characterisation and role in the growth and regeneration of dorsal root ganglion axons and growth cones." Mol Cell Neurosci 42(2): 102-115.

Voigt, T., K. Meyer, O. Baum and D. Schumperli (2010). "Ultrastructural changes in diaphragm neuromuscular junctions in a severe mouse model for Spinal Muscular Atrophy and their prevention by bifunctional U7 snRNA correcting SMN2 splicing." Neuromuscul Disord 20(11): 744-752.

Volkmann, N., D. DeRosier, P. Matsudaira and D. Hanein (2001). "An atomic model of actin filaments cross-linked by fimbrin and its implications for bundle assembly and function." J Cell Biol 153(5): 947-956.

Vos, M., E. Lauwers and P. Verstreken (2010). "Synaptic mitochondria in synaptic transmission and organization of vesicle pools in health and disease." Front Synaptic Neurosci 2: 139.

Walker, M. P., T. K. Rajendra, L. Saieva, J. L. Fuentes, L. Pellizzoni and A. G. Matera (2008). "SMN complex localizes to the sarcomeric Z-disc and is a proteolytic target of calpain." Hum Mol Genet 17(21): 3399-3410.

Wan, L., D. J. Battle, J. Yong, A. K. Gubitz, S. J. Kolb, J. Wang and G. Dreyfuss (2005). "The survival of motor neurons protein determines the capacity for snRNP assembly: biochemical deficiency in spinal muscular atrophy." Mol Cell Biol 25(13): 5543-5551.

Werdnig, G. (1971). "Two early infantile hereditary cases of progressive muscular atrophy simulating dystrophy, but on a neural basis. 1891." Arch Neurol 25(3): 276-278.

Westmark, P. R., C. J. Westmark, A. Jeevananthan and J. S. Malter (2011). "Preparation of synaptoneurosomes from mouse cortex using a discontinuous percoll-sucrose density gradient." J Vis Exp(55).

Weydt, P., S. M. Soyal, G. B. Landwehrmeyer and W. Patsch (2014). "A single nucleotide polymorphism in the coding region of PGC-1alpha is a male-specific modifier of Huntington disease age-at-onset in a large European cohort." BMC Neurol 14: 1.

Wigge, P., K. Kohler, Y. Vallis, C. A. Doyle, D. Owen, S. P. Hunt and H. T. McMahon (1997). "Amphiphysin heterodimers: potential role in clathrin-mediated endocytosis." Mol Biol Cell 8(10): 2003-2015.

Wilhelm, B. G., S. Mandad, S. Truckenbrodt, K. Krohnert, C. Schafer, B. Rammner, S. J. Koo, G. A. Classen, M. Krauss, V. Haucke, H. Urlaub and S. O. Rizzoli (2014). "Composition of isolated synaptic boutons reveals the amounts of vesicle trafficking proteins." Science 344(6187): 1023-1028.

Winkler, C., C. Eggert, D. Gradl, G. Meister, M. Giegerich, D. Wedlich, B. Laggerbauer and U. Fischer (2005). "Reduced U snRNP assembly causes motor axon degeneration in an animal model for spinal muscular atrophy." Genes Dev 19(19): 2320-2330.

Wirth, B. (2000). "An update of the mutation spectrum of the survival motor neuron gene (SMN1) in autosomal recessive spinal muscular atrophy (SMA)." Hum Mutat 15(3): 228-237.

Wirth, B., L. Brichta and E. Hahnen (2006). "Spinal muscular atrophy: from gene to therapy." Semin Pediatr Neurol 13(2): 121-131.

Wirth, B., L. Brichta, B. Schrank, H. Lochmuller, S. Blick, A. Baasner and R. Heller (2006). "Mildly affected patients with spinal muscular atrophy are partially protected by an increased SMN2 copy number." Hum Genet 119(4): 422-428.

Wirth, B., L. Garbes and M. Riessland (2013). "How genetic modifiers influence the phenotype of spinal muscular atrophy and suggest future therapeutic approaches." Curr Opin Genet Dev 23(3): 330-338.

Wirth, B., M. Herz, A. Wetter, S. Moskau, E. Hahnen, S. Rudnik-Schoneborn, T. Wienker and K. Zerres (1999). "Quantitative analysis of survival motor neuron copies: identification of subtle SMN1 mutations

in patients with spinal muscular atrophy, genotype-phenotype correlation, and implications for genetic counseling." Am J Hum Genet 64(5): 1340-1356.

Wirth, B., T. Schmidt, E. Hahnen, S. Rudnik-Schoneborn, M. Krawczak, B. Muller-Myhsok, J. Schonling and K. Zerres (1997). "De novo rearrangements found in 2% of index patients with spinal muscular atrophy: mutational mechanisms, parental origin, mutation rate, and implications for genetic counseling." Am J Hum Genet 61(5): 1102-1111.

Wishart, T. M., J. P. Huang, L. M. Murray, D. J. Lamont, C. A. Mutsaers, J. Ross, P. Geldsetzer, O. Ansorge, K. Talbot, S. H. Parson and T. H. Gillingwater (2010). "SMN deficiency disrupts brain development in a mouse model of severe spinal muscular atrophy." Hum Mol Genet 19(21): 4216-4228.

Wishart, T. M., C. A. Mutsaers, M. Riessland, M. M. Reimer, G. Hunter, M. L. Hannam, S. L. Eaton, H. R. Fuller, S. L. Roche, E. Somers, R. Morse, P. J. Young, D. J. Lamont, M. Hammerschmidt, A. Joshi, P. Hohenstein, G. E. Morris, S. H. Parson, P. A. Skehel, T. Becker, I. M. Robinson, C. G. Becker, B. Wirth and T. H. Gillingwater (2014). "Dysregulation of ubiquitin homeostasis and beta-catenin signaling promote spinal muscular atrophy." J Clin Invest 124(4): 1821-1834.

Wolf, M., A. M. Zimmermann, A. Gorlich, C. B. Gurniak, M. Sassoe-Pognetto, E. Friauf, W. Witke and M. B. Rust (2015). "ADF/Cofilin Controls Synaptic Actin Dynamics and Regulates Synaptic Vesicle Mobilization and Exocytosis." Cereb Cortex 25(9): 2863-2875.

Wu, C. Y., D. Whye, L. Glazewski, L. Choe, D. Kerr, K. H. Lee, R. W. Mason and W. Wang (2011). "Proteomic assessment of a cell model of spinal muscular atrophy." BMC Neurosci 12: 25.

Xu, W., A. M. Weissmiller, J. A. White, 2nd, F. Fang, X. Wang, Y. Wu, M. L. Pearn, X. Zhao, M. Sawa, S. Chen, S. Gunawardena, J. Ding, W. C. Mobley and C. Wu (2016). "Amyloid precursor protein-mediated endocytic pathway disruption induces axonal dysfunction and neurodegeneration." J Clin Invest 126(5): 1815-1833.

Yang, V. W., M. R. Lerner, J. A. Steitz and S. J. Flint (1981). "A small nuclear ribonucleoprotein is required for splicing of adenoviral early RNA sequences." Proc Natl Acad Sci U S A 78(3): 1371-1375.

Yanyan, C., Q. Yujin, B. Jinli, J. Yuwei, W. Hong and S. Fang (2014). "Correlation of PLS3 expression with disease severity in children with spinal muscular atrophy." J Hum Genet 59(1): 24-27.

Yao, J., Y. Sasaki, Z. Wen, G. J. Bassell and J. Q. Zheng (2006). "An essential role for beta-actin mRNA localization and translation in Ca2+-dependent growth cone guidance." Nat Neurosci 9(10): 1265-1273.

Yener, I. H., H. Topaloglu, S. Erdem-Ozdamar and D. Dayangac-Erden (2016). "Transcript levels of plastin 3 and neuritin 1 modifier genes in spinal muscular atrophy siblings." Pediatr Int.

Yonekawa, T., H. Komaki, Y. Saito, K. Sugai and M. Sasaki (2013). "Peripheral nerve abnormalities in pediatric patients with spinal muscular atrophy." Brain Dev 35(2): 165-171.

Young, P. J., T. T. Le, M. Dunckley, T. M. Nguyen, A. H. Burghes and G. E. Morris (2001). "Nuclear gems and Cajal (coiled) bodies in fetal tissues: nucleolar distribution of the spinal muscular atrophy protein, SMN." Exp Cell Res 265(2): 252-261.

Yu, A., Y. Shibata, B. Shah, B. Calamini, D. C. Lo and R. I. Morimoto (2014). "Protein aggregation can inhibit clathrin-mediated endocytosis by chaperone competition." Proc Natl Acad Sci U S A 111(15): E1481-1490.

Zatz, M., M. Vainzof and M. R. Passos-Bueno (2000). "Limb-girdle muscular dystrophy: one gene with different phenotypes, one phenotype with different genes." Curr Opin Neurol 13(5): 511-517.

Zenisek, D. and G. Matthews (2000). "The role of mitochondria in presynaptic calcium handling at a ribbon synapse." Neuron 25(1): 229-237.

Zerres, K. and S. Rudnik-Schoneborn (1995). "Natural history in proximal spinal muscular atrophy. Clinical analysis of 445 patients and suggestions for a modification of existing classifications." Arch Neurol 52(5): 518-523.

Zerres, K., S. Rudnik-Schoneborn, R. Forkert and B. Wirth (1995). "Genetic basis of adult-onset spinal muscular atrophy." Lancet 346(8983): 1162.

Zhang, H., L. Xing, W. Rossoll, H. Wichterle, R. H. Singer and G. J. Bassell (2006). "Multiprotein complexes of the survival of motor neuron protein SMN with Gemins traffic to neuronal processes and growth cones of motor neurons." J Neurosci 26(33): 8622-8632.

Zhang, L., X. Q. Guo, J. F. Chu, X. Zhang, Z. R. Yan and Y. Z. Li (2015). "Potential hippocampal genes and pathways involved in Alzheimer's disease: a bioinformatic analysis." Genet Mol Res 14(2): 7218-7232.

Zhang, Z., F. Lotti, K. Dittmar, I. Younis, L. Wan, M. Kasim and G. Dreyfuss (2008). "SMN deficiency causes tissue-specific perturbations in the repertoire of snRNAs and widespread defects in splicing." Cell 133(4): 585-600.

Zu, Y. L., K. Shigesada, E. Nishida, I. Kubota, M. Kohno, M. Hanaoka and Y. Namba (1990). "65-kilodalton protein phosphorylated by interleukin 2 stimulation bears two putative actin-binding sites and two calcium-binding sites." Biochemistry 29(36): 8319-8324.